이학박사학위논문

RAPGEF2/GEF26 의 생리적-병태생리적 기능

Physiological and pathophysiological roles of RAPGEF2/GEF26

2019 년 2 월

서울대학교 대학원

뇌인지과학과

허 근 정

RAPGEF2/GEF26 의 생리적-병태생리적 기능

Physiological and pathophysiological roles of RAPGEF2/GEF26

지도교수 이승복

이 논문을 이학박사학위논문으로 제출함
2018 년 12 월

서울대학교 대학원
뇌인지과학과
허근정

허근정의 박사학위논문을 인준함
2018 년 12 월

위 원 장 오 규 배 (인)
부위원장 이 승 복 (인)
위 원 기 창 욱 (인)
위 원 김 승 희 (인)
위 원 최 세 영 (인)

Physiological and pathophysiological roles of RAPGEF2/GEF26

Advisor: Seungbok Lee

A dissertation submitted in partial fulfillment of the requirement

for the degree of

DOCTOR of PHILOSOPHY

to the faculty of the
Department of Brian and Cognitive Sciences

at

SEOUL NATIONAL UNIVERSITY

by

Keunjung Heo

Thesis Committtee:

Lee Seungbok Chang-Seok K.

Seung H. Kim SE-YOUNG CHOI

Abstract

Physiological and pathophysiological roles of RAPGEF2/GEF26

Keunjung Heo
Department of Brain and Cognitive Sciences
The Graduate School
Seoul National University

Neurons are polarized cells, which allow all types of organelles to move bi-directionally based on microtubules (MTs). Because of the neuronal structure, understanding mechanisms of microtubule stability is signified for treatment of motor neuron diseases. This thesis is consisted of the research summary of the identification of the *RAPGEF2/GEF26* gene, which regulates microtubule stabilization to control neuromuscular junction (NMJ) growth and neuronal cell survival. My researches focus on functional role of RAPGEF2/GEF26 in FMRP-Futsch pathway modulation via BMP signaling and the pathogenic effect of RAPGEF2 p.E1357K variant, which has newly identified from a sporadic amyotrophic lateral sclerosis (ALS) patient through the whole exome sequencing (WES) analysis.

The first part of my thesis is focused on synaptic role of the GEF26 (human ortholog of RAPGEF2), which governs microtubule stability via BMP signaling to inhibit synaptic growth and neuronal degeneration. Specifically, GEF26 reveals to play in BMP receptor endocytosis by modulating endocytic internalization of surface BMP receptors. In addition, I clearly proved that GEF26 acts as an upstream molecule of Rap1 to control NMJ growth, motor function and neuronal cell survival. From the study, I contribute to pinpoint the GEF26 loss-of-function in regulation of microtubule stability by scrutinizing genetic relations between GEF26, Rap1, BMP-related components, and microtubule-associated protein (MAP).

The second part of my thesis is focused on defining the function of a *de novo* *RAPGEF2* variant (c.4069G>A; p.E1357K), which is discovered from whole exome sequencing analysis of sporadic ALS patients. In this study, abnormal morphology, activity and distribution of mitochondria, and decrease in microtubule stability were examined, when the RAPGEF2 function is disrupted by E1357K variant. In particular, defective mitochondrial distribution in distal axons was observed followed by the reduction of microtubule stability in transgenic flies expressing RAPGEF2-E1357K. Moreover, malfunction and aberrant morphology of mitochondria was confirmed to promote apoptotic cell death in RAPGEF2-E1357K expressing cells. From this research, I suspect that gain in toxicity due to RAPGEF2-E1357K variant weakens microtubule stability and microtubule-based trafficking of mitochondria, which leads to apoptotic cell death and motor dysfunction. Altogether, my thesis demonstrates that maintenance of microtubule stability is significant for neuronal survivability, which could contribute to find therapeutic target for treatment of neurological diseases.

Keywords: RAPGEF2/GEF26, BMP signaling pathway, microtubule stability, mitochondria trafficking, FMRP-Futsch pathway, synaptic growth, neuronal survival

***Student number*: 2014-21333**

Table of contents

List of Figures

Chapter I.

Chapter II.

Chapter III.

Abbreviations

α-TAT1	alpha tubulin acetyltransferase
ALS	Amyotrophic lateral sclerosis
ANG	Angiogenin
BAX	Bcl-2-associated X protein
BMP	Bone morphogenic protein
C9orf72	Chromosome 9 open reading frame 72
cNMP	cyclic Nucleotide-Monophosphate binding
Dad	Daughters against decapentaplegic
DCTN1	Dynactin-1
EB	End-binding
FMRP	Fragile X mental retardation protein
FUS	RNA binding protein (fused in Sarcoma)
FUTSCH	*Drosophila* MAP1B-like protein
GEF	Guanine Exchange Factor
Gbb	BMP ligand glass bottom boat
HDAC6	Histone deacetylase 6
JC-1	5,5',6,6'-tetrachloro-1,1',3,3'-tetraethylbenzimida zolylcarbocyanine iodide
KIF5A	Kinesin Family Member 5A
KRIT1	Krev1 interaction tRAPped gene 1
LIMK1	LIM kinase-1
Mad	R-Smad mother against Dpp
MAP	Microtubule associated protein
MAP1B	Microtubule associate protein 1B
Med	co-Smad media
MNs	Motor neurons
MT	Microtubule

MTOC	Microtubule organizing center
NMJ	Neuromuscular junction
OPTN	Optineurin
PDZ	Post-synaptic density, Discs large homologue, Zonula Occludens-1
PFN1	Profilin-1
P-Mad	Phosphorylation Mad
PTM	post-translational modification
RA	Ras Associating
RAPGEF2	RAP guanine nucleotide exchange factor 2
RNAi	RNA interference
ROS	Reactive oxygen species
SIRT2	NAD-dependent deacetylase
SOD1	Superoxide dismutase 1
Spartin	Troyer Syndrome protein
Spict	Spichthyin
TARDBP	TAR DNA binding protein
TBK1	TANK binding kinase 1
TDP-43	TAR DNA-binding protein 43
TGF-β	transforming growth factor-β
Tkv	The type I BMP receptor thickvein
TUBA4A	Tubulin alpha-4A
VCP	Valosin containing protein
VNC	Ventral nerve cord
WES	Whole-exome sequencing
Wit	The type II BMP receptor wishful thinking

Chapter I
Introduction

Neurons are polarized cells, which allow all types of cargoes e.g., synaptic vesicles or organelles to move bi-directionally based on microtubules (MTs) tracts from soma (also known as cell body) to the axonal terminals (Conde and Caceres, 2009). Because of the unique architecture of neurons, studying regulatory mechanism of microtubule is essential to understand neuronal properties (Conde and Caceres, 2009). Microtubules are governed by many microtubule-associated proteins (MAPs), which are involved in microtubule assembly and disassembly to control morphology and function of neurons based on the polarization (Forth et al., 2016). Disruption of microtubule polarity is proposed to alter mechanisms of microtubule organization and interrupt transport of organelles or local cues to activate intracellular signaling, which consequentially links with an early event on progression of neurological diseases by causing neuronal cell death (Stokin et al., 2006). Therefore, the molecular mechanisms of microtubule stability and dynamics are important for maintaining proper microtubule function during the neuronal development, plasticity and degeneration.

The properties and function of microtubule is characterized by the two processes, which are polymerization (assembly), and the de-polymerization (disassembly) (Inoue et al., 1995; Desai et al., 1997). The microtubule assembly and disassembly are structurally regulated by nucleotide exchangeable (E) site on β-tubulin (Conde and Caceres, 2009). When the E site on β-tubulin contacts with the catalytic domain of α-tubulin at the plus-end of microtubules, GTP caps polymerize microtubules, which leads microtubule stabilization (Gundersen et al., 2002; Conde and Caceres, 2009). After the polymerization, microtubule is de-polymerized by

hydrolyzing GTP-bound tubulins to GDP-bound tubulins at the plus-end of microtubules (Gundersen et al., 2002; Conde and Caceres, 2009). At the minus-end of microtubules, the contact between E site on β-tubulin and the catalytic domain of α-tubulin occurs with the absence of GTP caps, therefore microtubules plus-ends grow faster than the minus-ends (Gundersen et al., 2002; Conde and Caceres, 2009). The polymerization process stabilizes microtubules and activates various intracellular signals, whereas the de-polymerization process continuously modifies microtubule structures by generating forces to find target area, which occur mostly at the synaptic terminals (Gundersen et al., 2002; Conde and Caceres, 2009). Therefore, understanding the molecular mechanisms, which control microtubule polymerization and de-polymerization processes are important for neuronal outgrowth and cell death (Figure 1).

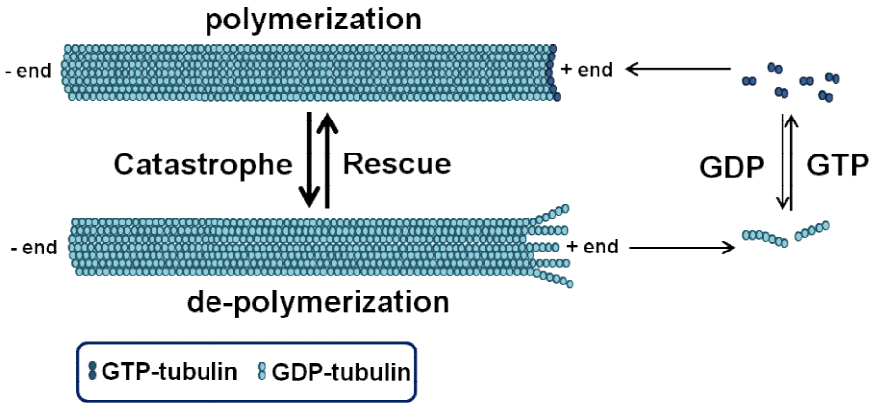

Figure 1. A model for microtubule stability and instability
The microtubule polymerization is mediated by addition of GTP-bound tubulin. After the polymerization, microtubule is de-polymerized by hydrolyzing GTP-bound tubulin to GDP-bound tubulin. The transition form of de-polymerization to polymerizaiton is known as rescue, while the form of polymerization to de-polymerizaiton is known as catastrophe.

These processes are largely controlled by post-translational modifications (PTMs), e.g., acetylation, detyrosination, tyrosination, and phosphorylation (Janke and Kneussel, 2010; Janke and Bulinski, 2011; Brill et al., 2016). Among the numerous PTMs, microtubule acetylation (stable) is considered as a significant tubulin modification, since the function of motor microtubule-associated proteins (MAPs) e.g., delivering vesicles or organelles to the target area, and maintaining axonal identities, is affected by microtubule stabilization (Conde and Caceres, 2009). In addition, the microtubule nucleation, which is important for axonal projection is controlled by microtubule stability (Conde and Caceres, 2009). Moreover, the neuromuscular junction (NMJ) growth or growth cone is regulated by microtubule stability (Dent et al., 1999; Roo et al., 2000; Wang et al., 2007; Nahm et al., 2013). Microtubule de-stabilization causes neuronal cell death, which further links with neurological diseases, such as ALS. Therefore, maintenance of microtubule stabilization is important for proper cellular processes.

I. Amyotrophic lateral sclerosis (ALS)

ALS is one of neurodegenerative diseases defined by muscle weakness and spastic paralysis resulting from loss of motor neurons (MNs) selectively (Taylor et al., 2016). Nearly 10% of ALS cases belong to familial forms (fALS) whereas the remaining are sporadic cases (sALS). After the discovery of the first ALS-causing gene *SOD1*, dozens of genes, e.g., *TARDBP*, *FUS*, *C9orf72,* and *PFN1*, were identified as important

genetic factors in pathogenesis of ALS (Schymick et al., 2007; Chen et al., 2008; Brown et al., 2017; De Vos et al., 2017). The genes affected in ALS are associated with numerous cellular pathways, e.g., protein homeostasis, RNA processing, and cytoskeletal organization (Brown et al., 2017; De Vos et al., 2017; Al-Chalabi et al., 2017). On the basis of the investigations in cellular and animal disease models, possible pathogenic mechanisms underlying degeneration of motor neurons in ALS, including protein misfolding, altered autophagy, impaired RNA regulation, defective axonal transport, and mitochondrial dysfunction have been proposed (Al-Chalabi et al., 2017; Turner et al., 2017). Among the pathways, protein aggregation is known as a hallmark for ALS pathogenesis in the studies of *SOD1*, *VCP*, *OPTN*, *TBK1* and *SQSTM1*. Studies related to RNA processing are rapidly increasing the knowledge of how *TDP-43*, *TARDBP*, *FUS* and *C9orf72* cause ALS pathology (Brown et al., 2017; Cozzolino et al., 2012). Unlike the other cellular pathways, only a few genes correlated with cytoskeletal organization have been discovered in ALS research: *DCTN1*, *PFN1*, and *TUBA4A* (Shi et al., 2010; Magrane et al., 2012; Chesi et al, 2013; Renton et al., 2014; De Vos et al., 2017).

ALS pathogenesis: regulation of microtubule-dependent process

The axonal transport of organelles, which move along the cytoskeletal organization, has been highlighted as an important pathological mechanism for neuronal function in ALS studies. One study showed that the axonal transport is disrupted by SOD1 (p.G93A) mutation (Kieran et al., 2005; Bilsland et al., 2010). Both Kieran et al. study

and Bilsland et al., study imply that the microtubule-dependent transport of organelles is important for ALS pathology. Another study with TUBA4A protein strengthens the significance in regulation of the microtubule-dependent process. When the function of microtubule protein, TUBA4A, is disrupted, it is known to promote motor neuron dysfunction (Smith et al., 2014). Such studies imply that dysregulation of microtubule-dependent process could be primary causes for ALS pathology.

II. Microtubule structure, organization and function

The microtubule cytoskeleton is important structure to regulate neuronal processes, such as proliferation and differentiation (Kapitein et al., 2015). Microtubules are polymerized structures, which is composed of α- and β-tubulin heterodimers to form protofilaments (Kapitein et al., 2015). Microtubule nucleation is derived from the microtubule organizing centers (MTOCs, also known as centrosomes) at minus-ends of microtubules (Kapitein et al., 2015). The MTOCs is composed of γ-tubulin ring complex (γ-TuRC), which is involved in polymerization of α- and β-tubulin into microtubule structure (Kollman et al., 2011; Kapitein et al., 2015). And then the microtubule structure continues modification under the growing and retracting status by circulating the modes of depolymerization, which predominately destabilize GDP-bound tubulins at the minus-end, and the mode of polymerization, which stabilize GTP-bound tubulins by capping at the plus-end (Kapitein et al., 2015).

Post-translational modifications (PTMs) of tubulin

The microtubule function is regulated by PTMs of tubulin, which is important for understanding the microtubule properties to define the specific neuronal function (Janke et al., 2011; Song et al., 2015). Many PTMs have been discovered, such as acetylation, and detyrosination (Janke et al., 2011). Microtubule function is determined based on the involvement of distinctively associated tubulin folding factors from the free form of tubulin to the specialized form of microtubules (Song et al., 2015). Among the modifications, acetylation of α-tubulin at lysine 40 (K40) represents stable microtubule during the formation of axon and synapse (Reed et al., 2006; Song et al., 2015). Microtubule acetylation is mediated by α-tubulin acetyl transferase 1 (α-TAT1), whereas histone deacetylase 6 (HDAC6) or sirtuin 2 (SIRT2) involved in microtubule deacetylation (Hubbert et al., 2002; North et al., 2003; Shida et al., 2010). The structurally stabilized microtubules are important for activities of microtubule-associated components during neuronal development and plasticity (Witte et al., 2008). If microtubule is destabilized, microtubule-based axonal transport disrupts and causes neuronal cell death, which is a well-known mechanism of neuronal diseases, such as amyotrophic lateral sclerosis (ALS) (Kim et al., 2010). Kim et al. study clearly showed the axonal transport defects in mutation of ALS-related genes, *TDP-43* and *FUS*. Therefore, maintenance of stable microtubule is important for neuronal survival.

The microtubule dynamic and function is also regulated by various microtubule-related motor and non-motor proteins, which activity is affected depend

on stable microtubules (Kapitein et al., 2015). The motor MAPs, such as kinesin and dynein regulate microtubule dynamics by controlling transport of cargoes whereas the non-motor MAPs act in interaction at plus-end of microtubules e.g., end-binding (EB), stabilizing microtubules e.g., tau and MAP1B, or severing microtubules e.g., spastin and katanin (Akhmanova et al., 2008; Hirokawa et al., 2010; Subramanian et al., 2012).

Microtubule-associated proteins (MAPs)

The role of MAP1B or Tau is well-known for regulation of neuronal outgrowth. Previously, the MAP1B is known to form microtubule loop structures during growth cone movement (Tanaka and Sabry, 1997; Luo et al., 1997; Dent et al., 1999). The production of microtubule loop (also called hairpin loop) structure is related to pause movement of the growth cone by stabilizing microtubules (Dent et al., 1999). The hairpin loop structure was also found in MAP1B-like protein *futsch* mutant (Hummel et al., 2000; Roo et al., 2000). Hummel et al. study revealed that Futsch is an essential molecule for microtubule-dependent modulation of axonal and dendritic development, and Roo et al. study discovered another role of the Futsch in regulation of NMJ growth. The abnormal Futsch localization or the reduction of transcription level is linked with disease progression (Coyne et al., 2014). Coyne et al. study clearly presented that defects in life span or motor activity in fly TDP-43 mutants were ameliorated after expressing the Futsch.

Microtubule-associated motor proteins

For the motor MAPs, the role of dynein or kinesin is well-documented. Stable microtubules provide axonal tracks for vesicles or organelles to transport based on neuronal polarization (Franker et al., 2013; Hammond et al., 2008). The directionality of movement is made by activity of motor proteins e.g., dynein (retrograde movement), or kinesin (anterograde movement) in axons (Zhao et al., 2001; Hammond et al., 2008; Hirokawa et al., 2010). From the previous studies, impairment in activity of motor protein is known to correlate with ALS diseases (Williamson et al., 1999; Rao et al., 2003; Fischer et al., 2004). In particular, Williamson et al. study clearly proved that the axonal transport defect is important for ALS pathogenesis by discovering motor neuron cell death due to the accumulated toxicity from interference in both kinesin- or dynein-mediated trafficking found from ALS patient carrying SOD1 mutation. Similar results were documented from other studies, which have reported the loss of kinesin-1 (KIF5A) or dynein could be causative factors for ALS diseases (Rao et al., 2003; Fischer et al., 2004). Overall, understanding mechanism of microtubule stability could help to find a therapeutic target to cure neuronal diseases.

III. Microtubule-dependent transport of mitochondria

The stable microtubule delivers various components, such as organelles or vesicles. Among the organelles transport, mitochondria trafficking is critical for causing

neuronal survival, since it is indispensable for delivering cellular energy. The morphology and distribution of mitochondria are dynamically altered throughout the fission and fusion events (Mattson et al., 2008). The mitochondria function is important for generation of ATP or endogenous reactive oxygen species (ROS), and maintenance of intracellular Ca^{2+} homeostasis, which are indispensable mechanisms for neuronal survival (Mattson et al., 2008; Sheng et al., 2012; 2017). Mitochondrial dysfunction causes interruption in energy production, and susceptibility from oxidative stress or toxicity, which lead to neuronal cell death. In particular, mitochondrial transport in motor neurons is critical due to the unique feature, which requires high energy consumption compared to other cellular types (Carri et al., 2017). According to the previous studies, the regulation of mitochondria transport is based on MAPs function (Stamer et al., 2002; Bettencourt da Cruz et al., 2005; Jimenez-Mateos et al., 2006). Stamer et al. study found that the neuronal MAP Tau regulates mitochondria trafficking depends on stable microtubules. In addition, Bettencourt da Cruz et al. study reported that MAP1B regulates mitochondria trafficking, which is further linked with neuronal degeneration. From studies, mitochondrial dysfunction is well-known pathogenic mechanism to progress motor neuron diseases, such as ALS.

IV. The signaling for regulation of microtubule stability

To maintain the stable microtubule status, various intracellular signaling or cues are involved in regulation of MAPs. From the previous studies, the correlation between

microtubule stabilization and BMP signaling has identified (Wang et al., 2007; Nahm et al., 2013). The level of presynaptic acetylated α-tubulin was decreased in BMP type I receptor *thickveins* (*Tkv*) mutant, implying that the absence of BMP signaling disrupt the microtubule stabilization (Wang et al., 2007). Wang et al., study also discovered that the microtubule-based axonal transport is interrupted in BMP receptor *Wit* mutant. Importantly, BMP signaling pathway is known to regulate microtubule stability by modulating FMRP expression (Nahm et al., 2013).

BMP pathway

BMP signaling is important for synaptic growth and homeostasis (Goold et al., 2007; Deshpande and Rodal, 2016). The canonical BMP signaling cascade is triggered by combination of type I and II receptors (Miyazono et al., 2010). In fly model, the BMPR-II (Wit) activated by BMP ligand (Gbb), which acts towards retrograde pathway after releases from the muscle, activates the BMPR-I (Sax and Tkv), and R-Smad (Mad) effector in consequential manner (Marques et al., 2002; McCabe et al., 2003; Deshpande et al., 2016). Phosphorylated Mad (P-Mad) further translocates into nucleus with the co-Smad media (Med) to regulate transcriptional factors, such as trio, a Rac GTPase, and I-Smad (Dad), a negative BMP signaling modulator (Ball et al., 2010; Zhao et al., 2015; Deshpande et al., 2016). In non-canonical BMP signaling, Wit receptor activates LIM kinase-1 (LIMK1) effector via a Mad-independent pathway to control synaptic growth and microtubule stability (Eaton et al., 2002; Piccioli et al., 2014). Overall, the both canonical or non-canonical BMP signaling are crucial for

microtubule-dependent regulation of synaptic growth (Ruiz-Canada et al., 2004; Wang et al., 2007; Nahm et al., 2013; Piccioli et al., 2014). However, the clear mechanism of how BMP signaling pathway regulates synaptic function is still not known.

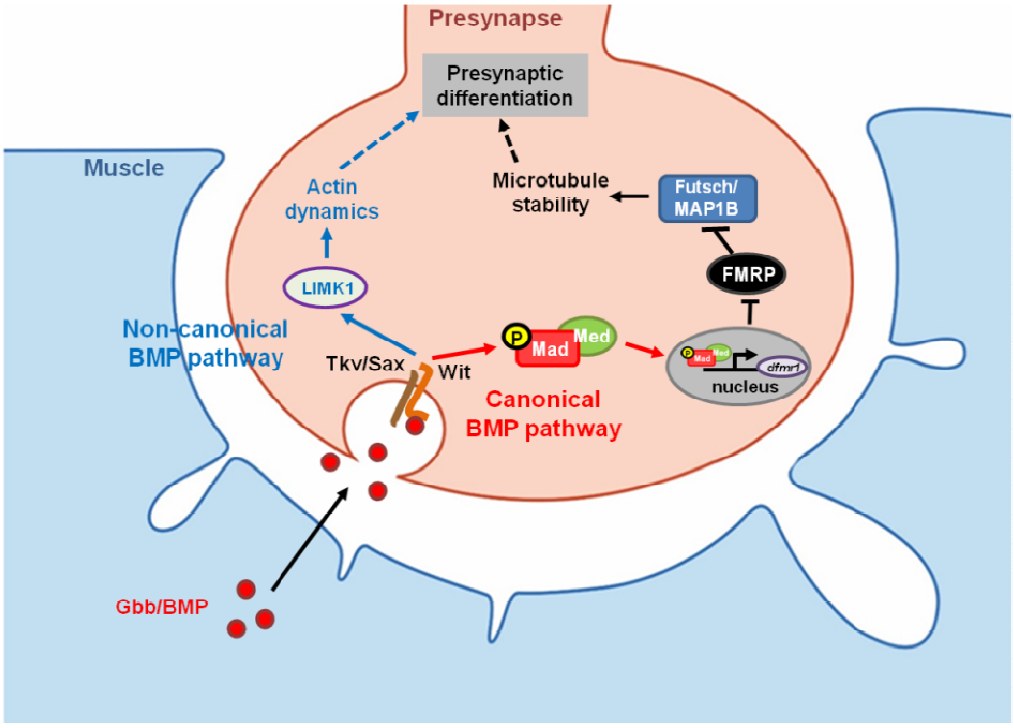

Figure 2. BMP signaling at fly NMJ
BMP ligand (Gbb) binds to the BMPR-II (Wit) in retrograde manner. The The canonical BMP signaling is initiated by Wit activation, which forms complex with BMPR-I (Tkv and Sax) to activate Mad. Phosphorylated Mad (P-Mad) moves to the nucleus with the co-Smad media (Med) and modulates transcriptional factor, such as *dfmr1*. Activation of FMRP and Futsch modulates microtubule stability to control NMJ growth and neuronal cell survival. The non-canonical BMP signaling is initiated from LIM kinase-1 (LIMK1) activation by Wit receptor via a Mad-independent pathway to control synaptic growth and microtubule stability

One mechanism of BMP signaling is that the internalization and trafficking of BMP receptors through the endocytic and endosomal pathway to control the activity of

BMP-related or -target proteins, which are the important for NMJ growth and neuronal survival (Deshpande et al., 2016). The phenotypes of formation of satellite bouton, a small bouton protruding three or less from the main synaptic branch is displayed when the BMP signaling is interrupted by disruption in BMP receptor internalization or endosomal sorting (O'Connor-Giles et al., 2008; Deshpande et al., 2016). Another mechanism of BMP signaling is regulation of microtubule stabilization, since previous studies have reported axonal transport defects in several BMP regulators, such as spichthyin (Spict) and Troyer Syndrome protein (Spartin), or MAPs such as Futsch and FMRP (Wang et al., 2007; Nahm et al., 2013). Therefore, define regulatory role of BMP signaling might provide important clues to understand the synaptic development, plasticity and degeneration.

Recently, my lab has reported that the Spartin modulates synaptic growth via BMP signaling pathway and FMRP-Futsch pathway (Nahm et al., 2013). Nahm et al. study clearly supports how BMP signaling pathway regulates microtubule stability by modulating expression of FMRP and Futsch. Although many studies have found the role of MAPs correlated with BMP signaling during synapse development, it was still limited to understand how defects in microtubule architecture regulated by BMP signaling could link with neuronal degeneration and disease pathogenesis. My research has focused on how microtubule stability regulated by BMP signaling further induces not only synaptic growth but also neuronal degeneration by using a novel BMP regulator *RAPGEF2* gene.

V. RAPGEF2/PDZGEF1/GEF26

RAPGEF2 (also called PDZGEF1) is known as GEF for Rap1 to affect various cellular processes, for example migration (Asha et al., 1999; Boettner et al., 2003; Bos, 2005; Singh et al., 2006; Boettner et al., 2007; Boettner et al., 2009). The RAPGEF2 is composed of cyclic nucleotide-monophosphate binding domain (cNMP), Ras exchange motif and Ras-associated domain (RA), two GEFs for Ras domains (RasGEF), which are important for Rap1 activation (Figure 3). The RAPGEF2 also has proline-rich motif domain (PDZ), which is important for mediation of signal transduction and two low complexity domains (LCD) (Figure 3). Since the guanine nucleotide exchange factors (GEFs) act as activator to transmit GDP-bound status to GTP-bound status, GEF activity is important for initiation of intracellular signaling (Droppelmann et al., 2014). From previous studies, the loss of *RAPGEF2* expression has known to disrupt neuronal migration in brain or organ morphogenesis in various animal models (Lee et al., 2002; Magliozzi et al., 2013; Ye et al., 2014). However, the studies to identify synaptic role of RAPGEF2 correlated with controlling of neuronal growth and survival was limited.

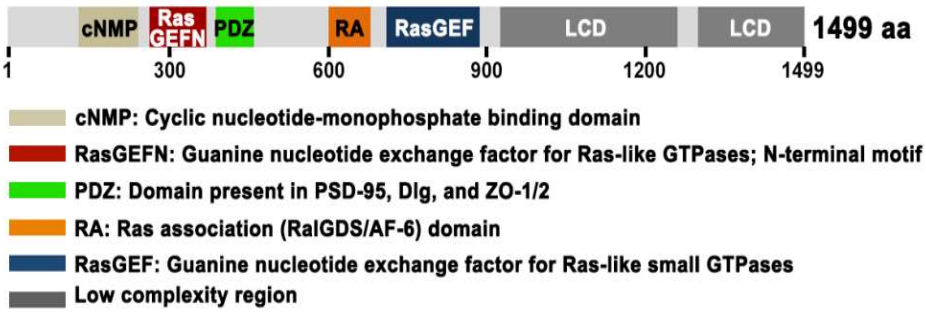

Figure 3. Molecular characterization of RAPGEF2
Human RAPGEF2 is consisted of cNMP, two RasGEF, PDZ, RA, and two LCD domains. cNMP domain activates GEF for Rap1. RA domain and two RasGEF domains stabilize active GEF conformation. PDZ domain triggers biological processes, such as signal transduction system.

VI. Purpose of my research

RAPGEF2 is known as a GEF for Rap1, which convert GDP to GTP-bound Rap1 through the seven domains, which are a cyclic NMP, RA, PDZ, and two RasGEF, and LCD domains (Bos et al., 2001). RAPGEF2 is a Rap1 GTPase, and Rap1 activity mediates microtubule stabilization by interacting with Rap1-binding protein, KRIT1 (Pannekoek et al., 2009; Liu et al., 2011). Although Rap1 was known to control microtubule dynamics, a direct correlation between the function of RAPGEF2 and microtubule dynamics was largely unknown (Krendel et al., 2002; Grabham et al., 2003; Smolen et al., 2007; Pannekoek et al., 2009; Post et al., 2013; Wilson et al., 2013). Previously, my lab studied regulatory mechanism of synaptic growth, which is governed by modulation of microtubule stability via BMP signaling pathway. Therefore, I was focus on the studies to determine the synaptic role of RAPGEF2 in modulation of BMP pathway at synaptic terminal. The synaptic role of Gef26 (fruit fly ortholog of RAPGEF2) was examined through epistatic relations between the Gef26, BMP components and MAPs. My first work revealed that the loss of Gef26 promotes synaptic overgrowth and progressive neurodegeneration in brain by governing microtubule stability via BMP signaling over-activation at synapses.

After the study in fly NMJ model, further research was done using a *de novo* RAPGEF2 variant (c.4069G>A; p.E1357K), which was identified from whole exome sequencing (WES) analysis of sporadic ALS patients. The E1357K variant is located at LCD domain, which is position at C-terminal of RAPGEF2. Impairment in LCD domain was known to increase cellular toxicity (Shin et al., 2016). My second work was to define the pathogenic effects of *de novo* RAPGEF2 variant. To study, skin fibroblasts obtained from an ALS patient carrying RAPGEF2-E1357K variant were used. In the patient fibroblasts, reduction of microtubule stability, and disruption of mitochondrial morphology and function were examined. In particular, the mitochondrial distributions in distal axons and NMJs were diminished in transgenic flies carrying RAPGEF2-E1357K mutation. My second research revealed that RAPGEF2 gain-in-toxic function from E1357K variant interfere microtubule stability and mitochondrial distribution, which further induces apoptotic cell death and motor dysfunction. Altogether, I found RAPGEF2 loss-of-function and gain-in-toxic function caused by RAPGEF2-E1357K variant in regulation of microtubule stability. In conclusion, my thesis suggests that the regulatory mechanism of microtubule stability can be central to develop therapeutic target for motor neuron diseases.

VII. Literature Cited

1. Conde C, and Caceres A. (2009). Microtubule assembly, organization and dynamics in axons and dendrites. Nat review Neurosci. *10*, 319-332.
2. Forth S, Hsia K, Shimamoto Y, Kapoor TM. (2016). Asymmetric friction of nonmotor MAPs can lead to their directional motion in active microtubule networks. Dev Cell. *157*(2), 420-432.
3. Stokin GB, and Goldstetin LS. (2006). Axonal transport and Alzheimer's disease. Annu Rev Biochem. *75*, 607-627.
4. Desai A. and Mitchison TJ. (1997). Microtubule polymerization dynamics. Annu Rev Cell Dev Boil. *13*, 83-117.
5. Ioue S, and Salmon ED. (1995). Force generation by microtubule assembly/disassembly in mitosis and related movements. Mol Biol Cell. *6*(12), 1619-1640.
6. Gundersen GG. (2002). Evolutionary conservation of microtubule-capture mechanisms. Nat Rev Mol Cell Biol. *3*(4), 296-304.
7. Janke C, and Kneussel M. (2010). Tubulin post-translational modifications: encoding functions on the neuronal microtubule cytoskeleton. Trends Neurosci. *33*(8), 362-372.
8. Janke C, and Bulinski JC. (2011). Post-translational regulation of the microtubule cytoskeleton: mechanisms and function. Nat Rev Mol Cell Biol. *12*(12), 773-786.
9. Brill MS, Kleele T, Ruschkies L, Wang M, Marahori MA, Reuter MS, Hausrat TJ, Weigand E, Fisher M, Ahles A, Engelhardt S, Bishop DL, Kneussel M, and Misgeld T. (2016). Branch-Specific microtubule destabilization mediates axon branch loss during NMJ synapse elimination. Neuron. *92*(4), 845-856.
10. Dent EW, Callaway JL, Szebenyi G, Baas PW, Kalil K. (1999). Reorganization and movement of microtubules in axonal growth cones and developing interstitial branches. J Neurosci. *19*(20), 8894-8909.
11. Roo J, Hummel T, Ng N, Klambt C, and Davis GW. (2000). Drosophila Futsch regulates synaptic microtubule organization and is necessary for synaptic growth. Neuron. *26*(2), 371-382.
12. Wang X, Shaw WR, Tsang HT, Reid E, and O'Kane CJ. (2007). Drosophila spichthyin inhibits BMP signaling and regulates synaptic growth and axonal microtubules. Nat Neurosci. *10*(2), 177-185.
13. Nahm M, Lee MJ, Parkinson W, Lee M, Kim H, Kim YJ, Kim S, Cho YS, Min BM, Bae YC, Broadie K, Lee S. (2013). Spartin regulates synaptic

growth and neuronal survival by inhibiting BMP-mediated microtubule stabilization. Neuron. *77*(4), 680-695.

14. Taylor JP, Brown RH, Cleveland DW. (2016). Decoding ALS: from genes to mechanism. Nature. 2016;539(7628):197-206.
15. Brown RH, Al-Chalabi A. (2017). Amyotrophic Lateral Sclerosis. New Engl J Med. 2017;377(2):162-72.
16. De Vos KJ, Hafezparast M. (2017). Neurobiology of axonal transport defects in motor neuron diseases: Opportunities for translational research? Neurobiol Dis. 2017;105:283-99.
17. Chen J, Shi X, Padmanabhan R, Wang Q, Wu Z, Stevenson SC, et al. (2008). Identification of novel modulators of mitochondrial function by a genome-wide RNAi screen in Drosophila melanogaster. Genome Res. 2008;18(1):123-36.
18. Schymick JC, Talbot K, Traynor BJ. (2007). Genetics of sporadic amyotrophic lateral sclerosis. Hum Mol Genet. 2007;16:R233-R42.
19. Al-Chalabi A, van den Berg LH, Veldink J. (2017). Gene discovery in amyotrophic lateral sclerosis: implications for clinical management. Nat Rev Neurol. 2017;13(2):96-104.
20. Turner MR, Al-Chalabi A, Chio A, Hardiman O, Kiernan MC, Rohrer JD, et al. (2017). Genetic screening in sporadic ALS and FTD. J Neurol Neurosur Ps. 2017;88(12):1042-4.
21. Cozzolino M, Carri MT. Mitochondrial dysfunction in ALS. (2012). Prog Neurobiol. 2012;97(2):54-66.
22. Shi P, Strom AL, Gal J, Zhu H. (2010). Effects of ALS-related SOD1 mutants on dynein- and KIF5-mediated retrograde and anterograde axonal transport. Biochim Biophys Acta. 2010;1802(9):707-16.
23. Magrane J, Sahawneh MA, Przedborski S, Estevez AG, Manfredi G. (2012). Mitochondrial dynamics and bioenergetic dysfunction is associated with synaptic alterations in mutant SOD1 motor neurons. J Neurosci. 2012;32(1):229-42.
24. Renton AE, Chio A, Traynor BJ. (2014). State of play in amyotrophic lateral sclerosis genetics. Nat Neurosci. 2014;17(1):17-23.
25. Chesi A, Staahl BT, Jovicic A, Couthouis J, Fasolino M, Raphael AR, et al. (2013). Exome sequencing to identify de novo mutations in sporadic ALS trios. Nat Neurosci. 2013;16(7):851-U98.
26. Kieran D., Hafezparast M., Bohnert S., Dick J. R., Martin J., Schiavo G., et al. (2005). A mutation in dynein rescues axonal transport defects and extends the life span of ALS mice. J. Cell Biol. 169, 561–567.

27. Bilsland L. G., Sahai E., Kelly G., Golding M., Greensmith L., Schiavo G. (2010). Deficits in axonal transport precede ALS symptoms in vivo. Proceedings of the National Academy of Sciences of the United States of America, 2010. *107*(47): p. 20523-20528.
28. Smith B. N., Ticozzi N., Fallini C., Gkazi A. S., Topp S., Kenna K. P., et al. (2014). Exome-wide rare variant analysis identifies TUBA4A mutations associated with familial ALS. Neuron 84, 324–331.
29. Kapitein LC, and Hoogenraad CC. (2015). Building the neuronal microtubule cytoskeleton. Neuron. *87*(3), 492-506.
30. Kollman JM, Merdes A, Mourey L, and Agard DA. (2011). Microtubule nucleation by γ-tubulin complexes. Nat Rev Mol Cell Biol. *12*(11), 709-721.
31. Song Y, and Brady ST. (2015). Post-translational modifications of tubulin: pathways to functional diversity of microtubules. Trends Cell Biol. *25*(3), 125-136.
32. Reed NA, Cai D, Blasius TL, Jih GT, Meyhofer E, and Verhey KJ. (2006). Microtubule acetylation promotes kinesin-1 binding and transport. Curr Biol. *16*(21), 2166-2172.
33. Shida T, Cueva JG, Xu Z, Goodman MB, and Nachury MV. (2010). The major alpha-tubulin K40 acetyltransferase alphaTAT1 promotes rapid ciliogenesis and efficient mechanosensation. Proc Natl Acad Sci USA. *107*(50), 21517-22.
34. Hubbert C, Guardiola A, Shao R, Kawaguchi Y, Ito A, Nixon A, Yoshida, M., Wang, X.F., and Yao, T.P. (2002). HDAC6 is a microtubule-associated deacetylase. Nature. *417*(6887), 455-458.
35. North BJ, Marshall BL, Borra MT, and Denu JM, and Verdin E. (2003). The human Sir2 Ortholog, SIRT2, is an NAD+−dependent tubulin deacetylase. Mol Cell. *11*(2), 437-444.
36. Witte H, Neukirchen D, and Bradke F. (2008). Microtubule stabilization specifies initial neuronal polarization. J Cell Biol. *180*(3),619-632.
37. Kim SH, Shanware NP, Bowler MJ, and Tibbetts RS. (2010). Amyotrophic lateral sclerosis-associated proteins TDP-43 and FUS/TLS function in a common biochemical complex to co-regulate HDAC6 mRNA. J Biol Chem *285*(44), 34097-34105
38. Akhmanova A, and Steinmetz MO. (2008). Tracking the ends: a dynamic protein network controls the fate of microtubule tips. Nat Rev Mol Cell Biol. *9*(4), 309-322.

39. Hirokawa N, Niwa S, and Tanaka Y. (2010). Molecular motors in neurons: transport mechanisms and roles in brain function, development and disease. Neuron. *68*(4), 610-638.
40. Subramanian R, and Kapoor TM. (2012). Building complexity: insights into self-organized assembly of microtubule-based architectures. Dev Cell. *23*(5), 874-885.
41. Tanaka E, Sabry J. (1995). Making the connection: cytoskeletal rearrangements during growth cone guidance. Cell. *83*:171–176.
42. Luo L, Jan LY, and Jan YN. (1997). Rho family GTP-binding proteins in growth cone signaling. Curr Opin Neurobiol. 7, 81–86.
43. Hummel T, Krukkert K, Roos J, Davis G, and Klambt C. (2000). *Drosophila* Futsch/22C10 is a MAP1B-like protein required for dendritic and axonal development. Neuron. *26*(2), 357-370.
44. Coyne AN, Siddegowda BB, Estes PS, Johannesmeyer J, Kovalik T, Daniel SG, Pearson A, Bowser R, and Zarnescu DC. (2014). Futsch/MAP1B mRNA is a translational target of TDP-43 and is neuroprotective in a *Drosophila* model of amyotrophic lateral sclerosis. J Neurosci. *34*(48), 15962-15974.
45. Franker MA, and Hoogernraad CC. (2013). Microtubule-based transport – basic mechanisms, traffic rules and role in neurological pathogenesis. J Cell Sci. *126*, 2319-2329.
46. Hammond JW, Cai D, and Verhey KJ. (2008). Tubulin modifications and their cellular functions. Curr Opin Cell Biol. *20*, 71-76.
47. Zhao C, Takita J, Tanaka Y, Setou M, Nakagawa T, Takeda S, Yang HW, Terada S, Nakata T, Takei Y, Saito M, Tsuji S, Hayashi Y, Hirokawa N. (2001). Charcot-Marie-Tooth disease type 2A cause by mutation in a microtubule motor KIF1Bβ. Cell. *105*, 587-597.
48. Williamson TL, and Cleveland DW. (1999). Slowing of axonal transport is a very early event in the toxicity of ALS-linked SOD1 mutants to motor neurons. Nat Neurosci. *2*, 50-56.
49. Rao MV, and Nixon RA. (2003). Defective neurofilament transport in mouse models of amyotrophic lateral sclerosis: A review. Neuroschemical Research. *28*(7),1041-1047.
50. Fischer LR, Culver DG, Tennant P, Davis AA, Wang M, Castellano-Sanchez A, Khan J, Polak MA, and Glass JD. (2004). Amyotrophic lateral sclerosis is a distal axonopathy: evidence in mice and man. Exp Neurol. *185*, 232-240.
51. Mattson MP, Gleichmann M, Cheng A. (2008) Mitochondria in neuroplasticity and neurological disorders. Neuron. *60*(5):748-66.

52. Carri MT, D'Ambrosi N, and Cozzolino M. (2017). Pathways to mitochondrial dysfunction in ALS pathogenesis. Biochem Biophys Res Commun. *483*(4):1187-93.
53. Sheng ZH, and Cai Q. (2012). Mitochondrial transport in neurons: impact on synaptic homeostasis and neurodegeneration. Nat Rev Neurosci. *13*,77–93.
54. Sheng ZH. (2012). The Interplay of Axonal Energy Homeostasis and Mitochondrial Trafficking and Anchoring. Trends Cell Biol. *27*(6), 403-416.
55. Stamer K, Vogel R, Thies E, Mandelkow E, and Mandelkow EM. (2002). Tau blocks traffic of organelles, neurofilaments, and APP vesicles in neurons and enhances oxidative stress. J Cell Biol. *156*(6), 1051-1063.
56. Bettencourt da Cruz A, Schwarzel M, Schulze S, Niyyati M, Heisenberg M, and Kretzschmar D. (2005). Disruption of the MAP1B-related protein FUTSCH leads to changes in the neuronal cytoskeleton, axonal transport defects, and progressive neurodegeneration in *Drosophila*. Mol Biol Cell. *16*(5), 2433-2442.
57. Jimenez-Mateos EM, Gonzalez-Billault C, Dawson HN, Vitek MP, and Avila J. (2006). Role of MAP1B in axonal retrograde transport of mitochondria. Biochem J. *397*(1), 53-59.
58. Aberle H, Haghighi AP, Fetter RD, McCabe BD, Magalhaes TR, and Goodman CS. (2002). Wishful thinking encodes a BMP type II receptor that regulates synaptic growth in *Drosophila*. Neuron. *33*, 545-558.
59. Marques G, Bao H, Haerry TE, Shimell MJ, Duchek P, Zhang B, and O'Connor MB. (2002). The *Drosophila* BMP type II receptor wishful thinking regulates neuromuscular synapse morphology and function. Neuron. *33*, 529-543.
60. Wang X, Shaw WR, Tsang HT, Reid E, and O'Kane CJ. (2007). *Drosophila* spichthyin inhibits BMP signaling and regulates synaptic growth and axonal microtubules. Nat Neurosci. *10*(2), 177-185.
61. Nahm M, Lee MJ, Parkinson W, Lee M, Kim H, et al. (2013) Spartin regulates synaptic growth and neuronal survival by inhibiting BMP-mediated microtubule stabilization. Neuron. 77: 680-695.
62. Goold CP, and Davis GW. (2007). The BMP ligand Gbb gates the expression of synaptic homeostasis independent of synaptic growth control. Neuron. *56*(1), 109-123.
63. Deshpande M, and Rodal AA. (2016). The Crossroads of Synaptic Growth Signaling, Membrane Traffic and Neurological Disease: Insights from *Drosophila*. Traffic. *17*(2), 87-101.

64. Miyazono K, Kamiya Y, and Morikawa M. (2010). Bone morphogenetic protein receptors and signaling transduction. J Biol Chem. *147*(1), 35-51.
65. Aberle H, Haghighi AP, Fetter RD, McCabe BD, Magalhaes TR, and Goodman CS (2002). Wishful thinking encodes a BMP type II receptor that regulates synaptic growth in *Drosophila*. Neuron. *33*(4),545-558.
66. Marques G, Bao H, Haerry TE, Shimell MJ, Duchek P, Zhang B, and O'Connor MB. (2002). The *Drosophila* BMP type II receptor Wishful Thinking regulates neuromuscular synapse morphology and function. Neuron. *33*(4), 529-543.
67. McCabe BD, Marques G, Haghighi AP, Fetter RD, Crotty M. L, Haerry TE, Goodman CS, O'Connor MB. (2003). The BMP homolog Gbb provides a retrograde signal that regulates synaptic growth at the *Drosophila* neuromuscular junction. Neuron. *39*, 241-54.
68. Ball RW, Warren-Paquin M, Tsurudome K, Liao EH, Elazzouzi F, Cavanagh C, An BS, Wang TT, White JH, Haghighi AP. (2010). Retrograde BMP signaling controls synaptic growth at the NMJ by regulating trio expression in motor neurons. Neuron. *66*(4), 536-549.
69. Zhao G, Wu Y, Du L, Li W, Xiong Y, Yao A, Wang Q, and Zhang YQ. (2015). *Drosophila* S6 kinase like inhibits neuromuscular junction growth by downregulating the BMP receptor thickveins. PloS Genetics. e1004984.
70. Eaton BA, and Davis GW. (2005). LIM Kinase 1 controls synaptic stability downstream of the type II BMP receptor. Neuron. *47*(5), 695-708.
71. Piccioli ZD, and Littleton JT. (2014). Retrograde BMP signaling modulate rapid regulate activity-dependent synaptic growth by presynaptic LIM Kinase regulation of cofilin. J Neurosci. *34*(12),4371-4381.
72. Ruiz-Canada C, Ashley J, Moeckel-Cole S, Drier E, Yin J, Budnik V. (2004). New synaptic bouton formation is disrupted by misregulation of microtubule stability. Neuron. *42*(4), 567-580.
73. O'Connor-Giles KM, Ho LL, and Ganetzky B. (2008). Nervous Wreck interacts with thickveins and the endocytic machinery to attenuate retrograde BMP signaling during synaptic growth. Neuron. *58*(4), 507-518.
74. Droppelmann CA, Campos-Melo D, Volkening K, and Strong MJ. (2014). The emerging role of guanine nucleotide exchange factors in ALS and other neurodegnerative diseases. Front Cell Neurosci. 8: 282.
75. Asha H, deRuiter ND, Wang MG, and Hariharan IK. (1999). The Rap1 GTPase functions as a regulator of morphogenesis in vivo. EMBO J. *18*, 605–615.

76. Boettner B, Harjes P, Ishimaru S, Heke M, Fan HQ, Qin Y, Van Aelst L, Gaul U. (2003). The AF-6 homolog canoe acts as a Rap1 effector during dorsal closure of the Drosophila embryo. Genetics *165*, 159-169.
77. Bos JL. (2005). Linking Rap to cell adhesion. Curr Opin Cell Biol. *17*, 123-128.
78. Singh SR, Oh SW, Liu W, Chen X, Zheng Z, and Hou SX. (2006). Rap-GEF/Rap signaling restricts the formation of supernumerary spermathecae in *Drosophila melanogaster*. Devlop. Growth Differ. *48*, 169-175.
79. Boettner B, Van Aelst L. (2007). The Rap GTPase activator *Drosophila* PDZ-GEF regulates cell shape in epithelial migration and morphogenesis. Mol Cell Biol. *27*, 7966-7980.
80. Boettner B, Van Aelst L. (2009). Control of cell adhesion dynamics by Rap1 signaling. Curr Opin Cell Biol *21*, 684-93.
81. Lee JH, Cho KS, Lee J, Kim D, Lee SB, Yoo J, Cha GH, Chung J. (2002). *Drosophila* PDZ-GEF, a guanine nucleotide exchange factor for Rap1 GTPase, reveals a novel upstream regulatory mechanism in the mitogen-activated protein kinase signaling pathway. Mol Cell Biol *22*, 7658-66.
82. Maglizzi, R., Low, T.Y., Weijts, M.W., Cheng, T., Spanjaard, E., Mohammed, S., Venn, A., Ovaa, H., Rooij, J., Zwartkruis, J.T., Bos JL, Bruin A, Heck JR, and Guardavaccaro D. (2013). Control of Epithelial Cell Migration and Invasion by the IKKβ- and CK1α-Mediated Degradation of RAPGEF2. Dev Cell. *27*(5), 574-585.
83. Ye T, Ip PK, Fu KY, and Ip NY. (2014). Cdk5-mediated phosphorylation of RapGEF2 controls neuronal migration in the developing cerebral cortex. Nat Commun. 5:4826.
84. Grabham PW, Reznik B, Goldberg DJ. (2003). Microtubule and Rac 1-dependent F-actin in growth cones. J Cell Sci. 116(18):3739-48.
85. Krendel M, Zenke FT, Bokoch GM. (2002). Nucleotide exchange factor GEF-H1 mediates cross-talk between microtubules and the actin cytoskeleton. Nat Cell Biol. 4(4):294-301.
86. Post A, Pannekoek WJ, Ross SH, Verlaan I, Brouwer PM, Bos JL. (2013). Rasip1 mediates Rap1 regulation of Rho in endothelial barrier function through ArhGAP29. P Natl Acad Sci USA. 110(28):11427-32.
87. Smolen GA, Schott BJ, Stewart RA, Diederichs S, Muir B, Provencher HL, et al. (2007). A Rap GTPase interactor, RADIL, mediates migratio f n oneural crest precursors. Gene Dev. 21(17):2131-6.

88. Wilson CW, Parker LH, Hall CJ, Smyczek T, Mak J, Crow A, et al. (2013). Rasip1 regulates vertebrate vascular endothelial junction stability through Epac1-Rap1 signaling. Blood. 122(22):3678-90.
89. Bos JL, Rooij J, and Reedquist KA. (2001). Rap1 signalling: Adhering to new models. Nat Rev Mol Cell Bio. 2(5):369-377.
90. Pannekoek WJ, Kooistra MR, Zwartkruis FJ and Bos JL. (2009). Cell–cell junction formation: The role of Rap1 and Rap1 guanine nucleotide exchange factors. Biochim Biophys Acta. 1788(4):790-6
91. Liu JJ, Stockton RA, Gingras AR, Ablooglu AJ, Han J, Bobkov AA, et al. (2011). A mechanism of Rap1-induced stabilization of endothelial cell-cell junctions. Mol Biol Cell. 22(14):2509-19.
92. Shin J, Salameh JS and Richter JD. Impaired neurodevelopment by the low complexity domain of CPEB4 reveals a convergent pathway with neurodegeration. Sci Rep. 2016;6:29395.

Chapter II*
The RapGEF2 controls NMJ growth and neuronal survival by modulating microtubule stability via retrograde BMP signaling

*This chapter has been largely reproduced from an article published by Heo, K., Nahm, M., Lee, M.-J., Kim, Y.-E., Ki, C.-S., Kim S.H., and Lee, S. Molecular Brain. 10: 62. (2017). Figures 2 and 13 were reproduced from data provided as part of collaboration by Dr. M. Nahm. Figures 4C-4F were reproduced from data provided as part of collaboration by M.-J. Lee.

I. Abstract

Rap is known as an important GTPases for synaptic plasticity and it is activated by neuronal specific activator RAPGEF2 (also known as Gef26). However, synaptic role of RAPGEF2 was not known. Our research goal is to prove the synaptic mechanism of Gef26 at neuromuscular junction (NMJ). First, presynaptic Gef26 is important for synaptic growth by examining NMJ overgrowth in *gef26* mutants was restored to normal when presynaptic *gef26* is expressed. Next, we discovered that Gef26 acts as an upstream molecule of Rap1 to regulate synaptic growth. Interestingly, we examined abundance of satellite boutons, which are small boutons protruding three or less from main synaptic branch in *gef26* mutant. This clue led us to suspect the Gef26 role in regulation of BMP signaling. To study the genetic mechanisms of Gef26 and BMP signaling, we scrutinized epistatic relations between Gef26 and BMP pathway related components. As results, we concluded that Gef26/Rap1 inhibits retrograde BMP signaling pathway. In addition, we proved that Gef26/Rap1 regulates microtubule stability via FMRP-Futsch pathway by governing expression level of FMRP. Moreover, we confirmed that loss of Gef26 causes shorten lifespan, progressive motor dysfunction and neuronal cell death. Taken together, our study demonstrates that Gef26 acts on microtubule stability to control NMJ growth and neuronal cell survival via suppressing retrograde BMP signaling.

II. Introduction

Synapses are specialized structures, which allow neuron-to-neuron communication. To coordinate synaptic development and maintenance, retrograde BMP signaling is known as an important intracellular cue. The BMP signaling is indispensable for synaptic development and plasticity (Aberle et al., 2002; Marques et al., 2002). In canonical BMP pathway, BMP ligand (Gbb) secreting from muscle binds to BMPR-II (Wit) in retrograde pathway (McCabe et al, 2003). The Wit activation forms complex with BMPR-I (Tkv and Sax), which further activates effector molecule Mad (Collins et al, 2007). When the Mad is phosphorylated (P-Mad), regulates synaptic growth by modulating transcriptional level of *trio* or *dfmr1* (Ball et al, 2010; Nahm et al., 2013).

Here, we identified function of a novel gene, *Gef26* (fruit fly homolog of *RAPGEF2*), which regulates synaptic growth via BMP signaling pathway. Previously, Gef26 is known as a GEF for Rap1, which convert GDP to GTP-bound Rap1 to activate developmental processes, e.g., eye, productive organs, dorsal closure (Asha et al., 1999; Boettner et al., 2003; Bos, 2005; Singh et al., 2006; Wang et al., 2006; Boettner et al., 2009; Gloerich et al., 2011). In particular, RAPGEF2 is known to function in neuronal morphogenesis (Hisata et al., 2007; Bilasy et al., 2009; Lee et al., 2011; Maeta et al., 2016). Bilasy et al. study proved that the RAPGEF2 is essential for early developmental stage in brain. In addition, Maeta et al. study presented that neuronal morphology and migration were altered in RAPGEF2 knockout mice, implying that RAPGEF2 functions in neuronal migration. Moreover, RAPGEF2 is known to act in integrin- and cadherin-mediated regulation of surface adherens

junctions (AJs), which structure is important for neuronal development (Boettner et al., 2000; Sawye et al., 2009; Boettner et al., 2009; Spahn et al., 2012; Wang et al., 2013). Despite previous studies, the regulatory mechanism of Gef26 in synaptic development and neuronal survival was unclear.

In this study, role of presynaptic Gef26 is important for synaptic growth by finding NMJ overgrowth with abundant formation of satellite bouton in *gef26* mutants is restored by presynaptic *gef26* overexpression. Next, Gef26 proves to act as an upstream molecule of Rap1 by examination of genetic interaction. Moreover, regulatory role of Gef26 in BMP signaling clearly reveals by test of epistatic relations between Gef26 and BMP components. In particular, internalization of BMP receptor was blocked in *gef26* mutants by examining massive accumulation of BMP receptor at surface area. The Gef26 is also revealed to regulate microtubule stability via FMRP-Futsch pathway. Lastly, I found that shorten lifespan, progressive motor dysfunction and neuronal cell death in *gef26* mutant. Taken together, I suggest that Gef26 is a novel regulator to control NMJ development and neuronal cell survival by governing BMP signaling and microtubule stability.

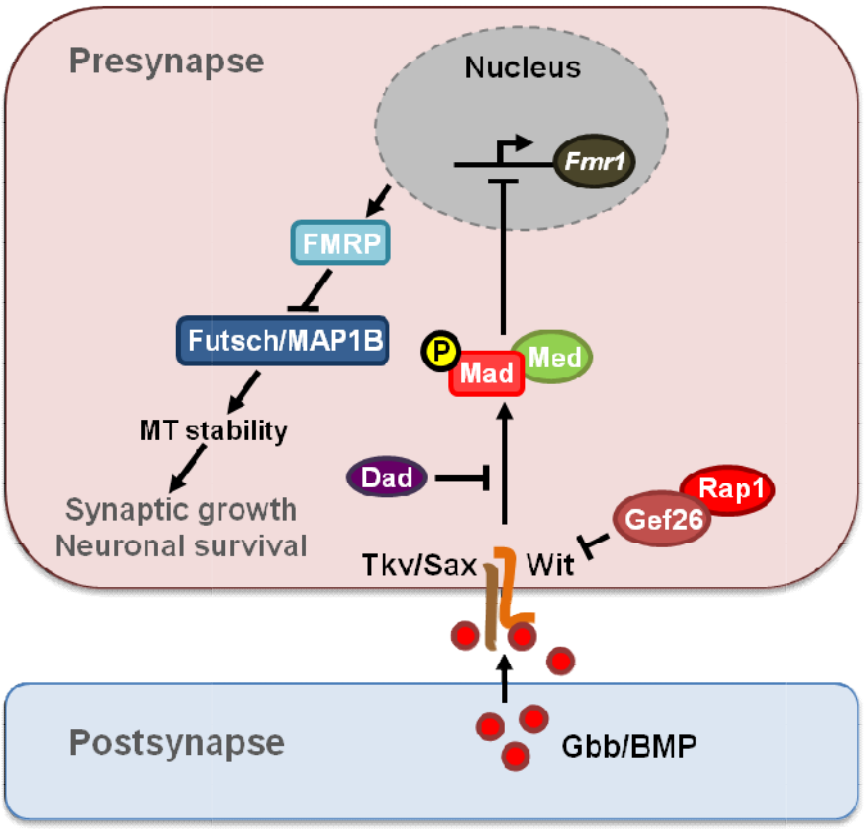

Figure 1. The presynaptic function of Gef26 in regulation of microtubule stability via BMP signaling at the NMJ

The Gef26, an upstream molecule of Rap1, inhibits endocytic internalization of BMPR-II (Wit) to regulate microtubule stability. Loss of Gef26 induces accumulation of surface Wit, increases P-Mad level, reduces transcription level of *Fmr1*, and increases Futsch/MAP1B to modulate microtubule stability to control NMJ growth and neuronal cell survival.

III. Materials and methods

1. Fly strains and genetics

Flies were maintained on fleshly provided medium at 25°C. For this study, we considered w^{1118} strain as wild-type control and used pan-neuronal *C155-GAL4* (Lin and Goodman, 1994) and muscle *BG57-GAL4* (Budnik et al. 1996) GAL4 drivers followed by previous studies (Nahm et al., 2013). The *gef26* null mutant, $gef26^{6}$ was generally gifted from S. Hou (NIH National Cancer Institute). wit^{A12}, wit^{B11}, tkv^{1}, tkv^{7}, dad^{J1E4}, $rap1^{Mi11950}$ (refer as $rap1^{M}$), $endoA^{\Delta 4}$, $dap160^{\Delta 1}$, Df*(2L)BSC5* (*gef26* deficiency, breakpoints 26B1-2;26D1-2), $\text{Rap1}^{\text{HMJ21898}}$ ($UAS\text{-}rap1^{RNAi2}$) were received from Bloomington Stock Center (Bloomington, IN, USA), whereas $\text{PDZ-GEF}^{\text{KK102612}}$ ($UAS\text{-}gef26^{RNAi}$), and $\text{Rap1}^{\text{KK107785}}$ ($UAS\text{-}rap1^{RNAi1}$) were earned from the Vienna Drosophila Resources Center (Vienna, Austria). Transgenic strains carrying *UAS-gef26* and $UAS\text{-}Myc\text{-}rap1^{CA}$ were generated using w^{1118} strain as a background followed by standard manuals (Nahm et al., 2013). For rescue experiments, interchromosomal combinations (*C155-GAL4;* $gef26^{6}$ and *Df*; *UAS-gef26*) were constructed followed by previously reported procedures (Robertson et al., 1988). The generated rescue lines were then verified by complementary test. For intragenic suppression experiments, 1) $tkv^{1}/gef26^{6}$ 2) tkv^{7}/Df 3) *Df*; $UAS\text{-}myc\text{-}rap1^{CA}$ 4) $tkv^{1},rap1^{M}$ 5) $tkv^{7},rap1^{M}$ were recombined each other. For BMP receptor trafficking experiment, *Df; UAS-Flag-tkv,* and *UAS-HA-gef26/UAS-Flag-tkv* were also recombined. The recombinants were identified by phenotypic and immunochemical analysis.

2. Molecular biology

Full-length of *gef26* and *rap1* cDNA was obtained from total RNA extracted from *Drosophila* S2R+ cells by reverse transcription PCR and introduced into the pUAST (Invitrogen, Carlsbad, CA, USA) or pUAST-Myc vector to generate *UAS-gef26* and *UAS-Myc-rap1*. The *UAS-Myc-rap1*^{CA} was produced by PCR-based mutagenesis using two single primer reactions for substitution of glutamine to glutamate at 63 positions. The information of primers were followed; 5'-ATGGCCGTGAACTCCT CCGTACCC-3', 5'-TACGGAGGAGTTCACGGCCATGCG-3', 5'-GGGAGATCTG CCACCATGGAACAAAAACTCATCTCAGAAGAGGATCTGATGCGTGAGTAC AAAATC-3', and 5'-GGGTCTAGATAGCAGA ACACATAGGGAC-3'.

For quantitative real-time PCR (qPCR) reaction, we used SYBR Select Master Mix (Applied Biosystems, Foster City, CA, USA) and an ABI 7500 Real Time PCR System (Applied Biosystems). Total RNA was extracted from third instar larvae brain of w^{1118}, *Gef26* and *rap1* mutants using Trisure kit (Bioline, Taunton, MA, USA). Then, the first-strand cDNA synthesis was obtained using a superscript III cDNA synthesis kit (Invitrogen). Relative quantification was analyzed by comparative CT method followed by Applied Biosystems manual. The primers for *dfmr1* were: forward 5'-GGATCAGAACATACCACGTG-3', and reverse 5'-CTGGCAGCT ATCGTGGAGGCG-3' and the primers for *rp49* were: forward 5'-CAC CAGTCGGATCGATATGC3' and reverse 5'-CACGTTGTGCACCAGGAACT-3'. The expression of *rp49* was used for control, and we performed the experiments in triplicate.

3. Cell culture and transfection

Fly origin neuronal (BG2-c2) cells were maintained at 25°C in M3 medium (Sigma-Aldrich, St. Louis, MO, USA) containing 10% heat-inactivated fetal bovine serum (Gibco, Carlsbad, CA, USA), 10 μg/ml insulin (Sigma-Aldrich) and penicillin-streptomycin. For transfection, 1μg DNA and 5μg double-strand RNA (dsRNA) were used with Cellfectin II by following manufacture protocol (Invitrogen). For endocytic trafficking assay, BMP receptors with Myc- and Flag-tagged (*pAc-Myc-tkv-Flag*) or *pAc-Myc-wit* were used. *Gef26* cDNA was introduced into pAc5.1 vector (Invitrogen) to produce *pAc-HA-Gef26*. *Gef26* dsRNA was generated using two single primer reaction containing T7 promoter sequences at both ends. The primers were 5'-GTGGCCGGCTCTACCAGT-3' and 5'-TGGTACGCG AGTCGAACG-3'.

4. BMP receptor internalization assay

To examine internalization of *tkv*, BG2-c2 cells were transfected with *pAc-Myc-tkv-Flag* and *Gef26* dsRNA and cultured for 72h. After treatment of 100ug/ml cycloheximide (Sigma-Aldrich) for 5 h to remove new protein synthesis and detect solely extracellular *tkv* were labeled with anti-Myc antibody (1:200, Cell Signaling, Danvers, MA, USA) for 1 h at 4 °C. Then, internalization of *tkv* is allowed using serum containing BMP ligand Gbb for 10 min at 25 °C. To remove surface remained anti-Myc antibody, cells were vigorously washed with cold-acidic buffer (0.5 M NaCl, 0.2 M acetic acid, pH 4.0) for 15 min, and fixed in 4% formaldehyde for 10 min. The fixed cells were consequentially permeabilized with 0.2% Triton X-100 for 10 min, blocked

with PBT-0.2 containing 1% BSA for 1 h, incubated with mouse anti-Flag primary antibody (1:500, Sigma-Aldrich) overnight at 4 °C to label both total *tkv*, and stained with FITC-conjugated secondary antibody (1:200, Jackson ImmunoResearch, West Grove, PA, USA). Finally, the samples were mounted in SlowFade antifade medium (Invitrogen). Internalization of another BMP receptor *wit* was additionally analyzed by following same protocol.

5. The analysis of BMPR internalization

Quantification of fluorescence intensity was followed as previously described (Wang et al., 2007). To quantify inside of bouton fluorescence intensity, ImageJ were used. The percentage of internalized Myc-Tkv intensity within 0.5 μm from HRP-labeled was calculated from the cells showing similar intensity of total Tkv. To quantify outside of bouton intensity, the percentage of surface labeled Myc-Tkv intensity from outside of a 2.5 μm from HRP-labeled was calculated. This experiment was performed triplicates.

6. Western blotting

Ten third instar larvae brains were isolated and homogenized in cold lysis buffer (25 mM Tris-HCl, pH 7.5, 150 mM NaCl, 0.5% Triton X-100, and protease inhibitors). The probs were incubated with anti-Myc (1:1000, Cell Signaling) or β-actin (1:10000, Sigma-Aldrich) at 4 °C overnight. The β-actin was accounted as control. The western blot probes were analyzed by densitometric measurements.

7. FM1-43FX dye uptake assays

FM1-43FX dye uptake assay was followed by previously described (Verstreken et al., 2008; Nahm et al., 2013). The larvae were dissected by preserving motor neurons from CNS in HL3 saline without Ca^{2+}. After the cutting of motor neurons, the samples are quickly incubated for 1 min with labeling solution in HL3 saline containing 90 mM KCl, 5 mM Ca^{2+}, and 4 μM FM1-43FX (Molecular Probes, Eugene, OR, USA) to label synaptic vesicle. After stimulation, the samples were washed with Ca^{2+}-free HL3 saline for 10 min and fixed for 30 min in 4% formaldehyde. The samples were mounted in SlowFade antifade medium (Invitrogen). Images were collected using a Plan Apo 40x 0.90 NA Water objective of FV300 laser-scanning confocal microscope (Olympus, Tokyo, Japan) followed by washing. Images were analyzed using FLOUVIEW image analysis software (Olympus).

8. NMJ immunostaining

Third-instar larvae were dissected in HL3 solution without Ca^{2+} (Stewart et al, 1994). The tissues were fixed in 4% formaldehyde for 20 min, and permeabilized with PBS containing 0.1% Triton X-100 for 30 min, blocked with PBT-0.1 containing 0.2% BSA for 1 hr, incubated with primary antibodies overnight at 4 ^{o}C. Monoclonal antibodies of anti-HRP (1:200), anti-Futsch (1:50), anti-CSP (1:300), anti-NC82 (1:50), and anti-Dlg (1:500) are obtained from the Developmental Studies Hybridoma Bank (DSHB). The primary antibodies anti-GluRIIC (1:200), anti-PS1 (1:500) were generally gifted from corresponders from following references (Marrus et al., 2004; Persson et al., 1998).

Additionally primary antibodies anti-P-Mad (1:100, Cell Signaling), anti-Flag (1:500, Sigma-Aldrich), anti-Myc (1:200, Cell Signaling) were used. The FITC-, Cy3- and Cy5-conjugated secondary antibodies were used (1:200, Jackson ImmunoResearch). All images mounted in SlowFade antifade medium (Invitrogen)were analyzed with either Olympus 300 or Zeiss 800 confocal microscope using a C Apo 40x W or Plan Apo 63x 1.4 NA objective. For vinblastine treatment experiment, 1 μM vinblastine sulfate (Sigma-Aldrich) was supplemented in standard fly food.

Quantified number of total bouton and satellite bouton were done at NMJ 6/7 or NMJ 4 from abdominal segment 2. Fewer than three boutons projecting from the main branch were only counted for quantification of satellite boutons (Nahm et al., 2013). We normalized overall boutons number to muscle size from all samples, since nerve branches expand parallel with the muscle area expansion during developmental process followed by previous protocol (Wan et al., 2000).

9. Immunohistochemistry and caspase-3 staining

Fly heads were surgically dissected and fixed with 4% paraformaldehyde for overnight at 4 °C. The brain tissues were embedded in paraffin wax and serial sectioned in frontal oriented position (5-μm) using RM2255 microtome (Leica, Wetzlar, Germany). The serial sectioned samples from the whole brain were dewaxed and hematoxylin and eosin-stained followed by reference manual (Nahm et al., 2013). For quantification, brain vacuoles with diameters > 5 μm were counted from the sections of whole brain.

For caspase-3 assay, fly brains were removed, our lab immunostaining

manual were followed. Then, the samples were incubated with primary antibodies anti-Elav (1:10, DSHB, 7E8A10), anti-Repo (1:10, DSHB, 8D12), and anti-cleaved caspase-3 (1:100, Cell Signaling) in blocking buffer for 2 days at 4 °C, and incubated with FITC-, Cy3- or Cy5-conjugated secondary antibodies (1:200, Jackson ImmunoResearch) for overnight at 4 °C. The sample finally mounted in SlowFade antifade medium (Invitrogen). Images were collected with a Zeiss LSM 700 laser-scanning confocal microscope using C-Apo 40x 1.20 W objective lens. For pairwise comparisons, student's t tests were executed. (*p<0.001; error bars indicate SEM).

10. TUNEL assay

TUNEL assay was followed by manufacture protocol using *in situ* cell death detection kit (Roche, Mannheim, Germany). Fly heads were incised and fixed overnight in 4% formaldehyde at 4°C. The samples were sequentially dehydrated, embedded in paraffin, and 5-μm serial sectioned in a frontal orientation. Three consecutive frontal sections from middle of brain are then deparaffinized, rehydrated, permeabilized with 0.1% sodium citrate and 0.1% Triton X-100 for 15 min at room temperature. After washing with PBS, the samples were consequentially incubated with TUNEL reaction mixture in a dark humid chamber for 1 hr at 37 °C and DAPI for 5 min at room temperature. To quantify TUNEL-positive cells, images were acquired with a LSM 800 laser-scanning confocal microscope using a C Apo 20x objective from the mounted samples in SlowFade antifade medium (Invitrogen).

11. Climbing assay and lifespan analysis

For locomotor ability analysis, the aged flies grown at 23 ^{o}C with 50% humidity for 2, 10, 20, 30, and 40-days were used (Ellis et al., 2010). Approximately 100 flies per each genotype were collected in 100 ml glass cylinder, and allow 5 min for acclimation. Climbing ability was analyzed at 30 s after the 5 s gentle vortexing. The climbing assays were performed triplicates.

For lifespan analysis, flies were raised at 23 ^{o}C camber with 50% to 55% humidity followed by previous lab manual. The 10 flies were maintained in each vial and the foods were transferred into clean medium every two days. The number of 2, 10, 20, 30, and 40-days-old flies were quantified and these experiments were performed triplicates.

12. Statistical analysis

All data are expressed as mean $\pm$ SEM. For pairwise comparisons, student's t tests were executed. For multiple comparisons, we used one-way ANOVAs and multiple pairwise comparisons. (*P<0.001, **P<0.01, and ***P<0.05; error bars indicate SEM).

IV. Results

1. Domain structure of Gef26

The Gef26 protein is composed of Guanine Exchange Factor (GEF) function related cyclic nucleotide-monophosphate (cNMP) binding domain (amino acid 128-246), Ras-exchange motif domain (amino acids 279-400), PDZ domain (amino acid 415-497), Ras-associating (RA) domain (amino acid 757-843), and guanine exchange factor domains (amino acid 864-1164), which are highly conserved in human RAPGEF2 protein (Fig 2A).

2. Neuronal function of Gef26 restrains synaptic growth

To examine the synaptic role of *gef26*, we additionally characterized the NMJ growth phenotype in third-instar larvae of *gef26* null mutant ($gef26^{6}$), which is generally gifted from Steven X. Hou (Hou et al., 2013). This mutant is semi-lethal at pupal stage. We examined synaptic growth phenotype of *gef26* homozygous mutants ($gef26^{6}$). Compared to the wild-type, normalized overall bouton numbers in $gef26^{6}$ mutants were increased (Fig 2B-D). To enable quantification, the numbers of overall boutons in all analyzed Gef26 related samples were normalized to the muscle size area from now on (data not shown). Interestingly, hyper-pruning satellite boutons, which are small sized boutons derived from the three or less primary boutons or branch in $gef26^{6}$ mutants (Fig 2B and 2D).

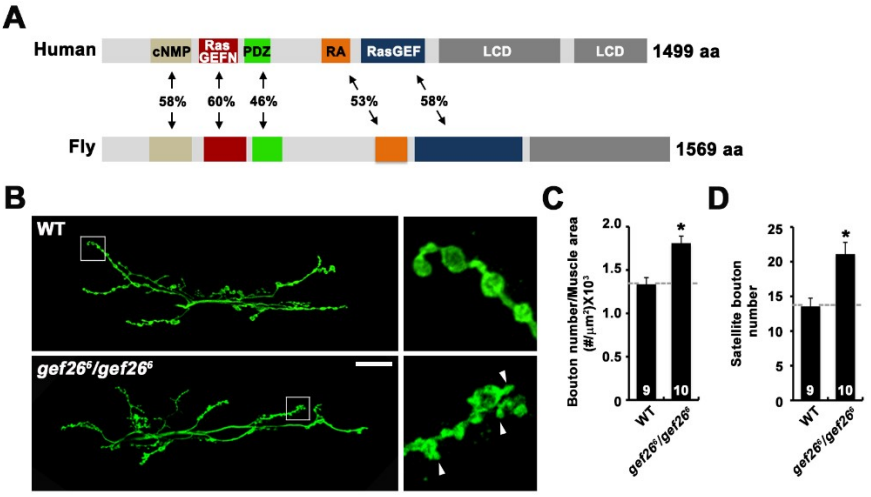

Figure 2. Domain structure and synaptic phenotypes of Gef26
(A) Domain structures of human and fruit fly RAPGEF2. Human RAPGEF2 contains cyclic nucleotide-monophosphate (cNMP) binding domain, two guanine exchange factor for Ras (Ras-GEF) domains, discs large homologue, zonula occludens-1 domain (PDZ) domain, Ras-associating (RA) domains, and two low-complexity domains (LCD). These domain structures of human RAPGEF2 are highly conserved in fly, implying the functionally significance of these amino acids. (B) NMJs 6/7 confocal images of third-instar larval in A2 segment were labeled with neuronal marker, anti-HRP. Note to the satellite boutons (arrowheads). Scale bar, 20 μm. (C, D) Bar graphs represent normalized number of total bouton (C) and satellite bouton number (D) in wild-type, *gef26*^{6}/*gef26*^{6}. All samples are compared to wild-type (*$P < 0.001$).

To eliminate the possibility of the off target effects, we obtained *Df(2L)BSC5* deficiency line (referred as *Df*) to examine the NMJ morphology in *gef26* hemizygous (*gef26*^{6}*/Df*) mutants. Synaptic overgrowth phenotype was still shown by 24% increases in normalized number of overall boutons at NMJ 6/7 and also 51% increases at NMJ 4 (Fig 3A-C). Increased formation of satellite boutons were constantly observed in *gef26*^{6}*/Df* by 39% increases at NMJ 6/7 and by 219% increases at NMJ 4 (Fig 3B and 3C). As results, we imply that the loss of function in Gef26 causes NMJ overgrowth.

To verify Gef26 role in synaptic growth regulation, we tested whether *gef26* is required for neuronal function or muscular function by generating a *UAS-gef26* line by allowing *gef26* cDNA to express in wild-type (w^{1118}) background. We then recombined neuronal or muscular expression of *UAS-gef26* in $gef26^{6}/Df$ mutants using a neuronal Gal4 (*C155-GAL4*) or a muscular Gal4 (*BG57-GAL4*). Compared with controls, superfluous populated total boutons and satellite boutons in neuronal expression of *UAS-gef26* in $gef26^{6}/Df$ mutants were rescued to the normal level (Fig 3A-C). However, overgrowth phenotypes of total boutons in muscle expression of *UAS-gef26* in $gef26^{6}/Df$ mutants were failed to rescue the phenotypes (Fig 3A-C). Altogether, these results imply that neuronal function of Gef26 is important for NMJ development.

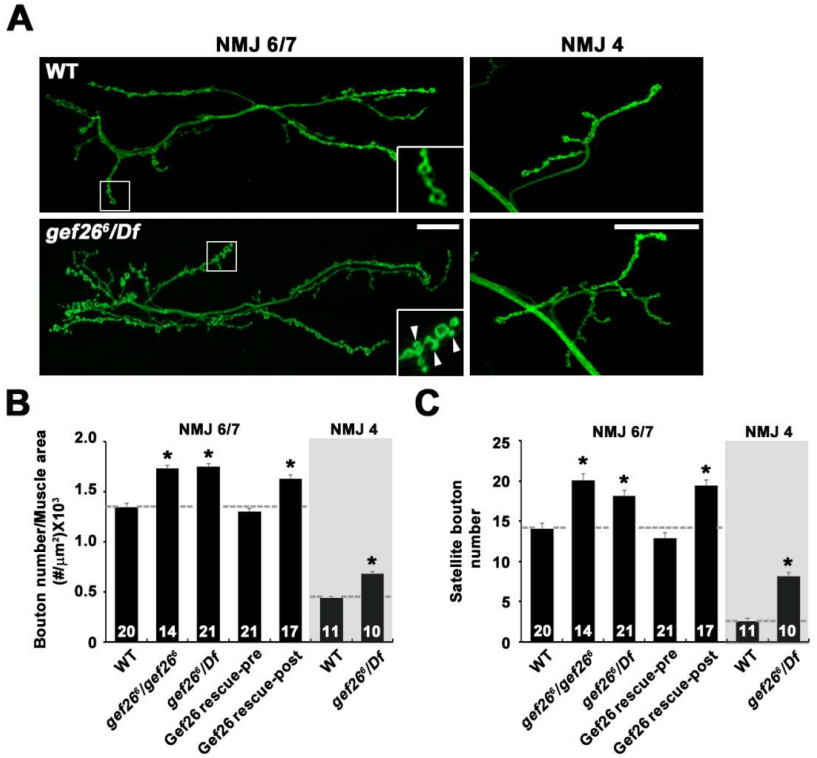

Figure 3. Loss of neuronal function of Gef26 causes NMJ overgrowth with overpruning of satellite boutons
(A) NMJ 6/7 images stained with anti-HRP in wild-type and *gef26*^{6}*/Df* mutants. Overpopulated total boutons with increased satellite boutons were observed in *gef26*^{6}*/Df* mutants compare to the wild-type. Scale bar, 20 μm (NMJ 6/7) and 10 μm (NMJ 4). Note to the satellite bouton (arrowhead). (B) Quantified number of total bouton and satellite bouton in indicated genotypes; wild-type, *gef26*^{6}, *gef26*^{6}*/Df*, *C155-GAL4*/+; *gef26*^{6}*/Df; UAS-gef26*/+ (Gef26 rescue-pre), *BG57-GAL4*/+; *gef26*^{6}*/Df*; *UAS-gef26*/+ (Gef26 rescue-post). (**P*<0.001; error bars denote SEM).

We additionally proved that neuronal knockdown of *gef26* induces synaptic overgrowth by using Gef26 RNA interference (RNAi) line. Neuronal expression of *gef26* dsRNA (*UAS-gef26*^{RNAi}) showed increased bouton number with excessive formation of satellite boutons (Fig 4A and 4B). Unlike the NMJ phenotypes in neuronal-knockdown of *gef26*, the bouton numbers were normal in muscle-knockdown of *gef26* (Fig 4A and 4B).

For further characterization of the satellite bouton in *gef26*^{6}*/Df* mutants, we labeled NMJs with Bruchpilot (NC82) marker and cystein-string protein (CSP) marker to examine the active zone and synaptic vesicles (Fig 4C and 4D). We also examined subsynaptic reticulum (SSR), and glutamate receptor by labeling NMJs with discs-large (Dlg) markers and double-labeling with Bruchpilot (NC82) marker or glutamate receptor IIC (GluRIIC) marker (Fig 4E and 4F). We verified that all of the markers were nicely conserved at the satellite boutons pruned in *gef26*^{6}*/Df* mutants (Fig 4C-F). From the results, we concluded that the satellite boutons observed in *gef26*^{6}*/Df* mutants are all functional synaptic boutons.

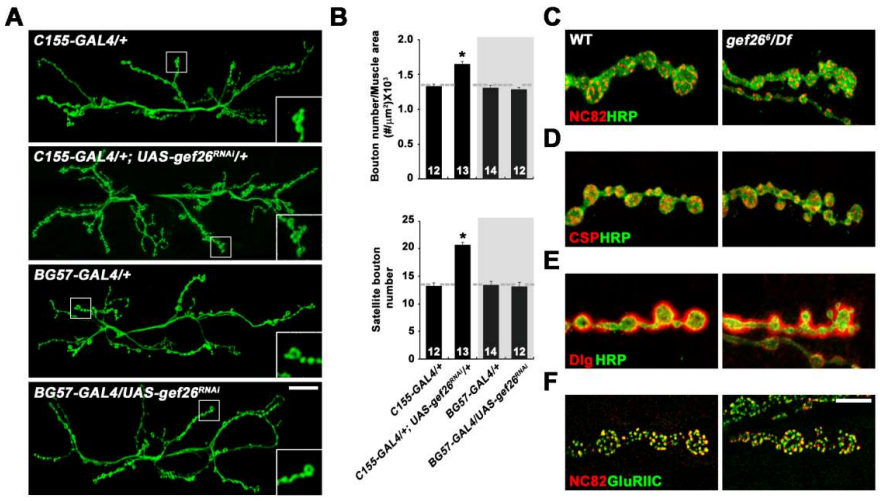

Figure 4. Satellite boutons are functional synaptic boutons in *gef26^{6}/Df* mutants
(A) NMJ 6/7 confocal images stained with anti-HRP in third-instar larvae of each indicated genotypes; *C155-GAL4*/+, *C155-GAL4*/+;; *UAS-gef26^{RNAi}*/+, *BG57-GAL4*/+, and *BG57-GAL4*/*UAS-gef26^{RNAi}*. The third-instar larvae of *C155-GAL4*/+;; *UAS-gef26^{RNAi}*/+ exhibited enhanced number of total boutons with hyperpruned satellite boutons. Scale bar, 20 μm. (B) Quantified number of total bouton and satellite bouton. All samples are compared with neuronal GAL4 and muscular GAL4 control (*P<0.001). (C-F) Characterization of satellite bouton displayed in *gef26^{6}/Df* mutants. NMJ 6/7 images double-labeled with anti-HRP and anti-NC82 (C), anti-CSP (D), or anti-Dlg (E), and double-labeled with anti-NC82 and anti-GluRIIC (F). Scale bar, 20 μm.

3. Gef26 is an upstream molecule of Rap1 to control NMJ growth

Previously, Gef26 is known as a Rap1-specific exchange factor for various developmental processes including wing, and eye development (Vossler et al., 1997; Asha et al., 1999; Singh et al., 2006; Noda et al., 2010). Despite the number of studies to define Gef26/Rap1 function, synaptic function of Gef26 targeting Rap1 was still not known. To define the synaptic role in Gef26 and Rap1, we obtained insertion of minos-element transposon in *rap1* gene (*rap1^{M}*), which is inserted downstream of ATG

starting codon. The *rap1*^{M} mutants showed increased NMJ growth with overpopulated satellite boutons, which are comparable to the *gef26*^{6} mutants (Fig 5A and 5B). To prove, we also examined the phenotypes using two Rap1 RNA interference (RNAi) lines and examine whether same NMJ growth phenotypes of *gef26* knockdown are shown in *rap1* knockdown third-instar larvae. Compared to the wild-type, the NMJ growth was dramatic increased by showing overpopulated synaptic boutons with excessive formation of satellite boutons at the NMJs in neuronal-specific knockdown of Rap1 expression (Fig 5A and 5B). In contrast, NMJ growth in muscular knockdown third-instar larvae of Rap1 expression was not changed (Fig 5A and 5B). These results suggest that Rap1 displayed phenotypic similarity of Gef26 during synapse growth.

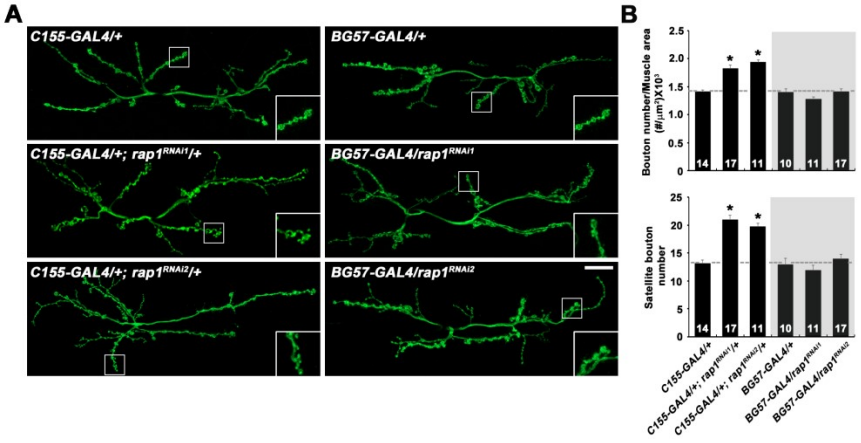

Figure 5. *rap1* mutants show phenotypic similarity of NMJ growth shown in *gef26*^{6}*/Df* mutants

(A-B) Excessive overall boutons and satellite boutons were shown in neuronal knockdown of Rap1 at NMJ. (A) NMJ 6/7 confocal images of neuronal and muscular specific knockdown of Rap1 NMJ. Scale bar, 20 μm. (B) Quantified number of total bouton and satellite bouton in indicated genotypes; *C155-GAL4*/+, *C155-GAL4*/+; *UAS-rap1*^{RNAi1}/+, *C155-GAL4*/+; *UAS-rap1*^{RNAi2}/+, *BG57-GAL4*/+, *BG57-GAL4*/+; *UAS- rap1*^{RNAi1}/+, and *BG57-GAL4*/+; *UAS-rap1*^{RNAi2}/+. All samples are compared with neuronal GAL4 and muscular GAL4 control (**P*<0.001; error bars denote SEM).

To examine the epistatic relationship of *gef26* and *rap1*, we examined NMJ morphology in neuronal expression of constitutively active Rap1-Q63E (*C155-GAL4*/+; *UAS-Myc-rap1*^{CA}/+). Compared to the wild-type, NMJ boutons were reduced by 76% in *C155-GAL4*/+; *UAS-Myc-rap1*^{CA}/+ third-instar larvae, suspecting Rap1 bi-directionally regulates synaptic growth (Fig 6A and 6B). Next, we examined trans-heterozygous interaction of Gef26 and Rap1 to test whether Rap1 mediates Gef26 in a common pathway during synaptic growth adjustment. While heterozygosity for either *gef26* (*gef26*^{6}/+) or *rap1* (*rap1*^{M}/+) show normal growth phenotype, trans-heterozygous mutation of *gef26* and *rap1* (*gef26*^{6}/+; *rap1*^{M}/+) showed overmuch NMJ growth including excessive satellite bouton formation (Fig 6B). This result implies that Rap1 and Gef26 reside in a same pathway for regulation of synaptic growth. To explore functional relationship between the Gef26 and Rap1, we further examined genetic interaction of Gef26 and Rap1. The excessive synaptic growth and satellite boutons seen at the NMJs in *gef26*^{6}/*Df*(*2L*) mutants is suppressed, when Rap1 expression is continuously activated in the *gef26* mutant background (*C155-GAL4*/+; *gef26*^{6}/*Df*; *UAS-Myc-rap1*^{CA}/+) (Fig 6B). From the results, we suspect that Gef26 acts as an upstream molecule of Rap1 for synaptic growth regulation.

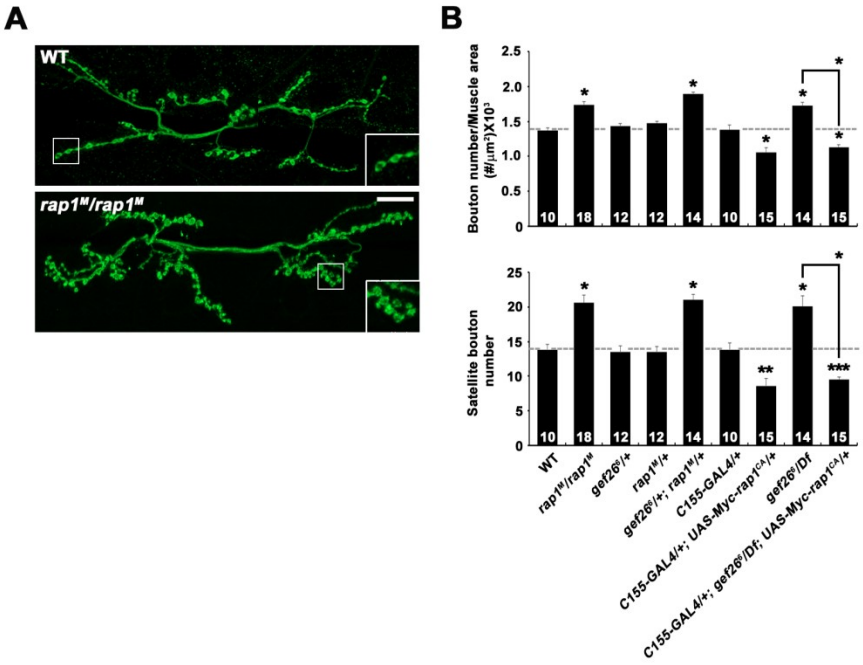

Figure 6. Gef26 acts as an upstream molecule of Rap1 in regulation of NMJ growth
(A) NMJ 6/7 confocal images labeled with anti-HRP. Scale bar, 20 μm. (B) Quantified number of total bouton and satellite bouton in indicated genotypes: wild-type, *rap1*^{M}/*rap1*^{M}, *gef26*^{6}/+, *rap1*^{M}/+, *gef26*^{6}/+; *rap1*^{M}/+, *C155-GAL4*/+, *C155-GAL4*/+; *UAS-Myc-rap1*^{CA}/+, *gef26*^{6}/*Df*, and *C155-GAL4*/+; *gef26*^{6}/*Df*; *UAS-Myc-rap1*^{CA}/+. We used one-way ANOVA and Student's t-test (**P*<0.001; ***P*<0.01; ****P*<0.05; error bars denote SEM).

4. Gef26/Rap1 blocks BMP pathway

BMP retrograde signaling pathway is significant for NMJ development (McCabe et al., 2003). Disruption of BMP signaling at synapse causes ectopic bouton division resulting in excessive satellite bouton formation (Sweeney et al., 2002; Dickman et al., 2006). Formation of satellite boutons shown in *gef26*^{6}/*Df* mutants implies that Gef26 play significant role in regulation of BMP signaling pathway. To prove the possibility, we scrutinized P-Mad levels (a well-known lead out of BMP signaling) in ventral

nerve cord (VNC) and the NMJ (McCabe et al., 2003; O'Connor-Giles et al., 2008; Ball et al., 2010). Compared to controls, the P-Mad accumulation was dramatically enhanced at both locations in *gef26*^{6}*/Df* mutants and *rap1*^{M} mutants, whereas such accumulation was repressed to normal level in neuronal expression of *UAS-gef26* in *gef26*^{6}*/Df* mutants background (Fig 7A and 7B). This illustrates that Gef26/Rap1 inhibits NMJ growth by down-regulation of BMP signaling.

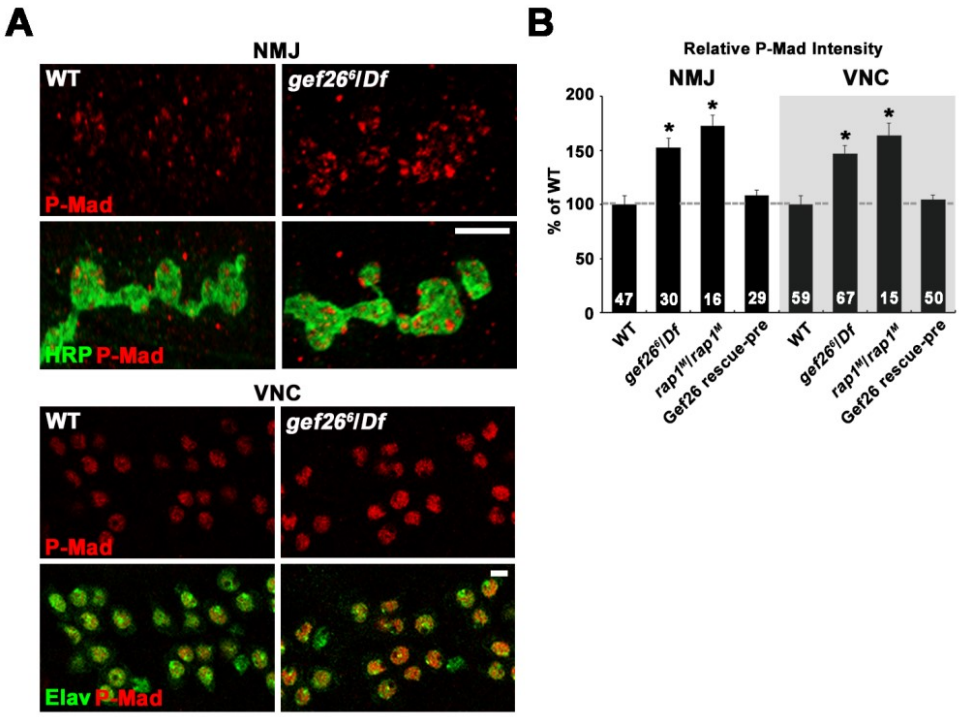

Figure 7. Gef26 regulates synaptic growth via BMP signaling inhibition
(A and B) Gef26 act in negative manner to regulate BMP signaling at synaptic terminal. (A) Images of NMJ 6/7 and VNC in wild-type and *gef26* mutants labeled with anti-pMad and anti-HRP. Scale bar, 20 μm and 5 μm. (B) Bar graphs of normalized pMad intensity to wild-type of indicated genotypes: wild-type, *gef26*^{6}*/Df*, *rap1*^{M}*/rap1*^{M} and *C155-GAL4*/+; *gef26*^{6}*/Df*; *UAS-gef26*/+ (Gef26 rescue-pre). (**P*<0.001; error bars denote SEM).

If NMJ overgrowth shown in the loss of neuronal function in Gef26 or Rap1 is truly affected by enhancement of retrograde BMP signaling, absence of BMP receptor would also display NMJ overgrowth. Previous studies refer that the neuronal expression of dominant-active type-I BMP receptor, thickveins (Tkv) or absence of the I-Smad, Daughters against decapentaplegic (Dad) induce overpopulated synaptic bouton by forming excessive satellite boutons (O'Connor-Giles et al., 2008; Nahm et al., 2013). To find the physical interactions between *gef26*, *rap1* and *tkv*, we genetically recombined *gef26*, *rap1* and *tkv* mutants. Unlike the $gef26^{6}/Df$ mutants, NMJs of heterozygosity for *tkv* ($tkv^{7}/+$) showed moderate synaptic development in wild-type background (Fig 8A and 8B). When single copy of *tkv* is expressed in $gef26^{6}/Df$ mutant background (tkv^{7},$gef26^{6}/+$,*Df*), the synaptic overgrowth in *gef26* mutants are suppressed to the similar range of synaptic growth seen at the NMJs of heterozygosity for *tkv* (Fig 8A and 8B). When both copies of *tkv* is expressed in *gef26* mutant background (tkv^{7},$gef26^{6}/\ tkv^{1}$,*Df*), synaptic growth is restrained to the similar level shown in homozygote mutant of *tkv* (tkv^{1}/tkv^{7}) NMJs (Fig 8A and 8B). Along with the epistasis of *gef26* and *tkv*, we also proved that the synaptic overgrowth in *rap1* mutant ($rap1^{M}/rap1^{M}$) is suppressed to the control level, when single copy of *tkv* are expressed in *rap1* mutant background ($tkv^{7}/+$; $rap1^{M}/rap1^{M}$) (Fig 8A and 8B). Altogether, we confirmed that the BMP signaling is important for Gef26/Rap1 functions during NMJ growth regulation in dose-dependent manner.

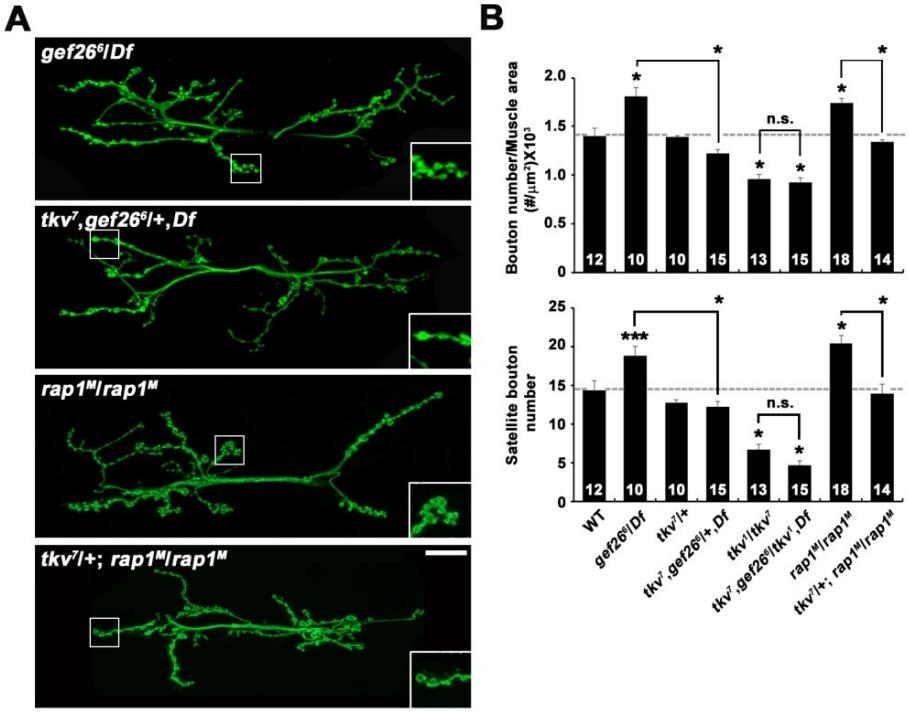

Figure 8. Gef26 restrains BMP signaling by genetically interact with BMP receptor Tkv

(A and B) The NMJ overgrowth in both *gef26* and *rap1* mutants are suppressed by BMP receptor *tkv* mutant. (A) Confocal image showing NMJ 6/7 synapse in genetic recombinants of Gef26, Rap1 and tkv. Scale bar, 20 μm. (B) Analysis of synaptic growth and satellite bouton formation in indicated genotypes: wild-type, $gef26^{6}/Df$, $tkv^{1}/+$, $tkv^{7},gef26^{6}/+,Df$, tkv^{1}/tkv^{7}, tkv^{7}, $gef26^{6}/tkv^{1},Df$, $rap1^{M}/rap1^{M}$, and $tkv^{7}/+$; $rap1^{M}/rap1^{M}$. We used one-way ANOVA and Student's t-test (*P<0.001; **P<0.01; ***P<0.05; n.s., not significant; error bars denote SEM).

To test whether Gef26 and Rap1 play roles in a common pathway with Dad, we examined NMJ growth in transheterozygous interaction of Gef26, Rap1, and Dad. Dad is a BMP inhibitor that negatively regulates BMP signaling (O'Connor-Giles et al., 2008). Compared to the wild-type, the NMJ growth in heterozygosity of *gef26* ($gef26^{6}/+$), *rap1* ($rap1^{M}/+$), or *dad* ($dad^{J1E4}/+$) third-instar larvae were normal (Fig 9A

and 9B). Unlike the heterozygosity of *gef26*, *rap1,* or *dad*, transheterozygotes of *gef26* and *dad* (*gef26*^{6}/+; *dad*^{J1E4}/+), or *rap1* and *dad* (*rap1*^{M}/+; *dad*^{J1E4}/+) third-instar larvae showed overpopulated synaptic boutons with excessive satellite boutons (Fig 9A and 9B). Hence, these results indicate that Gef26/Rap1 act in negative manner to regulate BMP signaling.

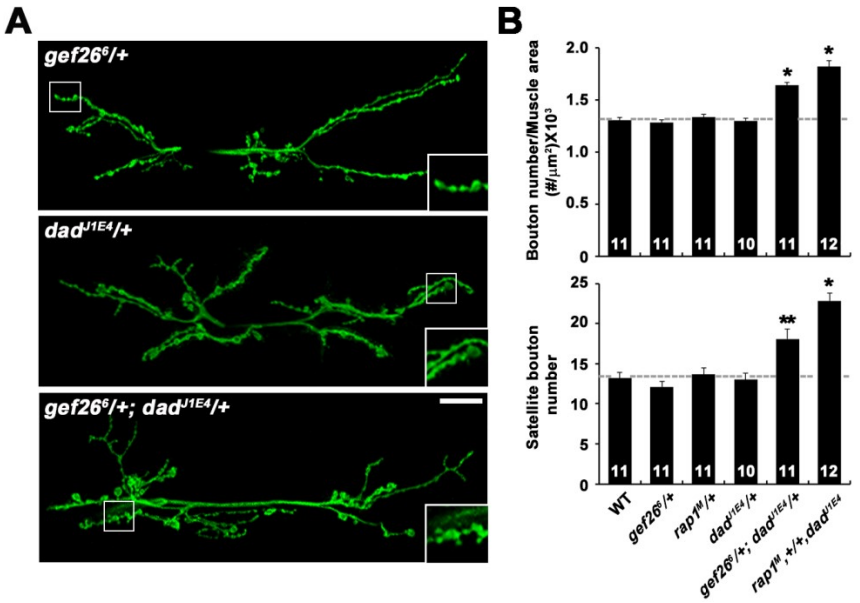

Figure 9. Gef26 mimics the role of Dad, a negative BMP regulator
(A and B) The overpopulated synaptic boutons with satellite boutons were observed in transheterozygous interaction of *gef26* and *dad*, or *rap1* and *dad* mutants. (A) Confocal images of *gef26*^{6}/+, *dad*^{J1e4}/+, and *gef26*^{6}/+; *dad*^{J1e4}/+. Scale bar, 20 μm. (B) Quantification of boutons and the satellite bouton of following genotypes: wild-type, *gef26*^{6}/+, *rap1*^{M}/+, *dad*^{J1e4}/+, *gef26*^{6}/+; *dad*^{J1e4}/+, and *rap1*^{M}/+; *dad*^{J1e4}/+. (**P*<0.001; ***P*<0.01; error bars denote SEM).

5. Gef26/Rap1 modulates synaptic growth by controlling *dfmr1* transcriptional level

The BMP signaling is significant for synaptic growth by regulating *Drosophila fmr1* (*dfmr1*), which is a Futsch repressor (Nahm et al., 2013). The *Drosophila* futsch also called as a MAP1B-like protein is a well-known regulator for maintenance of microtubule stability (Zhang et al., 2001; Lee et al., 2009; Nahm et al., 2013). For the reason, we suspect that Gef26/Rap1 might regulate microtubule (MT) stability by affecting dFMRP and MAP1B passing through BMP signaling pathway. To prove the hypothesis, we analyzed whether dFMRP is affected by Gef26/Rap1 by examining physical interaction between *dfmr1*, *gef26* and *rap1* at the NMJ terminal. Unlike control, the number of synaptic boutons were normal with average formed satellite boutons at the NMJs in the heterozygosity of *gef26* (*gef26*^{6}/+), *dfmr1* (*fmr1*$^{\Delta 50M}$/+) or *rap1* (*rap1*^{M}/+) third-instar larvae (Fig 10A and 10B). However, the number of synaptic boutons were significantly increased with excessive satellite boutons at the NMJs in the transheterozygotes of *gef26* and *dfmr1* (*gef26*^{6}/+; *fmr1*$^{\Delta 50M}$/+), and the transheterozygotes of *rap1* and *dfmr1* (*rap1*^{M},+/+, *fmr1*$^{\Delta 50M}$) third-instar larvae (Fig 8A and 8B). For further examination, we directly speculated expression level of *dfmr1* mRNA in third-instar larvae brain of the *gef26* and *rap1* mutants by conducting immunoprecipitation analysis by RT-PCR. The *dfmr1* mRNA level was significantly reduced in *gef26* and *rap1* mutants in comparison with the levels in wild-type controls (data now shown). We also obtained parallel results of the *dfmr1* mRNA level in *gef26* and *rap1* mutants by using quantitative real-time PCR (Fig 10C). These results imply

that Gef26/Rap1 suppresses synaptic growth by affecting transcriptional level of *dFMR1* via BMP signaling.

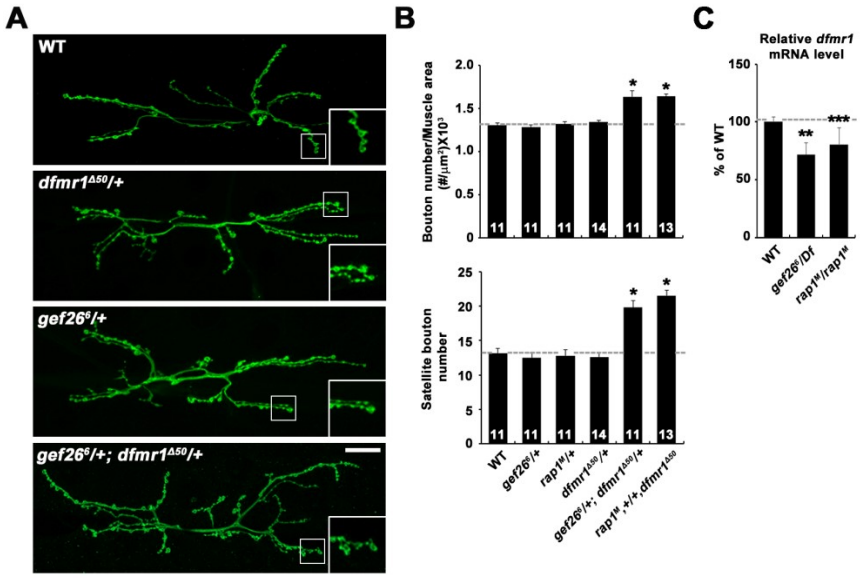

Figure 10. Gef26/Rap1 regulates transcription level of *dfmr1*
(A-C) Gef26/Rap1 genetically interacts with dfmr1 to control synaptic structure at the NMJ. (A) Images of NMJ 6/7 synapses labeled with anti-HRP. Scale bar, 20 μm. (B) Quantified number of total bouton and satellite bouton in indicated genotypes: wild-type, $gef26^{6}$/+, $rap1^{M}$/+, $fmr1^{\Delta 50M}$/+, $gef26^{6}$/+; $fmr1^{\Delta 50M}$/+, and $rap1^{M}$,+/+, $fmr1^{\Delta 50M}$. (C) Transcription of fmr1 was analyzed by quantitative PCR. Compare to the wild-type control, mRNA level of *fmr1* were reduced in *gef26* and *rap1* mutants. (*P<0.001; **P<0.01; ***P<0.05; error bars denote SEM).

6. Gef26/Rap1 acts on microtubule stability in Futsch-dependently

Translational level of Futsch is critical for synaptic bouton budding, and synaptic microtubule organization (Roos et al., 2000; Wan et al., 2000; Zhang et al., 2001; Pennetta et al., 2002). To examine the integrity of synaptic microtubule cytoskeleton structures at the NMJ terminals in *gef26* and *rap1* mutants, we visualized synaptic

microtubule at the NMJs labeled with Futsch (22C10) marker. The Futsch immunoreactivity was noticeably enhanced at the NMJ terminal in *gef26* and *rap1* mutants, compare to the wild-type (Fig 11A and 11B). Interestingly, loop-like structures, which are formed at nerve terminals, were increased in *gef26* and *rap1* mutants (data not shown). These results indicate that Gef26/Rap1 modulates microtubule stability.

Formation of loop structures is correlated with enhanced microtubule stability (Dent et al., 1999; Roos et al., 2000; Schober et al., 2007; Mosca et al., 2012; Nechipurenko et al., 2012). To characterize microtubule loop structure in *gef26* and *rap1* mutants, we applied pharmacological treatment at the mutant flies by feeding microtubule-destabilizing drug vinblastine (1 μM) followed by protocol (Nahm et al. 2013). Unlike the wild-type, the *gef26* and *rap1* mutants exhibited thicker synaptic branches with synaptic overgrown morphology without the vinblastine treatment (Fig 11C and 11D). With the presence of 1 μM vinblastine, outgrowth of synaptic boutons and thicker branches were restored to the average thickness of branches with normal synaptic bouton formation (Fig 11C and 11D). Altogether, these results imply that Gef26/Rap1 is involved in microtubule stability to regulate synaptic growth via BMP signaling pathway.

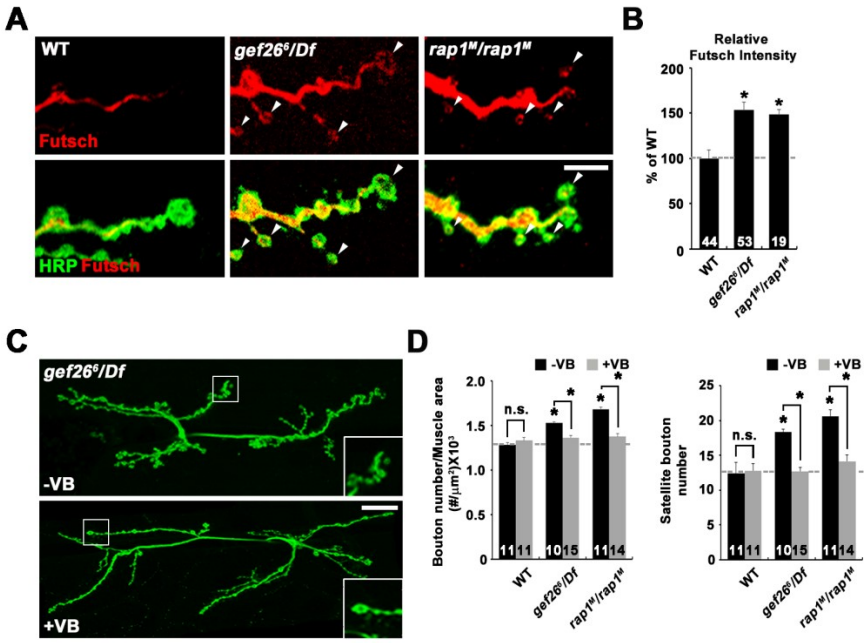

Figure 11. Gef26/Rap1 controls microtubule stabilization
(A-C) Defected synaptic morphology and microtubule cytoskeleton organization are displayed in *gef26* and *rap1* mutants. (A) NMJ 6/7 confocal images in wild-type, *gef26* and *rap1* mutants labeled with anti-Futsch and anti-HRP. Scale bar, 5 μm. Note to the excessive microtubule loops by arrowheads. (B) Bar graphs of normalized Futsch intensity in following genotypes: wild-type, $gef26^{6}/Df$, and $rap1^{M}/rap1^{M}$. (C and D) Altered microtubule structure and overpopulated synaptic boutons by forming excessive satellite boutons are rescued by the Vinblastine (VB) treatment in *gef26* and *rap1* mutants. (C) NMJs 6/7 confocal images in *gef26* mutants labeled with anti-HRP. Scale bar, 20 μm. (D) Quantified number of total bouton and satellite bouton in indicated genotypes; wild-type, $gef26^{6}/Df$, and $rap1^{M}/rap1^{M}$. All samples are compared with wild-type (*P<0.001; n.s., not significant; error bars denote SEM).

7. Gef26 restrains BMP signaling by controlling BMP receptor internalization

Since abnormal microtubule architecture, and increased number of satellite bouton were found in previously reported endocytic mutants e.g., *dap160*, *endophilin A*, and *nwk* (Koh et al., 2004; O;Connor et al., 2008; Nahm et al., 2013), Gef26 was suspected to participate in the process of BMP receptor endocytosis. To prove the

possibility, we first observed NMJ growth phenotype of transheterozygous interaction between *gef26*, *endophilin A* (*endoA*), *dap160*, and *nwk* mutants. Compared to the heterozygotes of *gef26* (*gef26*^{6}/+), *endophilin A* (*endoA*$^{\Delta 4}$/+), *dap160* (*dap160*$^{\Delta 1}$/+), or *nwk* (*nwk*^{2}/+) third-instar larvae, the overpopulated synaptic boutons and satellite boutons were observed at the NMJ in transheterozygotes of *gef26* and *endophilin A* (*gef26*^{6}/+; *endoA*$^{\Delta 4}$/+), or *gef26* and *dap160* (*gef26*^{6}/*dap160* $^{\Delta 1}$) third-instar larvae, recapitulating the phenotype observed in *gef26* mutants (Fig 12A and 12B). In contrast, synaptic boutons and satellite boutons were not altered at the NMJ in transheterozygotes of *gef26* and *nwk* (*gef26*^{6}/+; *nwk*^{2}/+) third-instar larvae (Fig 12A and 12B). These results indicate that Gef26 regulates synaptic growth through BMP-dependent pathway, which are parallel to the Nwk pathway.

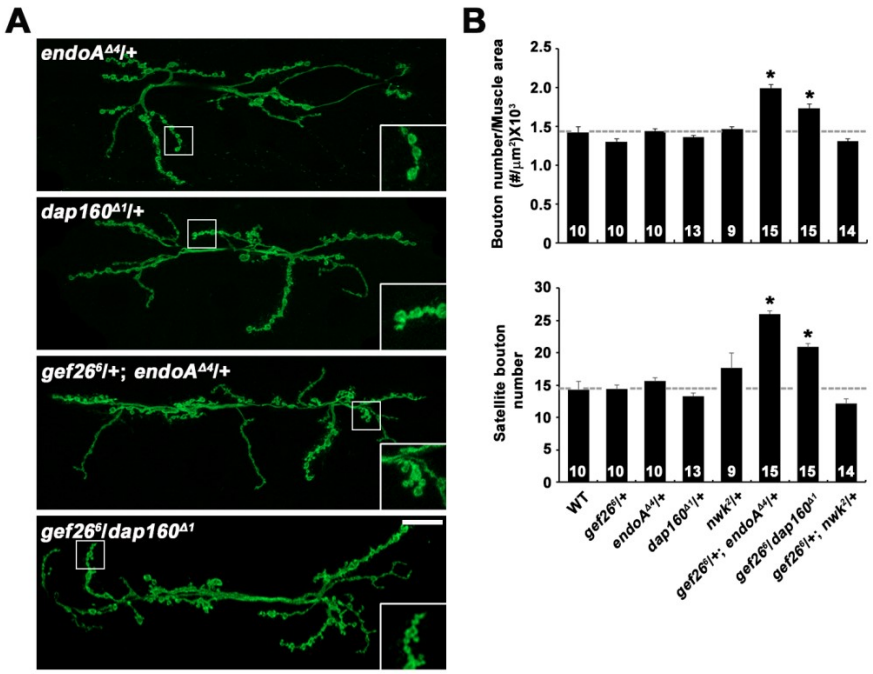

Figure 12. Gef26 genetically interacts with endocytic components
(A) NMJ 6/7 confocal images in *endoA*, *dap160*, $gef26^{6}$/+; $endoA^{\Delta 4}$/+ and $gef26^{6}/dap160^{\Delta 1}$ third-instar larvae. Scale bar, 20 μm. (B) Quantified number of total and satellite bouton in indicated genotypes: wild-type, $gef26^{6}$/+, $endoA^{\Delta 4}$/+, $dap160^{\Delta 1}$/+, nwk^{2}/+, $gef26^{6}$/+; $endoA^{\Delta 4}$/+, $gef26^{6}/dap160^{\Delta 1}$ and $gef26^{6}$/+; nwk^{2}/+. (*P<0.001; error bars denote SEM).

From the previous study, Gef26 is known to localize at plasma membrane (Gloerich et al., 2012; Consonni et al., 2014), therefore, we hypothesized that Gef26 might physically involve in BMP receptor endocytosis by regulating BMP signaling. To prove the hypothesis, we first confirmed that Gef26 is localized at plasma membrane at NMJ of flies, which are generated to carry a transgene of HA-Gef26 (Fig 13).

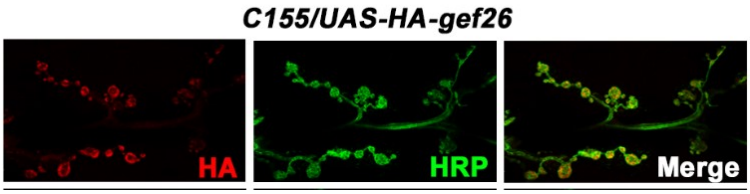

Figure 13. The presynaptic Gef26 is localized at plasma membrane
NMJ 6/7 images from third-instar larvae expressing UAS-HA-Gef26. Scale bar, 20 μm.

Next, we investigated whether Gef26 modulates BMP receptor internalization from plasma membrane by performing internalization assay in *Drosophila* neuronal (BG2-c2) cells expressing *pAc-Myc-tkv-Flag* or *pAc-Myc-wit-Flag* and *gef26* dsRNA. After 5 hr cycloheximide treatment for protein synthesis inhibition, we labeled surface *tkv* or *wit* with anti-Myc antibody, and allowed 10 min internalization using conditioned media. After acid washing, total level of *tkv* or *wit* was labeled with anti-

Flag antibody. Compared to the mock treated cells, internalized *tkv* or *wit* from surface area was reduced in cells expressing *gef26* dsRNA (Fig 14A-C). Rather internalized, most of the *tkv* or *wit* was accumulated at surface area in *gef26*-knockdown cells, suggesting that Gef26 is indispensable for the internalization of BMP receptors.

We additionally determined the impact of *gef26* loss-of-function on the level of surface Tkv at the NMJ. To do this, we generated flies expressing *UAS-Myc-tkv* in w^{1118} or *gef26* mutant background using *C155-GAL4* driver. Surface expression of Myc-Tkv was examined by stained with anti-Myc and anti-HRP antibodies, respectively. The ratio of Myc-Tkv to HRP signal from outside of 2.5 μm perimeter from HRP-labeled was importantly increased, while the ratio of Myc-Tkv to HRP signal from 0.5 μm of HRP-labeled was decreased in NMJs of *gef26* mutant background, compared with NMJs of wild-type (Fig 14D and 14E). We also examined level of endogenous Tkv through western blotting analysis using anti-Myc antibody, which label ectopically expressed Tkv in VNC of *C155-GAL4*/+; *UAS-Myc-tkv*/+ and *C155-GAL4*/+; $gef26^{6}$/*Df*; *UAS-Myc-tkv*/+ larvae. Endogenous Tkv level were consistent in *gef26* mutant background with the control, which indicates Gef26 is involved in regulation of Tkv receptor internalization (Fig 14F and 14G).

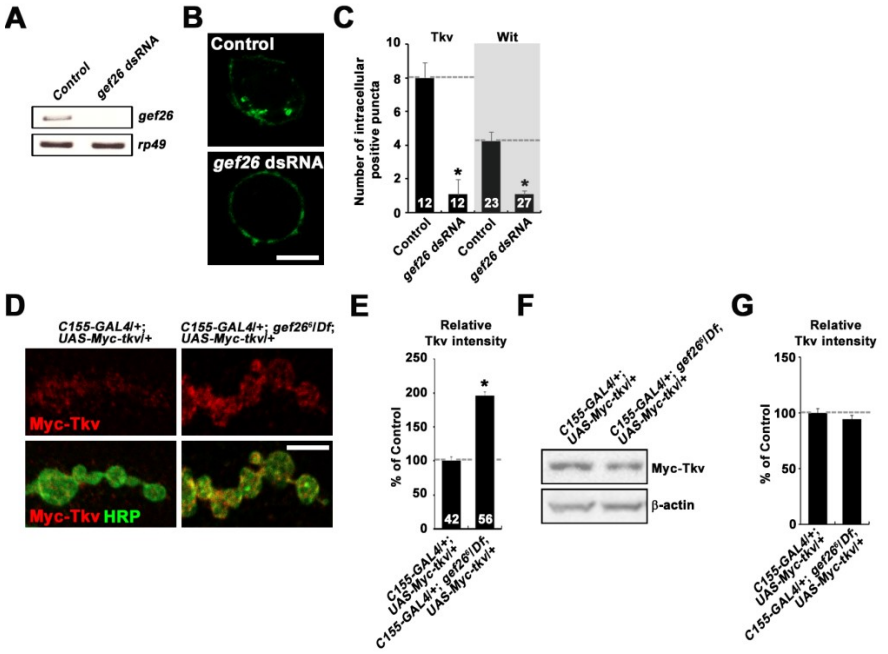

Figure 14. Gef26 regulates internalization of surface resided BMP receptors
(A-C) Gef26 is essential for endocytic internalization of BMPR. BG2-c2 cells were expressed with *pAc-Myc-tkv-Flag* or *pAc-Myc-Wit-Flag* in control or *gef26* dsRNA. Live control and Gef26-depleted cells were pre-labeled with anti-Myc (green) at 4°C and incubated at 25°C for 10 min to allow the internalization of the labeled surface receptors. Acidic wash was allowed for 15 min to remove pre-labeled surface receptors. (A) Reverse transcription (RT)-PCR analysis to confirm knockdown efficiency of Gef26. (B) Single confocal sections through the middle of control and *gef26*-knockdown cells are shown for the green channel only. Scale bar, 5 μm. (C) Quantification of the number of intracellular Myc-positive puncta per cell. Only cells with similar Flag signal (red) intensities were analyzed. (D and E) Levels of surface Tkv are increased at the NMJ of *gef26* mutants. (D) Images of NMJs 6/7 in *C155-GAL4*/+; *UAS-Myc-tkv*/+ and *C155-GAL4*/+; *gef26*^{6}*/Df*; *UAS-Myc-tkv*/+ third-instar larvae. NMJ preparations were sequentially stained with anti-Myc (red) and anti-HRP (green) under nonpermeant and permeant conditions. Scale bar, 5 μm. (E) Quantified ratio of surface Myc-Tkv to HRP intensity (**P* <0.001). (F and G) Total protein level of Tkv is constant in CNS extracted from *gef26* mutants with control larvae. (F) Western blot probe of central nerve system (CNS) obtained from the third-instar larvae using anti-Myc and anti-β-actin. (G) Western blot analysis was done by quantifying level of anti-Myc. β-actin was used as an internal control.

Finally, we examined whether Gef26 acts on synaptic vesicle endocytosis by stimulating NMJs with 90 mM K^+ and allowing 1 min FM1-43FX dye loading. Compared with wild-type controls, dye uptake was consistent in *gef26*^{6}*/Df* mutants (Fig. 15A and 15B). These results imply that Gef26 does not act in synaptic vesicle endocytosis at NMJs.

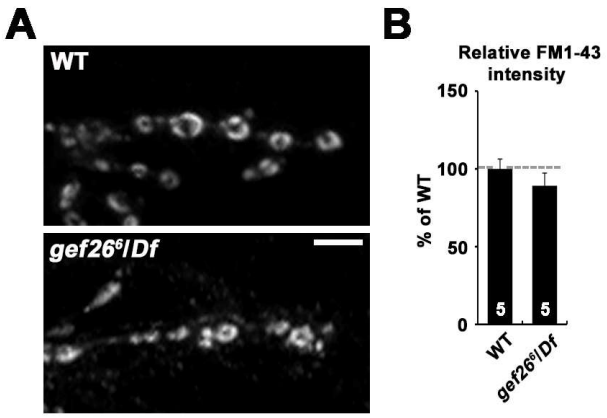

Figure 15. Synaptic vesicle endocytosis was normal at the NMJ in *gef26*^{6}*/Df* mutants
(A) NMJ 6/7 confocal images in wild-type and *gef26*^{6}*/Df* third-instar larvae, which are labeled with FM1-43FX dye after 90 mM K^+ in 5 mM Ca^{2+} stimulation. Scale bar, 20 μm. (B) Quantification of average FM1-43FX dye labeling of *gef26*^{6}*/Df* to wild-type.

8. Neuronal-knockdown of *gef26* expression in flies show shorten lifespan, age-dependent locomotor dysfunction and neuronal cell death

To find whether Gef26 affects neuronal survivals, we investigated the behavior of motor ability and survivorship in adult flies. Since *gef26* mutants are semi-lethal in adult stage, we used UAS-GAL4 system. The lifespan is progressively declined in neuronal knockdown of *gef26* flies (*C155-GAL4*/+; *UAS-gef26*^{RNAi}/+), compared to the

controls, while the lifespan in heterozygotes of *gef26* (*gef26*^{6}/+) is not changed (Fig 16A). We also performed locomotor assay using 2, 10, 20, 30, and 40-days-aged flies. In neuronal knockdown of *gef26* flies, severe locomotor dysfunction was observed (Fig 16B).

We next investigated neuropathological phenotype of Gef26 by performing histologic sections of 2, 10, 20, 30 and 40 days aged fly brains of Gef26 and staining with hematoxyline and eosin (H&E) to measure brain vacuoles, which is a hallmark of neurodegeneration in *Drosophila*. The neuronal knockdown of *gef26* flies showed increases of vacuoles age progressively, when *gef26* heterozygous shows the normal (Fig 16C and 16D).

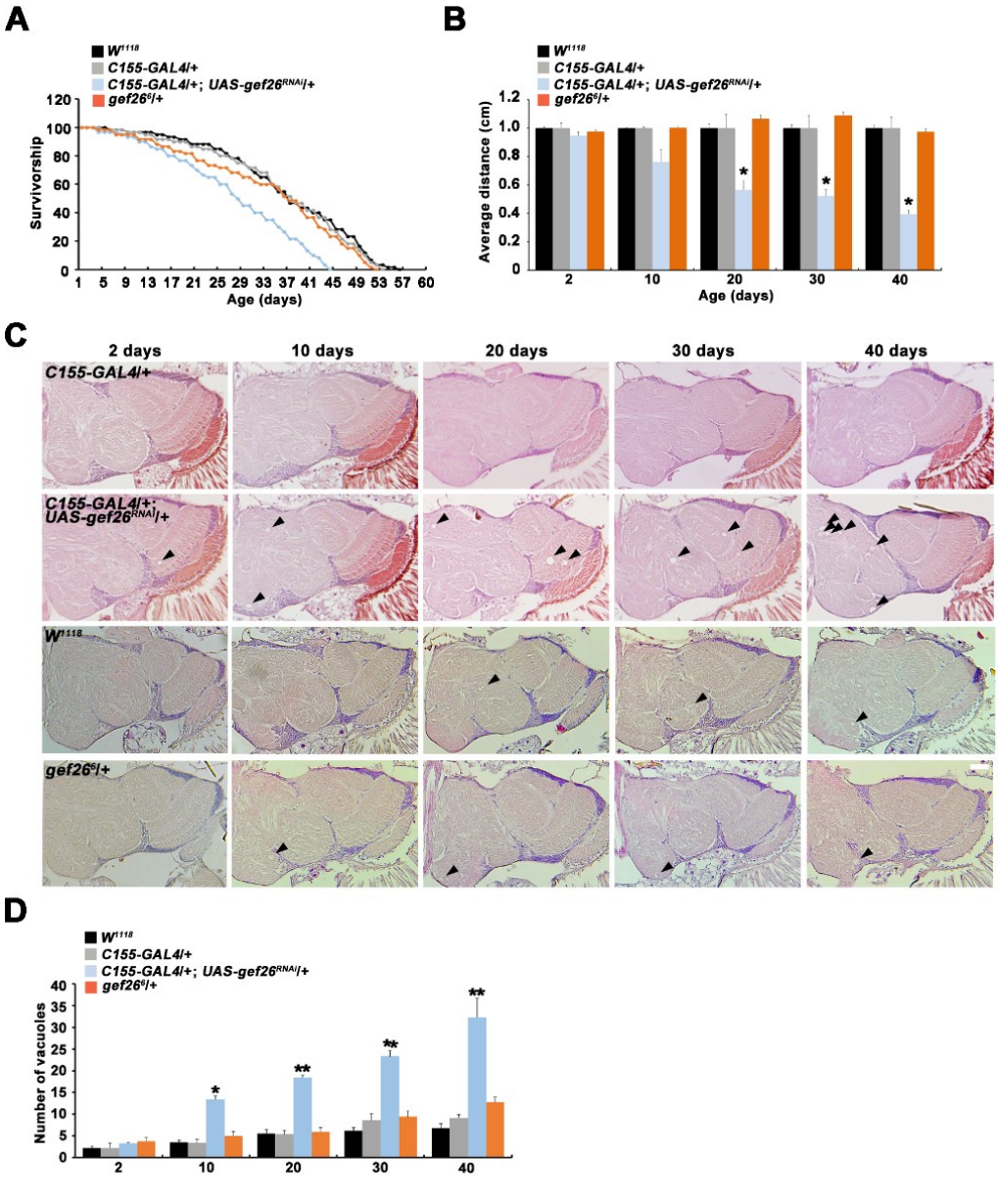
A
W1118
C155-GAL4/+
C155-GAL4/+; UAS-gef26RNAi/+
gef26e/+
Survivorship
Age (days)
B
Average distance (cm)
Age (days)
C
2 days
10 days
20 days
30 days
40 days
C155-GAL4/+
C155-GAL4/+; UAS-gef26RNAi/+
W1118
gef26e/+
D
Number of vacuoles

Figure 16. Neuronal-knockdown of *gef26* expression in flies show shorten lifespan, progressive motor dysfunction and neuronal degeneration
(A) Shorten life span was observed in *gef26*-knockdown flies compare to the wild-type. The genotypes were wild-type, *C155-GAL4*/+, $gef26^{6}$/+, and *C155-GAL4*/+; $UAS\text{-}gef26^{RNAi}$/+. (B) Climbing assay in a vertical graduated cylinder using 2, 10, 20, 30, 40-days-aged flies of indicated genotypes: *C155-GAL4*/+, *C155-GAL4*/+; $UAS\text{-}gef26^{RNAi}$/+. Defected locomotor ability was initially observed in 10-days-aged *gef26*-knockdowned flies (*C155-GAL4*/+; $UAS\text{-}gef26^{RNAi}$/+). Heterozygotes of *gef26* ($gef26^{6}$/+) was not defected. Sample size, n<60 per genotype. (C and D) Neurodegeneration were dramatically occurred in aged-*gef26*-knockdown flies (*C155-GAL4*/+; $UAS\text{-}gef26^{RNAi}$/+). (C) Images of H&E-stained frontal brain sections (5 μm) of 20-days-aged flies. Note to the vacuoles (>5 μm) as arrowheads. Scale bar, 20 μm. (D) Quantification of brain vacuolization (diameter <5 μm) in fly brain of following genotypes: wild-type, *C155-GAL4*/+, $gef26^{6}$/+, and *C155-GAL4*/+; $UAS\text{-}gef26^{RNAi}$/+. (*P<0.001; **P<0.01, error bars denote SEM).

To test whether the motor dysfunction and the neurodegeneration in *gef26*-knockdown flies are due to apoptotic cell death, we performed TUNEL assay in fly brains of *C155-GAL4*/+; $UAS\text{-}gef26^{RNAi}$/+. The TUNEL-positive cells are clearly labeled in positive control, which is treated with DNase I (Fig 17A). In *gef26 C155-GAL4*/+; $UAS\text{-}gef26^{RNAi}$/+ flies, severely increases of TUNEL-positive cells were observed in age-dependent manner, unlike the controls (Fig 17B and 17C).

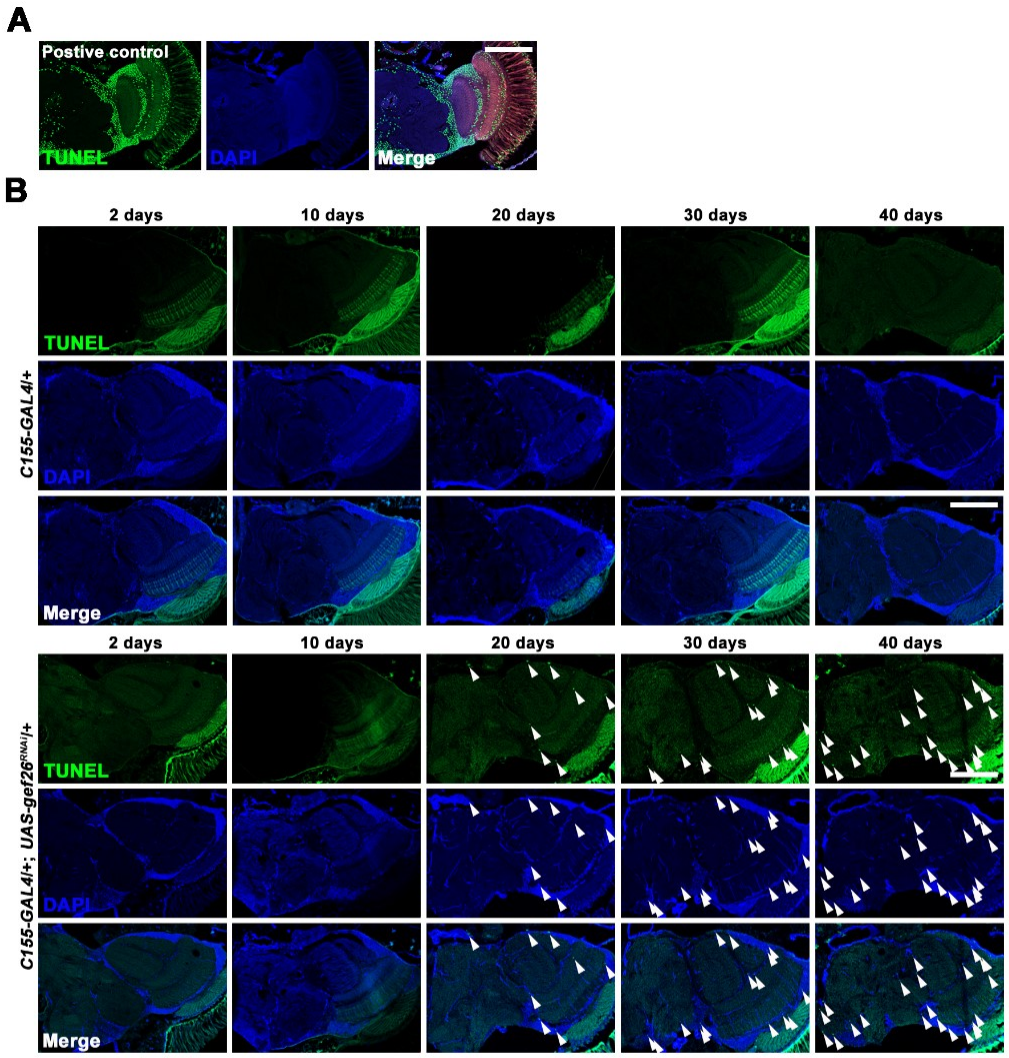
A
Postive control
TUNEL
DAPI
Merge
B
2 days
10 days
20 days
30 days
40 days
TUNEL
DAPI
Merge
C155-GAL4/+
C155-GAL4/+; UAS-gef26RNAi/+
C
C155-GAL4/+
C155-GAL4/+; UAS-gef26RNAi/+
Number of TUNEL positive cells
Age (days)
0
10
20
30
40
50
60
2
10
20
30
40
*

Figure 17. Apoptotic cell death was age-dependently increased in transgenic flies expressing dsRNA of *gef26*

(A) Positive control for TUNEL assay to test TUNEL reaction. (B and C) TUNEL-positive-cells analysis in three consecutive section from middle brain of *C155-GAL4*/+ and *C155-GAL4*/+; *UAS-gef26*^{RNAi}/+ flies. Scale bars, 20 μm. (B) TUNEL-labeled images from brain sections (5 μm). (C) TUNEL-positive cells in brain of *C155-GAL4*/+; *UAS-gef26*^{RNAi}/+ flies were induced age progressively compared with the *C155-GAL4*/+ flies. The sample size, n = 4 animals. All comparisons are with control (*P <0.001).

To characterize the apoptotic cell death, I performed caspase-3 staining assay. I stained fly brains of *C155-GAL4*/+; *UAS-gef26*^{RNAi}/+ flies with anti-caspase-3 (program cell death marker) and anti-Elav (neuronal marker) or with anti-Repo (glia marker) at 20-days-aged. The anti-caspase-3 signals were co-localized with anti-Elav, and not co-localized with anti-Repo in *C155-GAL4*/+; *UAS-gef26*^{RNAi}/+ fly brains (Fig 18A). I was unable to detect significant anti-caspase-3 signals in control fly brain (Fig 18A). As result, I concluded that the brain vacuolization shown in *C155-GAL4*/+; *UAS-gef26*^{RNAi}/+ flies were due to the neuronal cell death. Taken together, we concluded that Gef26 regulates not only NMJ growth, but also brain degeneration.

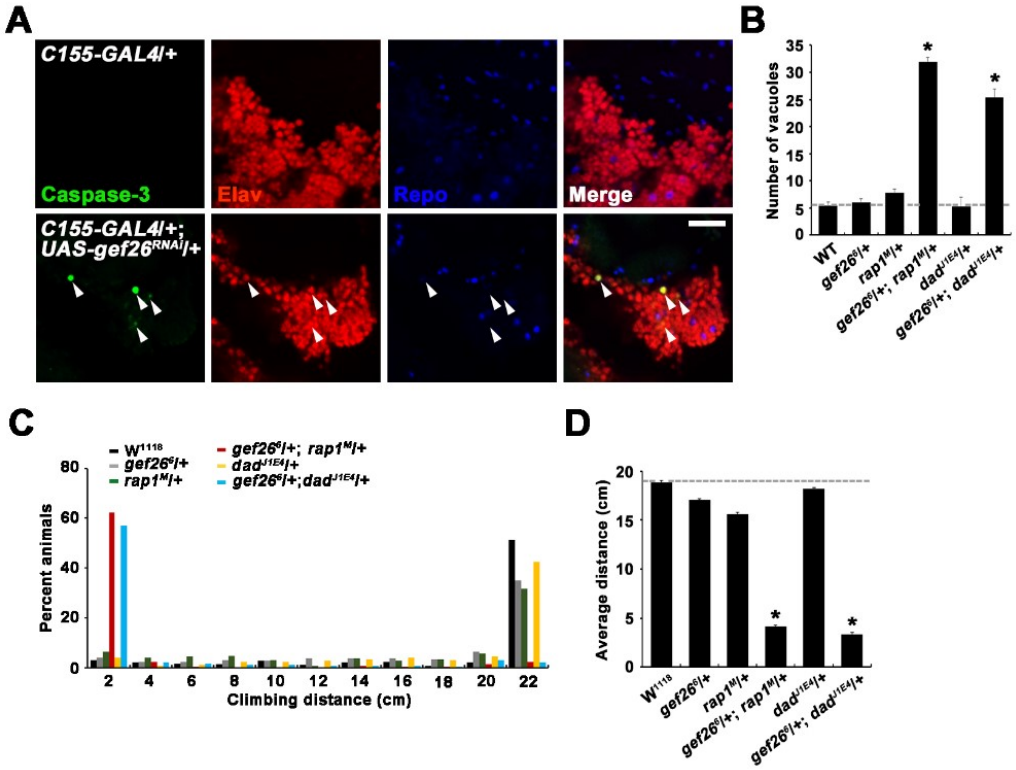

Figure 18. Neurodegeneration and motor dysfunction were observed in transheterozygous of *gef26* and *rap1* or *dad* flies

(A) Confocal images of 20-days-aged brain in *C155-GAL4*/+ and *C155-GAL4*/+; *UAS-gef26*^{RNAi}/+ flies stained with anti-caspase-3 either with anti-Elav or anti-Repo. Scale bar, 20 μm. (B) Quantification of brain vacuolization (diameter < 5 μm) in 20-days-aged fly brain of following genotypes: w^{1118}, *gef26*^{6}/+, *rap1*^{M}/+, *gef26*^{6}/+; *rap1*^{M}/+, *dad*^{J1E4}/+, *gef26*^{6}/+; *dad*^{J1E4}/+. All comparisons are made with w^{1118} (*P<0.001; error bars denote SEM). (C and D) Climbing assay in a vertical graduated cylinder using flies of indicated genotypes: w^{1118}, *gef26*^{6}/+, *rap1*^{M}/+, *gef26*^{6}/+;*rap1*^{M}/+, *dad*^{J1E4}/+, *gef26*^{6}/+; *dad*^{J1E4}/+. Locomotor activity was severely defected in 20-days-aged *gef26* and *rap1* or *dad* transheterozygous. (C) Distribution of distance climbed of each genotypes at 20-days-aged at 30 s period. (D) Locomotor activities were reduced in transheterozygous interactions of Gef26 and Rap1 or Dad. Sample size, n<50 per each genotype. All comparisons are made with w^{1118} (*P <0.001; error bars denote SEM).

To study whether these neuropathological phenotypes shown in *C155-GAL4*/+;; *UAS-gef26*^{RNAi}/+ flies was relevant to BMP signaling, brain vacuoles and

locomotor behavior were further quantified in genetic interaction of Gef26 and Rap1 or Dad. The massive vacuoles were examined in fly brains at 20-days-aged of *gef26*^{6}/+; *rap1*^{M}/+ and *gef26*^{6}/+; *dad*^{J1E4}/+ flies (Fig 18B). Also, the 20-days-aged of *gef26*^{6}/+; *rap1*^{M}/+ and *gef26*^{6}/+; *dad*^{J1E4}/+ flies showed motor dysfunction, compared to the control flies (Fig 18C and 18D). Altogether, the results imply that the age-dependently occurring motor dysfunction or neurodegeneration in *gef26* mutant is correlated with over-activation of BMP signaling.

V. Discussion

This study suggests that Gef26 regulates microtubule stability via BMP signaling for controlling synaptic growth. When the Gef26 function is absence, synapses are overgrown with formation of “satellite” boutons, which characterize as small boutons protruding from a main synaptic terminal, at the NMJ. Enhancement of satellite bouton suspects us to investigate Gef26 function related to BMP signaling. To study, genetic interaction with Gef26 and BMP components were executed through immunocytological analysis. From the study, Gef26 reveals to suppress P-Mad level by acting as an upstream molecule of Rap1 at the NMJ. In addition, the accumulation of BMP receptors at cell surface area in depletion of *gef26* cells suggests that Gef26 controls internalization of surface resided BMP receptors. As results, this research claims that Gef26 is a new regulator of synaptic growth via BMP signaling.

In addition, this study proved that Gef26 regulates microtubule stability by suppressing Futsch level via BMP signaling. The study further discovered that Gef26 regulates neuronal survival by clearly showing age progressively shortens survivorship, motor dysfunction and neuronal degeneration in neuronal knockdown of Gef26 flies. We also confirmed that loss of Gef26 induces age-dependent neuronal cell death. Therefore, this study suggests that Gef26 governs NMJ growth and neurodegeneration by controlling stability of microtubule through BMP signaling pathway (Fig 19).

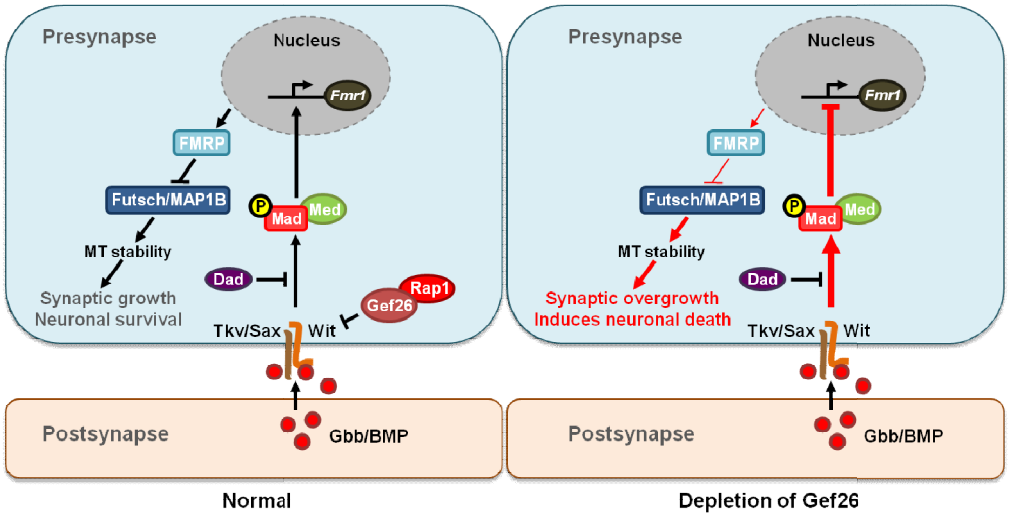

Figure 19. Loss of Gef26 causes NMJ overgrowth and microtubule over-stabilization by over-activating BMP signaling, which induces neuronal cell death
In normal condition, presynaptic Gef26 control NMJ growth and microtubule stability through inhibiting BMP pathway at the NMJ. When the presynaptic Gef26 is absent, the NMJ overgrows by over-activation of BMP signaling through accumulation of BMP receptors at cellular surface, and increases of P-Mad level, and over-stabilization of microtubules. These consequential effects further induce neuronal cell death.

How does Gef26 control microtubule stability via BMP signaling?

The P-Mad, which is a BMP key mediator, was accumulated at motor neuron nuclei in ventral nerve cord and synaptic terminal of *gef26* mutants. Previously, synaptic role of P-Mad was to modulate BMP targeted genes, whereas nuclear P-Mad possesses regulatory role of synaptic growth (Serpe et al., 2016). In order to regulate synaptic growth, the BMP pathway activated at synapses needs to be transported to the nucleus passing through the long projection of axons and initiates transcriptional regulators, such as *Trio*, or *Fmr1*. Hence, understanding the mechanism of microtubule-dependent transports of BMP-related components in axons need to be clarified. To understand,

mechanisms of motor proteins, which move bi-directionally on stable microtubules and correlated with the BMP signaling, need to be studied. In fact, a motor MAP, Khc-73, is documented to control nuclear P-Mad level (Liao et al., 2018). Therefore, investigation of Gef26 role correlated with the action of motor proteins, which could control regulatory switch of BMP targeted genes based on the stable microtubule in axons, might be interesting for the future studies.

Neurological disease pathogenesis: regulation of microtubule stability via BMP signaling

Impairment in regulation of microtubule stability has been reported as an important pathogenesis of neurological diseases, such as HSP and ALS (LaMonte et al., 2002; Aggad et al., 2014). In particular, malfunction of HSP-causative gene, Spartin, has been documented to cause neuronal cell death by blocking BMP signaling and microtubule stability (Nahm et al., 2013). Our data supports the previous studies, which suspected the correlation of modulation of microtubule stability through BMP signaling with progression of neurological diseases. We clearly presented that inhibition of BMP signaling caused by absence of Gef26 interrupts microtubule stability resulting of NMJ overgrowth and severe neuronal death in brain. For future study, it would be interested to define role of Gef26 in other diseases model.

VI. Literature Cited

1. Aberle H, Haghighi AP, Fetter RD, McCabe BD, Magalhaes TR, Goodman CS. (2002) wishful thinking encodes a BMP type II receptor that regulates synaptic growth in *Drosophila*. Neuron. 33:545-558.
2. Marques G, Bao H, Haerry TE, Shimell MJ, Duchek P, Zhang B, et al. (2002). The *Drosophila* BMP type II receptor Wishful Thinking regulates neuromuscular synapse morphology and function. Neuron. 33:529-543.
3. McCabe BD, Marques G, Haghighi AP, Fetter RD, Crotty ML, Haerry TE, et al. (2003). The BMP homolog Gbb provides a retrograde signal that regulates synaptic growth at the *Drosophila* neuromuscular junction. Neuron. 39:241-254.
4. Collins CA, and DiAntonio A. (2007) Synaptic development: insights from *Drosophila*. Current opinion in neurobiology. 17:35–42
5. Ball RW, Warren-Paquin M, Tsurudome K, Liao EH, Elazzouzi F, Cavanagh C, et al. (2010) Retrograde BMP signaling controls synaptic growth at the NMJ by regulating trio expression in motor neurons. Neuron. 66:536-549.
6. Nahm M, Lee MJ, Parkinson W, Lee M, Kim H, et al. (2013) Spartin regulates synaptic growth and neuronal survival by inhibiting BMP-mediated microtubule stabilization. Neuron. 77: 680-695.
7. Asha H, deRuiter ND, Wang MG, and Hariharan IK. (1999). The Rap1 GTPase functions as a regulator of morphogenesis in vivo. EMBO J. *18*, 605–615.
8. Boettner B, Harjes P, Ishimaru S, Heke M, Fan HQ, Qin Y, Van Aelst L, Gaul U. (2003). The AF-6 homolog canoe acts as a Rap1 effector during dorsal closure of the Drosophila embryo. Genetics. *165*, 159-169.
9. Bos JL. (2005). Linking Rap to cell adhesion. Curr Opin Cell Biol. *17*, 123-128.
10. Singh SR, Oh SW, Liu W, Chen X, Zheng Z, and Hou SX. (2006). Rap-GEF/Rap signaling restricts the formation of supernumerary spermathecae in *Drosophila melanogaster*. Devlop Growth Differ. *48*, 169-175.
11. Wang X, Shaw WR, Tsang HT, Reid E, and O'Kane CJ. (2007). *Drosophila* spichthyin inhibits BMP signaling and regulates synaptic growth and axonal microtubules. Nat Neurosci. *10*(2), 177-185.
12. Boettner B, Van Aelst L. (2009). Control of cell adhesion dynamics by Rap1 signaling. Curr Opin Cell Biol. *21*, 684-93.
13. Gloerich M, and Bos JL. (2011). Regulating Rap small G-proteins in time and space. Trends Cell Biol. 21:615–623.

14. Boettner B, Govek EE, Cross J, Van Aelst L. (2000). The junctional multidomain protein AF-6 is a binding partner of the Rap1A GTPase and associates with the actin cytoskeletal regulator profilin. Proc Natl Acad Sci USA. *97*(16), 9064-9.
15. Sawyer JK, Harris NJ, Slep KC, Gaul U. and Peifer M. (2009). The *Drosophila* afadin homologue Canoe regulates linkage of the actin cytoskeleton to adherens junctions during apical constriction. J Cell Biol. 186, 57–73.
16. Spahn P, Ott A, and Reuter R. (2012). The PDZ-GEF protein Dizzy regulates the establishment of adherens junctions required for ventral furrow formation in *Drosophila*. J Cell Sci. 15;125(Pt 16):3801-12.
17. Wang YC, Khan Z, and Wieschaus EF. (2013). Distinct Rap1 activity states control the extent of epithelial invagination via α-catenin. Dev Cell. *25*, 299-309.
18. Bilasy SE, Satoh T, Ueda S, Wei P, Kanemura H, Aiba A, Terashima T, and Kataoka T. (2009). Dorsal telencephalon-specific RA-GEF-1 knockout mice develop heterotopic cortical mass and commissural fiber defect. Eur. J. Neurosci. 29, 1994–2008.
19. Hisata S, Sakisaka T, Baba T, Yamada T, Aoki K, Matsuda M, and Takai Y. (2007). Rap1-PDZ-GEF1 interacts with a neurotrophin receptor at late endosomes, leading to sustained activation of Rap1 and ERK and neurite outgrowth. J. Cell Biol. 178, 843–860.
20. Lee KJ, Lee Y, Rozeboom A, Lee JY, Udagawa N, Hoe HS, and Pak DT. (2011). Requirement for Plk2 in orchestrated ras and rap signaling, homeostatic structural plasticity, and memory. Neuron 69, 957–973.
21. Maeta K, Edamatsu H, Nishihara K, Ikutomo J, Bilasy SE, and Kataoka T. (2016). Crucial role of Rapgef2 and Rapgef6, a family of Guanine Nucleotide Exchange Factors for Rap1 Small GTPase, in formation of Apical Suface Adherens Junctions and Neural Progenitor Development in the Mouse Cerebral Cortex. *3*(3) e0142-16.
22. Singh SR, Oh SW, Liu W, Chen X, Zheng Z, and Hou SX. (2006). Rap-GEF/Rap signaling restricts the formation of supernumerary spermathecae in *Drosophila melanogaster*. Devlop. Growth Differ. *48*, 169-175.
23. Lin DM, Goodman CS. (1994). Ectopic and increased expression of Fasciclin II alters motoneuron growth cone guidance. Neuron. 13:507-523.
24. Budnik V, Koh YH, Guan B, Hartmann B, Hough C, Woods D, et al. (1996). Regulation of synapse structure and function by the Drosophila tumor suppressor gene dlg. Neuron. 17:627-640.

25. Verstreken P, Ohyama T, Bellen HJ (2008) FM 1-43 labeling of synaptic vesicle pools at the Drosophila neuromuscular junction. Methods Mol Biol 440: 349-369.
26. Marrus SB, Portman SL, Allen MJ, Moffat KG, DiAntonio A. (2004). Differential localization of glutamate receptor subunits at the Drosophila neuromuscular junction. J Neurosci. 24:1406-1415.
27. Persson U, Izumi H, Souchelnytskyi S, Itoh S, Grimsby S, Engstrom U, et al. (1998). The L45 loop in type I receptors for TGF-beta family members is a critical determinant in specifying Smad isoform activation. FEBS Lett. 434:83-87.
28. Wan HI, DiAntonio A, Fetter RD, Bergstrom K, Strauss R, Goodman CS. (2000). Highwire regulates synaptic growth in *Drosophila*. Neuron. *26*(2):313-29
29. Ellis LL, and Carney GE. (2010). Mating alters gene expression patterns in *Drosophila melanogaster* male heads. BMC Genomics. 11:558.
30. Vossler MR, Yao H, York RD, Pan MG, Rim CS and Stork PJ. (1997). cAMP activates MAP kinase and Elk-1 through a B-Raf- and Rap1-dependent pathway. Cell. *89*(1):73-82.
31. Singh SR, Oh SW, Liu W, Chen X, Zheng Z, Hou SX. Rap-GEF/Rap signaling restricts the formation of supernumerary spermathecae in *Drosophila melanogaster*. Dev Growth Differ. 48:169-175.
32. Noda K, Zhang J, Fukuhara S, Kunimoto S, Yoshimura M, and Mochizuki N. (2010). Vascular endothelial-cadherin stabilizes at cell-cell junctions by anchoring to circumferential actin bundles through alpha- and beta-catenins in cyclic AMP-Epac-Rap1 signal-activated endothelial cells. Mol Biol Cell. *21*, 584-596.
33. Wang X, Shaw WR, Tsang HT, Reid E, O'Kane CJ. (2007). *Drosophila* spichthyin inhibits BMP signaling and regulates synaptic growth and axonal microtubules. Nat Neurosci. 10:177-185.
34. Sweeney ST, Davis GW. (2002). Unrestricted synaptic growth in spinster-a late endosomal protein implicated in TGF-beta-mediated synaptic growth regulation. Neuron. 36: 403-416.
35. Dickman DK, Lu Z, Meinertzhagen IA, Schwarz TL. (2006). Altered synaptic development and active zone spacing in endocytosis mutants. Curr Biol. 16:591-598.
36. McCabe BD, Marques G, Haghighi AP, Fetter RD, Crotty ML, Haerry TE, et al. (2003). The BMP homolog Gbb provides a retrograde signal that regulates

synaptic growth at the Drosophila neuromuscular junction. Neuron. 39:241-254.

37. O'Connor-Giles KM, Ho LL, Ganetzky B (2008) Nervous wreck interacts with thickveins and the endocytic machinery to attenuate retrograde BMP signaling during synaptic growth. Neuron 58: 507-518.

38. Ball RW, Warren-Paquin M, Tsurudome K, Liao EH, Elazzouzi F, Cavanagh C, et al. (2010). Retrograde BMP signaling controls synaptic growth at the NMJ by regulating trio expression in motor neurons. Neuron. 66:536-549.

39. Zhang YQ, Bailey AM, Matthies HJ, Renden RB, Smith MA, Speese SD, et al. (2001). Drosophila fragile X-related gene regulates the MAP1B homolog Futsch to control synaptic structure and function. Cell. 107:591-603.

40. Lee MH, Paik SK, Lee MJ, Kim YJ, Kim SD, Nahm MY, Oh SJ, Kim HM, Yim JB, Lee CJ, Bae YC and L SB. (2009). *Drosophila* Atlastin regulates the stability of muscle microtubules and is required for synapse development. Dev Biol. *330*(2), 250-262.

41. Roo J, Hummel T, Ng N, Klambt C, and Davis GW. (2000). Drosophila Futsch regulates synaptic microtubule organization and is necessary for synaptic growth. Neuron. *26*(2), 371-382.

42. Pennetta G, Hiesinger PR, Fabian-Fine R, Meinertzhagen IA, and Bellen HJ. (2002). Drosophila VAP-33A directs bouton formation at neuromuscular junctions in a dosage-dependent manner. Neuron. *35*(2):291-306.

43. Dent EW, Callaway JL, Szebenyi G, Baas PW, Kalil K. (1999). Reorganization and movement of microtubules in axonal growth cones and developing interstitial branches. J Neurosci. *19*(20), 8894-8909.

44. Schober JM, Komarova YA, Chaga OY, Akhmanova A, Borisy GG. (2007). Microtubule-targeting-dependent reorganization of filopodia. J Cell Sci. *120*, 1235-44.

45. Mosca TJ, Hong W, Dani VS, Favaloro V, Luo L. (2012). Trans-synaptic Teneurin signalling in neuromuscular synapse organization and target choice. Nature. *484*, 237-41.

46. Nechipurenko IV, Broihier HT. (2012). FoxO limits microtubule stability and is itself negatively regulated by microtubule disruption. J Cell Biol. *196*, 345-362.

47. Koh TW, Verstreken P, Bellen HJ. (2004). Dap160/intersectin acts as a stabilizing scaffold required for synaptic development and vesicle endocytosis. Neuron. *43*, 193-205.

48. Gloerich M, ten Klooster JP, Vliem MJ, Koorman T, Zwartkruis FJ, et al. (2012). Rap2A links intestinal cell polarity to brush border formation. Nat Cell Biol. 14: 793–801.
49. Consonni SV, Brouwer PM, van Slobbe ES, and Bos JL. (2014). The PDZ domain of the guanine nucleotide exchange factor PDZGEF directs binding to phosphatidic acid during brush border formation. PloS One. *9*(5):e98253.
50. Sulkowski MJ, Han TH, Ott C, Wang Q, Verheyen EM, Lippincott-Schwartz J, and Serpe M. (2016). A novel, noncanonical BMP pathway modulates synaptic maturation in drosophila neuromuscular junction. PloS Genet. *12*(1):e1005810.
51. Liao EH, Gray L, Tsurudome T, El-Mourzer W, Elazzouzi F, Baim C, Farzin S, Calderon MR, Kauwe G and Haghighi AP. (2018). Kinesin Khc-73/KIF13B modulates retrograde BMP signaling by influencing endosomal dynamics at the Drosophila neuromuscular junction. PLoS Genet. *14*(1):e1007184.
52. LaMonte BH, Wallace KE, Holloway BA, Shelly SS, Ascano J, Tokito M, Van Winkle T, Howland DS and Holzbaur EL. (2002). Disruption of dynein/dynactin inhibits axonal transport in motor neurons causing late-onset disease progressive degeneration. Neuron. *34*(5):715-27.
53. Aggad D, Veriepe J, Tauffenberger A and Parker JA. 2014. TDP-43 toxicity proceeds via calcium dysregulation nad necrosis in aging Caenorhabditis elegans motor neurons. J Neurosci. *34*(36): 12093-12103.

Chapter III*
The novel RAPGEF2 (p.E1357K) variant found in a sporadic ALS patient disrupts microtubule stability and mitochondrial distribution in distal axons

*This chapter has been largely reproduced from an article published by Heo, K., Lim, S.M., Nahm, M., Kim, Y.-E., Oh, K.W., Park, H.T., Ki, C.-S., Kim S.H., and Lee, S. Exp Neurobiol. (6): 550-563. (2018).

*Specially thank to Dr. M. Nahm, who helped the most with this study by providing technical help, reagents and heavy discussion.

Figures 1B, 3B, and 3C were reproduced from data provided as part of collaboration by Dr. Y.-E. Kim. Figure 5 was reproduced from data provided as part of collaboration by Dr. M. Nahm. Figures 6A, 6B, and 7B were reproduced from data provided as part of collaboration by Dr. S.M. Lim. Figure 7A was reproduced from data provided as part of collaboration by Dr. H.T. Park.

I. Abstract

Amyotrophic lateral sclerosis (ALS) is classified as a motor neuron (MN) disease, which causes death by muscle weakness and paralysis due to progressive degeneration in brain and spinal cord motor neurons. Recently, axonal transport has been highlighted as a neuropathological mechanism for neuronal function. Despite the evidence emphasizing the significance of axonal transport, the regulatory mechanism of how microtubule (MT)-dependent axonal transport could link with motor neuron diseases was still unclear. Our study proves how axonal transport could impact on motor neuron activity by generating transgenic flies and using skin fibroblasts obtained from ALS patients. RAPGEF2 is known for Rap1 activator, which has roles in various cellular processes during development. Previously, we discovered that RAPGEF2/Rap1 controls microtubule stability at the neuromuscular junction (NMJ) using *Drosophila* as research models. Contrary to the previous study, here we newly report that microtubule could also be destabilized by RAPGEF2 *de novo* missense variant, E1357K. We found the novel variant from trio exome sequencing analysis of ALS patients. Here, we show how RAPGEF2 influences microtubule-based trafficking of mitochondria, which supply the most of energy required in cells. We clearly show aberrant mitochondrial morphology and motility as microtubules are destabilized in the patient fibroblasts from electron microscopy (EM) analysis. In addition, we show impairment in mitochondrial distribution from proximal to distal axons and synaptic terminals in motor neurons of RAPGEF2-E1357K transgenic animals. Lastly, we confirm that the motor neuron of transgenic animals expressing RAPGEF2-E1357K

show ALS-like locomotor behavior. Our data conclude that gain of toxicity due to RAPGEF2-E1357K variant disrupts microtubule stability and microtubule-dependent trafficking of axonal mitochondria.

II. Introduction

ALS is one of neurodegenerative diseases defined by muscle weakness and spastic paralysis resulting from loss of motor neurons (MNs) selectively (Taylor et al., 2016; Brown et al., 2017). Because of the specialized features of motor neurons, finding genetic causes associated with cytoskeletal organization might provide new insights for pathogenic studies on ALS. Defects in organelles transport along microtubule (MT) networks are relevant in neurodegenerative processes (Mattson et al., 2008; Clark et al., 2016; De Vos et al., 2017; Carrie et al., 2017). In particular, modulation of mitochondrial transport along the microtubule network is critical for neuronal function, since mitochondria provide energy supplies to targeted areas e.g., synaptic terminals (Safiulina et al., 2013; De Vos et al., 2017). The mitochondria transport between soma, axons and the synaptic terminals are executed by microtubule-associated motor proteins (Frank et al., 2001). For neuronal activity, newly generated mitochondria in soma are delivered to dendrites along the axons, whereas the used mitochondria are transport back to soma for degradation (Sheng et al., 2017). Therefore, mitochondrial transport is crucial for energy homeostasis throughout the cells, especially in distal axons (Sheng et al., 2012; Fang et al., 2016; Sheng et al., 2017). The regulation of long-range mitochondrial movements depends on the microtubule polarity (Sheng et al., 2012). In this study, we identify a *de novo* variant in *RAPGEF2* gene, which affects mitochondrial transport depended on microtubule network.

RAPGEF2 (also called PDZ-GEF1) is known as Rap1 activator, which affects various cellular processes, e.g., migration (Hariharan et al., 1991; De Rooij et al., 1999;

Asha et al., 1999; Boettner et al., 2007; Asuri et al., 2008; Gloerich et al., 2011). Moreover, a previous study using transgenic mice expressing *RAPGEF2* shRNA has demonstrated that RAPGEF2 plays essential role in brain development (Ye et al., 2014). However, relationship between the RAPGEF2 function and human diseases remains unsolved. Here, we demonstrate how RAPGEF2 dysfunction due to the E1357K variant, which was found in an ALS trio study, impairs the mitochondrial transport. To address the relevance of microtubule stability and mitochondria, we analyzed mitochondria movement in the patient fibroblasts carrying RAPGEF2 (E1357K) variant. Skin fibroblasts obtained from the patient carrying the RAPGEF2 (E1357K) variant show destabilized microtubules, impaired mitochondrial movements, morphology and function. The combination of genetic and functional studies provides new insight into the development of ALS. Furthermore, we hope that future studies using this paradigm will contribute to expanding the understanding of ALS and its treatment.

III. Materials and methods

1. Subjects and exome sequencing

For this study, we were permitted by Institutional Review Boards (IRB) of Hanyang University Hospital and Samsung Medical Center. All participants submitted approval agreements for the study. We extracted genomic DNA from peripheral blood leukocytes obtained from ALS patients and their parents using a Wizard Genomic DNA Purification kit (Promega, Madison, WI, USA). This experiment was provided as part of collaboration by Ki-Wook Oh (Hanyang University).

To identify *de novo* variants, we analyzed ALS patients with living parents by application of whole exome sequencing (WES) analysis. The exome DNA were captured using Agilent SureSelect all Exon 50Mb kit (Agilent, Santa Clara, CA) and paired-end sequencing were executed using on an Illumina NextSeq500 machine (Illumina, San Diego, CA, USA). Reads was consequentially mapped to reference of human genome (GRCh37/hg19) using the Burrows-Wheeler Aligner (BWA), and allele frequency, which are less than 0.01 were selected as rare variants in the NHLBI Exome Sequencing Project (http://evs.gs.washington.edu/EVS/), 1000 Genomes Project (http://www.1000genomes.org/), and gnomAD (http://gnomad.broadinstitute.org/). This experiment was provided as part of collaboration with Young-Eun Kim (Hanyang University).

2. Cell culture and transfection

Human skin fibroblasts were collected through punch biopsy approaches as previously described (Lim et al., 2016). Patient fibroblasts were cultured in Dulbecco's modified Eagle's medium (DMEM) with 20% heat-inactivated FBS, 1% Penicillin/Streptomycin/ Fungizone, non-essential amino acids (Gibco, Grand Island, NY, USA), and sodium bicarbonate (Sigma-Aldrich). All fibroblasts at earlier passages (before 10) were used by passage-matched between control and patient. Fibroblasts were transfected with 1 μg plasmid DNA using FuGENE HD transfection reagent (Promega).

3. Molecular biology

The entire *RAPGEF2* and *Bcl-2-associated X* (*BAX*) open reading frame (ORF) was PCR-amplified from total human cDNAs and cloned into pEGFP-C1 vector (Clontech, Mountain view, CA, USA) to make *pEGFP-RAPGEF2-WT* and *pEGFP-BAX*. *RAPGEF2-E1357K* was generated through two-step PCR-based mutagenesis approach.

4. Fly stains

Flies were raised in medium at 25°C followed by lab manual. The *D42-GAL4*, and *D42-GAL4, UAS-mito-HA-GFP* lines were obtained from the Bloomington Stock Center (Bloomington, IN, USA). Transgenic lines of *UAS-HA-RAPGEF2-WT* and *UAS-HA-RAPGEF2-E1357K* were generated in the wild-type background strain using

standard manuals. The RAPGEF2^{KK102612} line (*UAS-gef26*^{RNAi}) was earned from the Vienna *Drosophila* Resources Center (Vienna, Austria).

5. Immunostaining and pharmacological treatment

Samples were fixed with 4% formaldehyde for 20 min at room temperature, permeabilized with PBS containing 0.2% Triton X-100 for 10 min and blocked in PBS containing 1% BSA for 1 h. Then, the samples were under primary antibody incubation for 1 h at room temperature and secondary antibody incubation for 30 min at room temperature. In this study, the used primary antibodies were listed: anti-Mitochondria (1:1000, Millipore, Burlington, MA, USA), anti-acetylated α-tubulin (1:500, Sigma-Aldrich), anti-tyrosinated α-tubulin (1:500, Milipore), and anti-total α-tubulin (1:500, Sigma-Aldrich). The FITC- and Cy5-conjugated HRP antibodies (1:200), FITC- and Cy3- conjugated secondary antibodies (1:200) were obtained from Jackson ImmunoResearch. The samples were mounted in SlowFade antifade medium (Invitrogen, Carlsbad, CA, USA). Images were collected using an LSM 700 laser-scanning confocal microscope (Carl Zeiss, Jena, Germany) using a C Apo 40x W or Plan Apo 63x 1.4 NA objective. For HDAC6 inhibitor treatment, human skin fibroblasts were treated with 1 μM tubastatin A (Sigma-Aldrich, St. Louis, MO, USA) for overnight at 37°C. After the washes, standard protocol was followed.

Dissected third-instar larvae in Ca^{2+}-free HL3 solution were fixed with 4% formaldehyde for 20 min. The fixed samples were sequentially treated with PBT-0.1 (PBS, 0.1% Triton X-100) solution for permeabilization, PBT-0.1 containing 0.2%

BSA solution for blocking, primary antibodies at 4°C and secondary antibodies for 30 min at room temperature. The primary antibodies, anti-HRP (1:200) and anti-Futsch (1:50) were obtained from DSHB (Iowa City, IA, USA), and anti-GFP (1:1000) obtained from Invitrogen. Images were collected using an LSM 700 laser-scanning confocal microscope (Carl Zeiss, Jena, Germany) using a C Apo 40x W or Plan Apo 63x 1.4 NA objective.

6. GEF activity assay

Rap1 activity was measured in patient fibroblasts using an Active Rap1 Pull-Down and Detection Kit following the manufacturer's protocols (Thermo Scientific, Waltham, MA, USA). Patient fibroblasts were rinsed gently with ice-cold TBS. Cells were collected in Lysis/Binding/Wash buffer, then centrifugation. For GTP treatment, lysates were placed for 15 min at 30°C with constant agitation after adding 0.5M EDTA pH 8.0 and 10mM GTP. Then BCA protein assay (Bio-Rad, Hercules, CA, USA) was performed to measure protein concentrations. GTP-bound active Rap1 was pulled down by GST-Raf1-RBD beads (Thermo Scientific) for 1 h at 4°C. The mixture was collected by centrifugation at 6,000 x g for 30 s. Then, the resin was incubated for 2 min at room temperature. The samples are then boiled for 5 min at 95°C, and subjected to western blot. The used primary antibodies were anti-Rap1 (1:1000, Thermo Scientific), and anti-GAPDH (1:1000, Santa Cruz Biotechnology, Dallas, TX, USA).

7. Western blotting

Homogenized cells in ice-cold lysis buffer containing 50 mM Tris-HCl, pH 7.4, 150 mM NaCl, 1% Triton X-100, 100 mM $CaCl_2$, and protease inhibitors) were subjected to western blot. The following primary antibodies were used: anti-acetylated α-tubulin (1:1000; Sigma-Aldrich), anti-tyrosinated α-tubulin (1:1000; Millipore), anti-total α-tubulin (1:1000; Sigma-Aldrich), anti-BAX (1:1000; BD, Franklin Lakes, NJ, USA), and anti-GAPDH (1:1000; Santa Cruz Biotechnology). The probes were analyzed using ImageJ software (NIH Image, Bethesda, MD, USA). For comparison, Student's *t*-test was used (*p<0.001) and the data are displayed as mean ± SEM.

8. Isolation of the mitochondrial fraction

The mitochondrial fraction was isolated from human skin fibroblasts using a Mitochondria/Cytosol Fractionation Kit following the manufacturer's protocols (BioVision, Milpitas, CA, USA). Briefly, skin fibroblasts were rinsed gently with ice-cold TBS. After collecting cells by centrifugation at 600 x g for 5 min at 4°C, cells were resuspended in cytosol extraction buffer mixture containing protease inhibitors (Sigma-Aldrich) and incubated on ice for 10 min. Subsequently, cells were homogenized with an ice-cold tissue grinder. Mitochondria and cytosolic fractions were segregated after the centrifugation at 10,000 x g for 30 min at 4°C.

9. Analysis of mitochondrial distribution in live cells

To examine mitochondrial distribution in live cultured cells, human skin fibroblasts were transfected with *Mito-RFP* for 48 h were placed in imaging dishes (Chamber slide Lab-Tek II 4; Fisher). Images were acquired by DeltaVision fluorescence microscopy (Applied Precision; Santa Clara, CA, USA) at a rate of one frame every 3 sec for 2 min. Mitochondrial lengths were measured in fixed fibroblasts expressing Mito-RFP using ImageJ software (NIH Image) followed by previously described (Fang et al., 2016). This experiment was provided as part of collaboration by Su Min Lim (Hanyang University).

10. Mitochondrial membrane potential analysis

The membrane potential of mitochondria ($\Delta\psi_m$) was analyzed in human skin fibroblasts using a Mitochondrial Potential Changes Detection Kit followed by manufacturer instructions (Sigma-Aldrich). Detection of mitochondrial membrane potential in live fibroblasts was achieved through labeling with membrane-permeant JC-1 dye. Skin fibroblasts were washed and incubated with JC-1 dye (5 μg/ml) for 20 min at 37°C. After washing, images were collected using a DeltaVision fluorescence microscopy system (Applied Precision; Santa Clara, CA, USA). Green fluorescence of JC-1 represents monomer form and red JC-1 fluorescence represents aggregates form. This experiment was provided as part of collaboration by Su Min Lim (Hanyang University).

11. Electron microscopy

Skin fibroblasts were fixed in PBS containing 4% paraformaldehyde and 2.5% glutaraldehyde for 24 h and washed with PBS. Then, the tissues were subjected to 70-nm sectioning after gradual dehydration in ethanol solutions and propylene oxide (Acros, New Jersey, USA), and stained with epoxy resins according to standard procedures. Images were acquired with a Hitachi electron microscope (ES500W, GATAN, Pleasanton, CA, USA). This experiment was provided as part of collaboration by Hwan Tae Park (Dong-A University).

12. Climbing assay

Locomotor ability from adult *Drosophila* was assayed as described previously (Heo et al., 2017). Approximately 45 flies were collected within 24 h post-eclosion, and ages for 20 days. The flies were transferred into fresh foods every 2 days by maintaining 10 flies per vial. For the assay, flies were transferred into a glass graduated cylinder and placed it for 5 min for adaptation. The climbed distance for individual flies at 30 s after the gentle tapping for 5 s were analyzed.

13. Statistical analysis

For comparison, Student's *t*-test was used (*P<0.001), and the data are presented as mean ± SEM.

IV. Results

1. Clinical features of an ALS patient carrying E1357K variant in *RAPGEF2* gene and the *RAPGEF2* domain structure

From the analysis of Korean ALS trios, a 28-year-old female patient was identified to carry a *de novo* RAPGEF2 (c.4069G>A, p.E1357K) variant (Fig 1A and 1B). The neurological examination was done by Ki-wook Oh from Hanyang University. The patient initially showed progressive weakness in both lower limbs followed by left and right arm weakness at 27-years old. In addition, her Needle electromyography (EMG) exhibited abnormal active potentials. According to the neurological examination, Dr. Oh diagnosed her with clinically probable ALS. For additional information, the patient was negative for genetic screening of other ALS causing genes, such as *C9orf72, SOD1, FUS, TARDBP, ANG*, and *OPTN*. At the time of publication, she is still alive for 121 months following the onset of ALS.

RAPGEF2 is known as a GEF for Rap1 during various developmental processes (Hariharan et al., 1991; Lee et al., 2002; Boettner et al., 2007). Human RAPGEF2 contains Ras signaling domains, such as a Ras-exchange motif, and Ras-associating (RA) domain, as well as GEF function related cyclic nucleotide-monophosphate (cNMP) binding domain, and two guanine exchange factor catalytic (Ras-GEF) domains, discs large homologue, zonula occludens-1 (PDZ) domain, and two low-complexity domains (LCD) (Fig 1C). Previously, abnormal function of LCD domain is known to induce cellular toxicity by increasing level of genes related to stress response and interrupting biogenesis of ribosomal RNA (rRNA) or actin

dynamics to restrain neuronal growth (Shin et al., 2016). The position of E1357K variant is located in LCD domain of human RAPGEF2, and it is highly conserved in other species, suggesting that this amino acid is functionally important (Fig 1C).

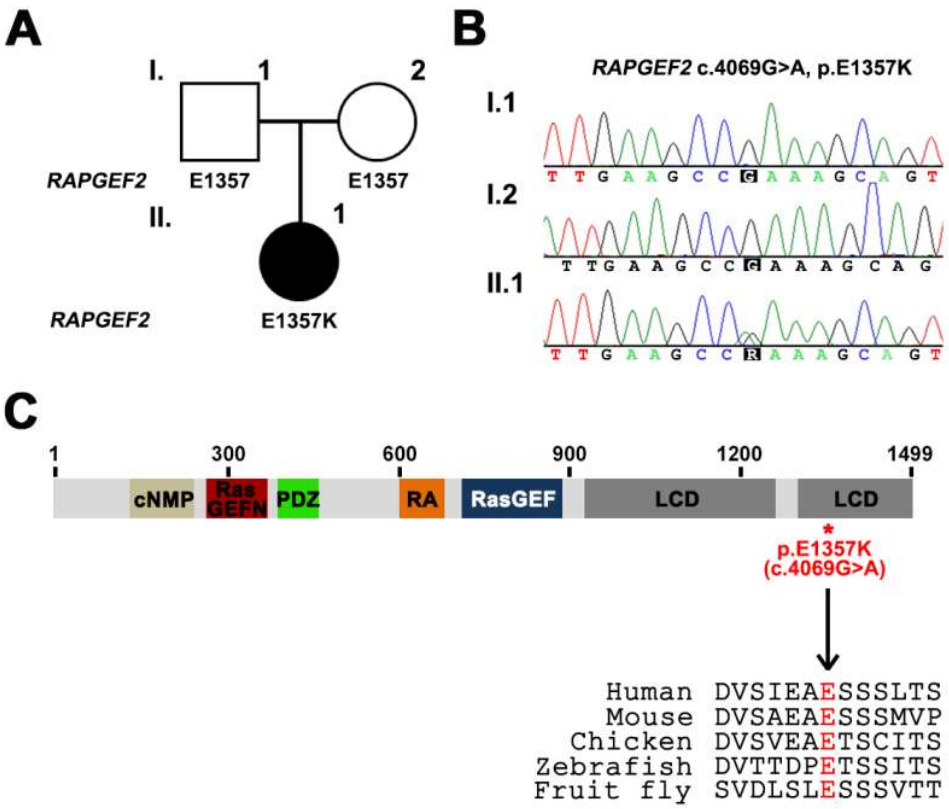

Figure 1. The discovery of a *de novo* RAPGEF2 (E1357K) variant through whole exome sequencing (WES) analysis of sporadic ALS patients
(A) ALS patient family pedigree. Note that unfilled square: unaffected male, unfilled circle: unaffected female, and filled circle: affected female. (B) Sanger sequencing analysis of the RAPGEF2 E1357K variant. (C) E1357K variant is marked at RAPGEF2 domain structure.

2. Identification of RAPGEF2 E1357K variant found from sporadic ALS patient

Our previous study established that Gef26, fly homolog of RAPGEF2 modulates microtubule (MT) stability through the microtubule-associated protein Futsch at the *Drosophila* neuromuscular junctions (NMJs) (Heo et al., 2017). We therefore investigated whether microtubule stability is affected in skin fibroblasts obtained from sporadic ALS patient carrying RAPGEF2 (E1357K) variant. Microtubule acetylation and tyrosylation have been proposed as post-translational modifications affecting microtubule dynamics, while acetylated microtubules represent stable microtubule population, whereas tyrosinated microtubules indicate dynamic microtubules (Westernmann et al., 2003; Conde et al., 2009; Wloga et al., 2010; Portran et al., 2017). Staining with specific antibody against acetylated α-tubulin revealed that the most of microtubule bundles were loss except for the perinuclear region in patient fibroblasts compared with healthy control (Fig 2A-C). Also, acetylated α-tubulin levels were reduced in patient fibroblasts, while the total α-tubulin levels were not affected (Fig 2A-C). Unlike the acetylated α-tubulin, tyrosinated or total α-tubulin in patient fibroblasts remained constant patterns or levels with the healthy controls (Fig 2A-D). We also examined the RAPGEF2 (E1357K) variant by expressing Flag-tagged RAPGEF2 constructs in Hela cells (Fig 2E). As results, we suspect that the microtubule is de-stabilized when RAPGEF2 function is disrupted by E1357K variant.

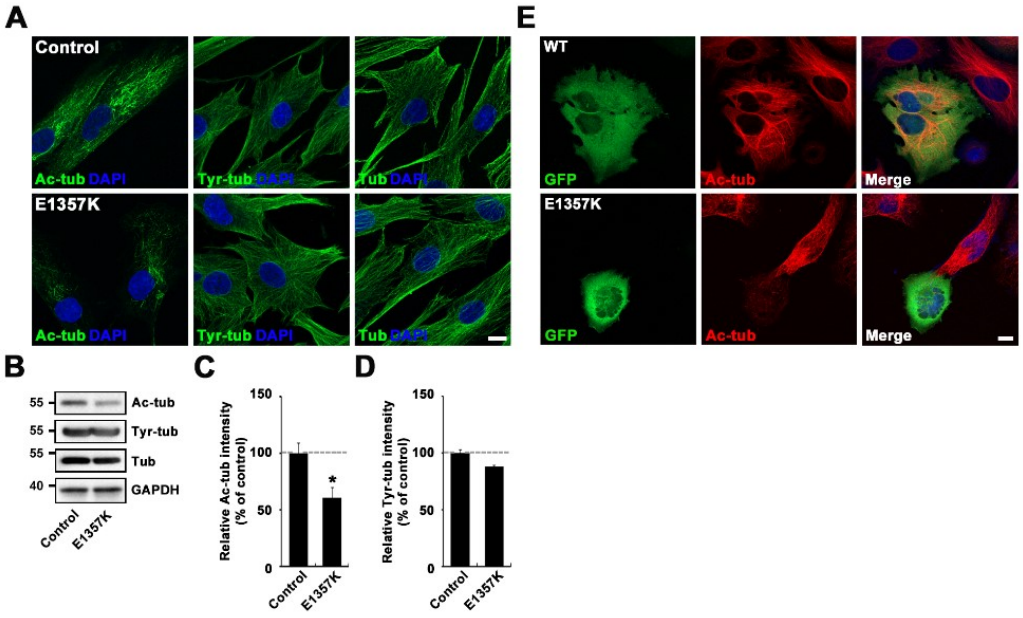

Figure 2. Patient fibroblasts show altered microtubule stability and network
(A-D) Expression level of acetylated α-tubulin is decreased, while tyrosinated or total α-tubulin remained constant in the patient fibroblasts. (A) Confocal images of fibroblasts labeled with Ac-tub, Tyr-tub or Total-tub (green) and DAPI (blue). Scale bar: 5 μm. (B) Western blot of fibroblasts from healthy control and a patient with the E1357K variant in RAPGEF2. The blots were incubated with anti-Ac-tub, anti-Tyr-tub, anti-Total-tub, and anti-GAPDH. (C and D) Quantitative analysis of three independent blots using ImageJ. Levels of Ac-tub or Tyr-tub were normalized to the levels of Total-tub. All comparisons are made with healthy controls (*P<0.001). (E) Images of Hela cells labeled with Ac-tub (green), Ac-tub (red) and DAPI (blue). Scale bar: 5 μm.

We additionally examined the distribution of acetylated α-tubulin in Hela cells by expressing other missense (c.1883C>T, p.T628I and c.3293G>A, p.R1098H) variants in *RAPGEF2* gene through next generation sequencing (Fig 3A). The position of p.T628I is located in RA domain whereas the p.R1098H variant is located in first LCD domain of human RAPGEF2 (Fig 3B and 3C). We also examined the RAPGEF2 (p.T628I and p.R1098H) variant by expressing Flag-tagged RAPGEF2 constructs in

Hela cells (Fig 3D). The distributions of acetylated α-tubulin and the localizations of RAPGEF2 T628I were severely altered, while the parameter in R1098H variant were consistent with the wild-type controls (Fig 3D). Since the patient carrying RAPGEF2 T628I also possesses pathogenic variant in FUS, we eliminated the variant for further experiment because it would be hard to interpret the phenotypes observed in the cells expressing T628I are truly due to the role of RAPGEF2. Altogether, these data suggest that RAPGEF2-E1357K variant is indispensable for MT stability.

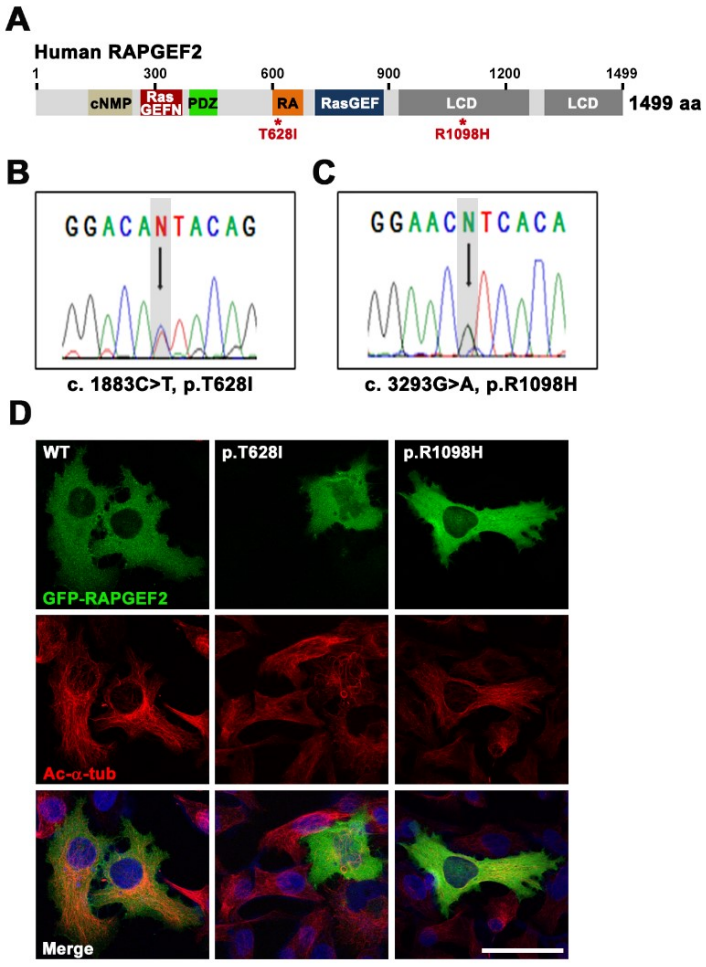

Figure 3. The distribution of acetylated α-tubulin was impaired in RAPGEF2 T628I variant, but normal in RAPGEF2 R1098H variant
(A) The p.T628I and p.R1098H variant are marked at RAPGEF2 domain structure. (B) Sanger sequencing analysis of the RAPGEF2 T628I and R1098H variant. (C) Images of Hela cells labeled with Ac-tub (green), Ac-tub (red) and DAPI (blue). Scale bar: 5 μm.

3. The RAPGEF2 E1357K variant regulates microtubule stability independently from the GEF activity towards Rap1

Since RAPGEF2 is known as an activator for Rap1 in various cellular levels, we also tested Rap1 activity in patient fibroblasts with E1357K variant through the active Rap1 pull-down assay. In brief, GTP-bound active Rap1 was pulled down for 1 h at 4°C with GST-Raf1-RBD beads (Thermo Scientific), which is known as a GST-fusion protein of Rap1-binding domain (RBD), and then western blot was performed using anti-Rap1 antibody. While total Rap1 level in controls and RAPGEF2 E1357K variant was consistent, the level of GTP-Rap1 was dramatically reduced in E1357K variant, compared with controls (Fig. 4A and 4B).

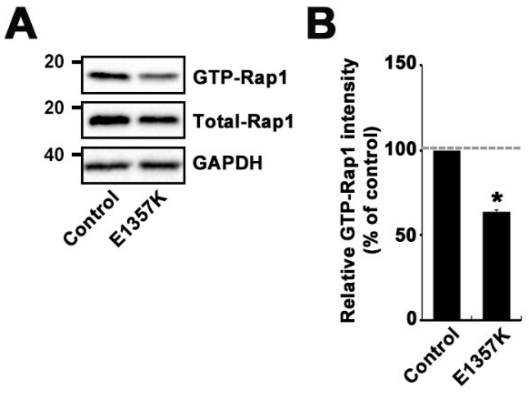

Figure 4. The level of GTP-Rap1 were dramatically reduced in the patient fibroblasts carrying E1357K variant compared with the controls
(A) GEF activity towards Rap1 was reduced in patient fibroblast with (E1357K) variant. Primary patient fibroblasts were collected for GTPγS treatment. Protein was incubated with GST-Raf1-RBD beads for 1 h at 4°C. The probe was incubated with anti-Rap1 and anti-GAPDH. (B) Quantitative analysis of blot was done by normalization of active-Rap1 intensity to GAPDH. Data are presented as mean ± SEM. All data are compared with RAPGEF2 control (*P<0.001).

We additionally examined the distribution of Rap1 in cells expressing RAPGEF2 E1357K variant. The RAPGEF2 was co-localized with Rap1 in cells expressing RAPGEF2 wild-type, and this phenomena was consistent in cells expressing RAPGEF2 E1357K (Fig 5A). These data imply that the E1357K variant in RAPGEF2 is indispensable for Rap1 function. Altogether, the results indicate that E1357K variant in RAPGEF2 is critical for regulation of microtubule stability by modulating Rap1 activity. From the previous studies, another RAPGEF family, Epac, is known to depend on the cAMP level (Vossler et al., 1997). To examine whether the addition of cAMP alters the localization of RAPGEF2, we compared the distribution of RAPGEF2 and Rap1 by treating cAMP. There was no changed before and after the treatment of cAMP in fibroblasts carrying RAPGEF2 E1357K compared to the

controls (Fig 5A and 5B). As results, we concluded that the RAPGEF2 function is not similar with the other RAPGEFs.

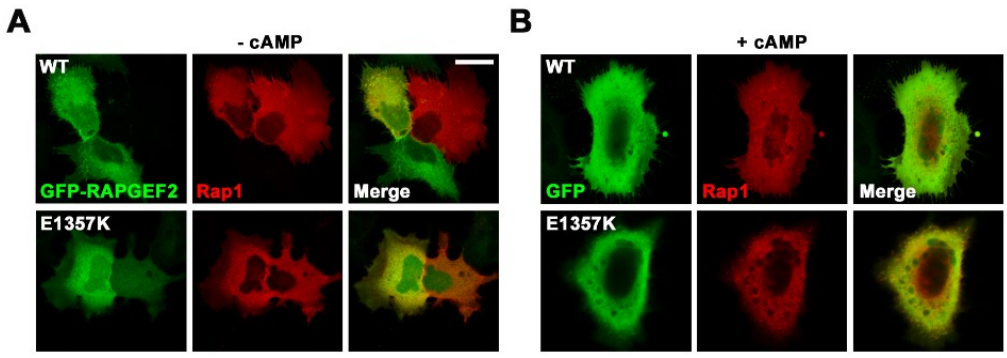

Figure 5. The expression of RAPGEF2 is Rap1-independent and cAMP-independent in the patient fibroblasts with RAPGEF2 E1357K variant
(A and B) Images of fibroblasts labeled with RAPGEF2 (green) and Rap1 (red). The expression of RAPGEF2 and Rap1 was examined from the fibroblasts in absence (A) or presence (B) of cAMP. Scale bar: 5 μm.

4. Mitochondrial distribution was altered in patient fibroblasts with RAPGEF2 E1357K variant

Abnormal organization of microtubule affects mitochondrial motility (Park et al., 2013). Therefore, we visualized the mitochondria in patient fibroblasts by employing mitochondrial targeted GFP (Mito-GFP) followed by previously described method (Kaasik et al., 2007; Zala et al., 2013). The live cell imaging experiment was performed by Su Min Lim from Hanyang University. We monitored Mito-GFP by time-lapse florescence microscopy for live imaging analysis of mitochondria movement. The mitochondrial movements were investigated by time course using DeltaVision fluorescence microscopy. Compared with the controls, mitochondrial fragmentation and attenuated movement were found in the patient fibroblasts carrying

the RAPGEF2-E1357K variant (Fig 6A and 6B). Similar defects of mitochondria were observed in fixed fibroblast cells (Fig 6C-E). To quantify changes in mitochondrial morphology, we measured mitochondrial length in similar positions of healthy or patient fibroblasts. The mitochondrial length in patient fibroblasts with RAPGEF2-E1357K variant were shorten compared to healthy control, while cell sizes are comparable (Fig 6C and 6D). Microtubules are stabilized by acetylation α-tubulin at lysine 40 residue and destabilized by α-tubulin deacetylases, such as, HDAC6 (Hubbert et al., 2002). To investigate whether the defect in mitochondrial distribution is due to microtubule de-stabilization, we tested whether attenuated tubulin acetylation in patient fibroblasts is restored by an HDAC6 inhibition. Tubastatin A is a potent HDAC6 inhibitor that rescues some axonal transport defects (Hubbert et al., 2002; d'Ydewalle et al., 2011; Guo et al., 2017). After the tubastatin A (1 μM) treatment, the aberrant patterns of acetylated α-tubulin and fragmented mitochondria were clearly restored to the normal pattern in the patient fibroblasts carrying the RAPGEF2-E1357K variant (Fig 6C-E). These results suggest that microtubule de-stabilization causes impairment in the mitochondrial distribution in the RAPGEF2-E1357K variant.

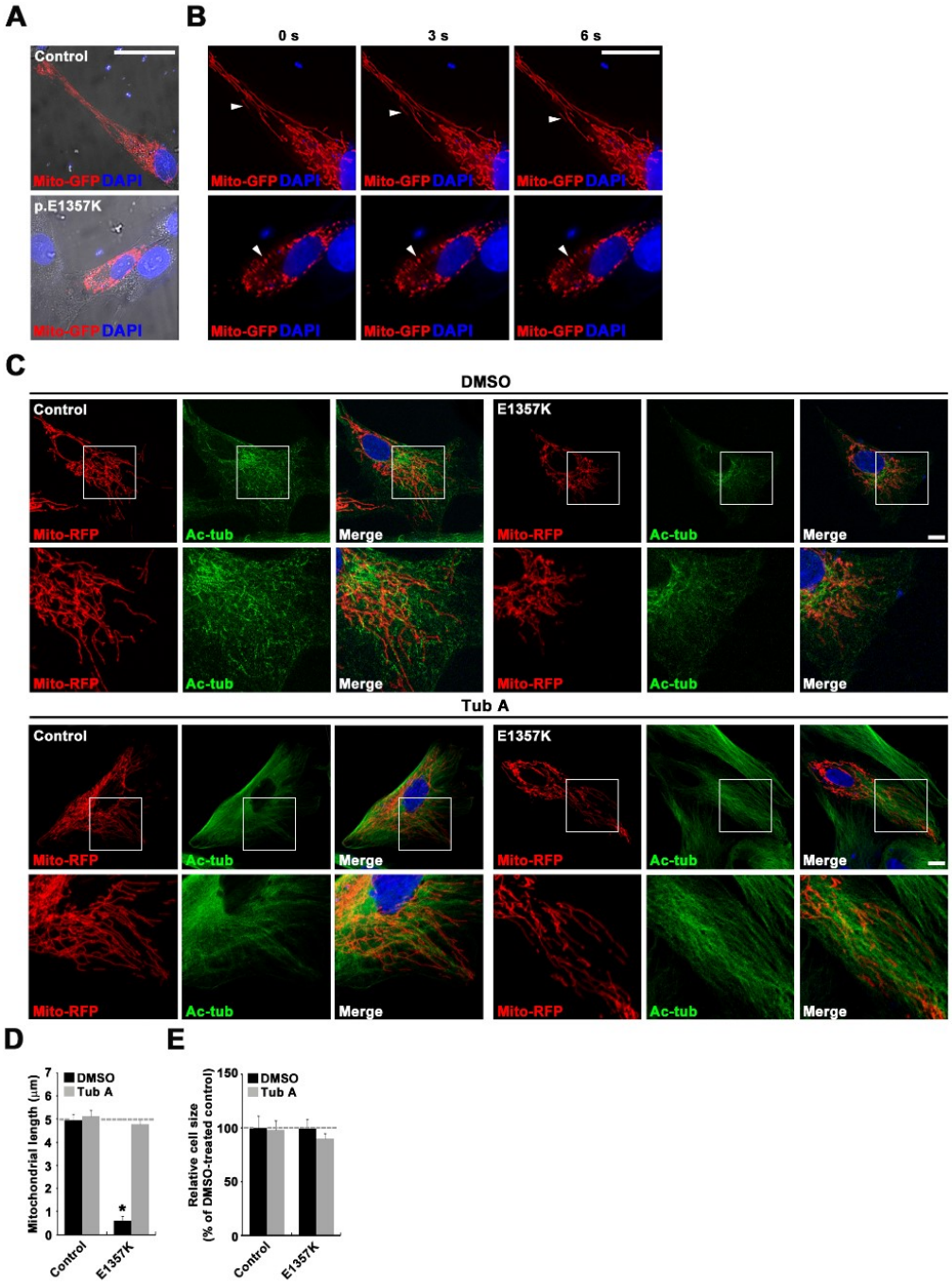

Figure 6. Inhibition of the HDAC6 restored impaired mitochondrial distribution in the patient fibroblasts carrying RAPGEF2-E1357K

(A and B) Live cell images of mitochondria labeled by Mito-RFP (red) and nuclei labeled by DAPI (blue) in skin fibroblasts. (A) Representative fluorescent microscopy images of the fibroblasts for healthy control and ALS patient. Fluorescent images are merged with the DIC image to better visualize the cell boundary. Scale bar: 25 μm. (B) Representative images from time-lapse series (0-6s). Note the moving mitochondria (arrowhead). Scale bar: 15 μm. (C) Confocal images of fibroblasts labeled with Ac-tub (green) or RFP-Mito (red) and DAPI (blue). In ALS patient fibroblast carrying RAPGEF2 E1357K variant, decreased acetylated α-tubulin and fragmented mitochondria were shown, and these are restored by treatment of 1 μM tubastatin A (Tub A). Scale bar: 5 μm. (D) The length of mitochondria in patient fibroblasts were shorter than those of controls, and the phenotypes are restored by tubastatin A (Tub A) treatment. (E) The analyzed fibroblasts showed similar cell sizes. Analyzed cell number: n=7 for control, n=6 for p.E1357K, n=11 for control (Tub A), n=11 for E1357K (Tub A). All comparisons are made with controls (*P<0.001).

5. Altered mitochondrial ultrastructure and activity were observed in dermal fibroblasts of the patient

To investigate further changes in the mitochondrial ultrastructure in skin fibroblasts of patient and healthy control, we performed transmission electron microscopy experiments helped by Hwan Tae Park from Dong-A University. In healthy control, typical mitochondrial features of membrane, cristae, and dense matrix were exhibited (Fig 7A). Unlike the control, patient skin fibroblast showed disturbed mitochondrial morphology displaying enlarged structures with loss of cristae and electron dense structure (Fig 7A). These results indicate that the mitochondria function is disrupted when RAPGEF2 is disrupted by the E1357K variant.

Aberrant mitochondrial motility and morphology are correlated with defective mitochondrial function (Chen et al., 2009; Sheng et al., 2012; Genin et al., 2016). Therefore, we monitored mitochondria function in living cells using JC-1 fluorescence dye to analyze membrane potential of mitochondria. The JC-1 dye differentially labels

mitochondrial activity depended on mitochondrial membrane potential (Smiley et al., 1991). This experiment was performed by Su Min Lim from Hanyang University. Unlike the healthy controls, decreased aggregates and increased monomers were observed in patient fibroblasts with RAPGEF2-E1357K variant, indicating reduced mitochondrial membrane potential (Fig 7B). These results clearly exhibit attenuated mitochondria activity in the RAPGEF2-E1357K variant.

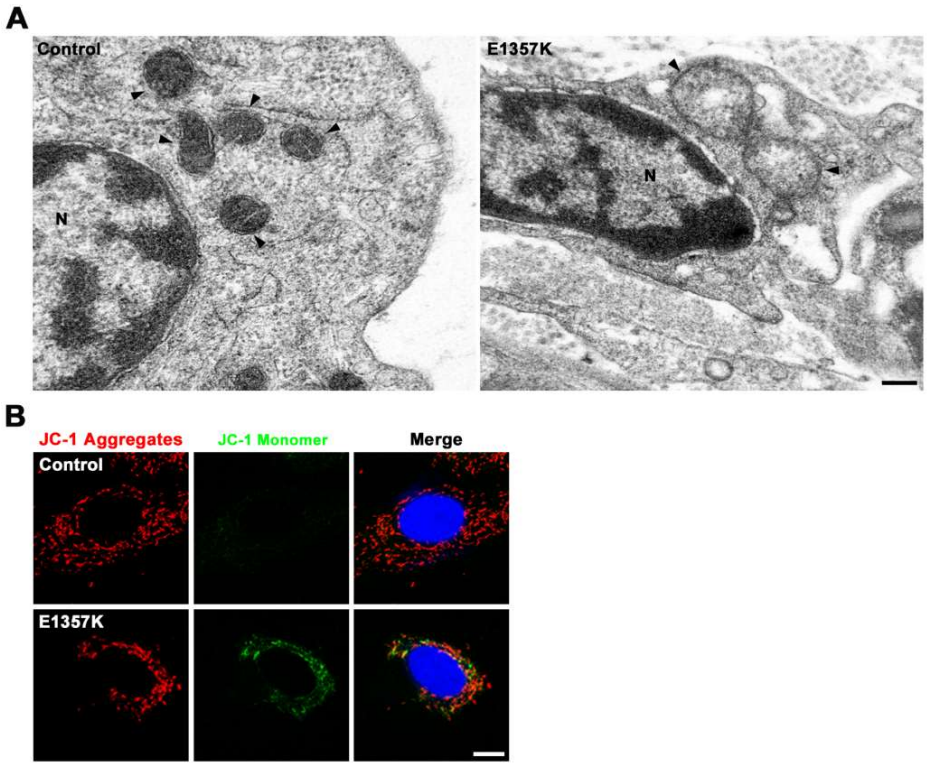

Figure 7. Mitochondrial ultrastructure and activity are impaired in patient fibroblasts

(A) Electron microscopic images of mitochondria in skin fibroblasts from healthy control and patient. Enlarged size of mitochondria with absence of cristae was observed in patient fibroblast. Note the nucleus (N), and mitochondria (arrowhead). Scale bar: 0.2 μm. (B) Mitochondrial membrane potential ($\Delta\psi_m$) was reduced in patient fibroblast carrying the E1357K variant. Representative images of fibroblasts using JC-1 dye, an indicator of mitochondrial membrane polarization. Scale bar: 15 μm.

The control fibroblasts used in this study were obtained from male at age 43, whereas the patient fibroblasts were obtained from the female at age 27. To diminish the possibility which phenotypic differences are due to different genetic background, we initially examined the level of acetylated α-tubulin from the skin fibroblasts obtained from one male at age 43 (control used in this paper) and two females whose ages were 35 and 57. We confirmed that the levels of acetylated α-tubulin was consistent in all three control fibroblasts (Fig. 8A and 8B). Thus, we used fibroblast obtained from male at age 43 as a heathy and non-ALS control in this study because he is available skin biopsy for EM study.

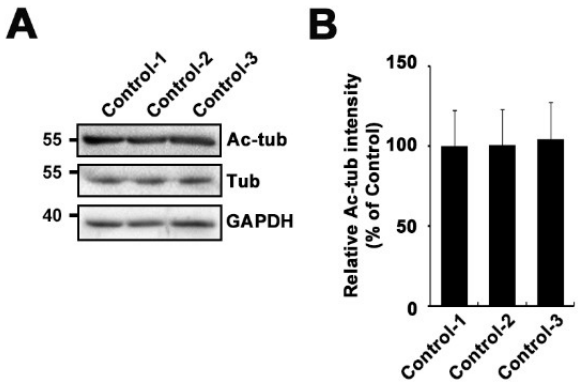

Figure 8. The phenotypic differences shown at the controls and the patient fibroblasts are not due to the different genetic background
(A) Western blot of fibroblasts from three different healthy controls. The blots were incubated with anti-Ac-tub, anti-Total-tub, and anti-GAPDH. (B) Quantitative analysis of three independent blots using ImageJ. Levels of Ac-tub were normalized to the levels of Total-tub. All comparisons are made with healthy controls. Note to the control-1: Male, 43 age; control-02: Female, 35 age; control-03: Female, 57 age. Scale bar: 5 μm.

6. Motor neurons of flies expressing human RAPGEF2-E1357K exhibit defective mitochondrial distribution

Previously, many studies have documented that microtubule networks regulate axonal mitochondria trafficking in fly motor neurons (Pilling et al., 2006; Wang et al., 2009; Schwarz et al., 2013; Sandoval et al., 2014; Babic et al., 2015). Therefore, we investigated whether motor neuron specifically over-expression of RAPGEF2-E1357K variant affects axonal mitochondrial distribution *in vivo*. To do this, we generated HA-tagged human RAPGEF2 wild-type (*HA-RAPGEF2-WT*) and E1357K (*HA-RAPGEF2-E1357K*) transgenic flies using standard protocols. First, we confirmed that the expression levels of RAPGEF2 were consistent between the wild-type and E1357K mutant (data not shown). Next, we tested whether the stable microtubules are affected in motor neurons over-expressing RAPGEF2 wild-type (*HA-RAPGEF2-WT*) and RAPGEF2-E1357K mutant (*HA-RAPGEF2-E1357K*). The intensity of acetylated-α-tubulin in 100-μm lengths of axons and the NMJs over-expressing RAPGEF2 wild-type were consistent with the controls (Fig 9A, C-E). Interestingly, unlike the RAPGEF2 wild-type, the level of the acetylated-α-tubulin was reduced in axons and the NMJs expressing RAPGEF2-E1357K mutant, while the intensity of acetylated-α-tubulin in axons and the NMJs depleting *gef26* expression (Gef26 KD) were increased (Fig 9A, C-E). We obtained similar results of MAP1B-like protein Futsch levels, which is decreased in motor neurons over-expressing RAPGEF2-E1357K mutant, increased in Gef26 KD larvae and unchanged in RAPGEF2 wild-type compared to the controls (Fig 9B,C,F,G). These results imply that the regulatory mechanism of

microtubule stability in RAPGEF2-E1357K variant is not loss-of-function or gain-of-function.

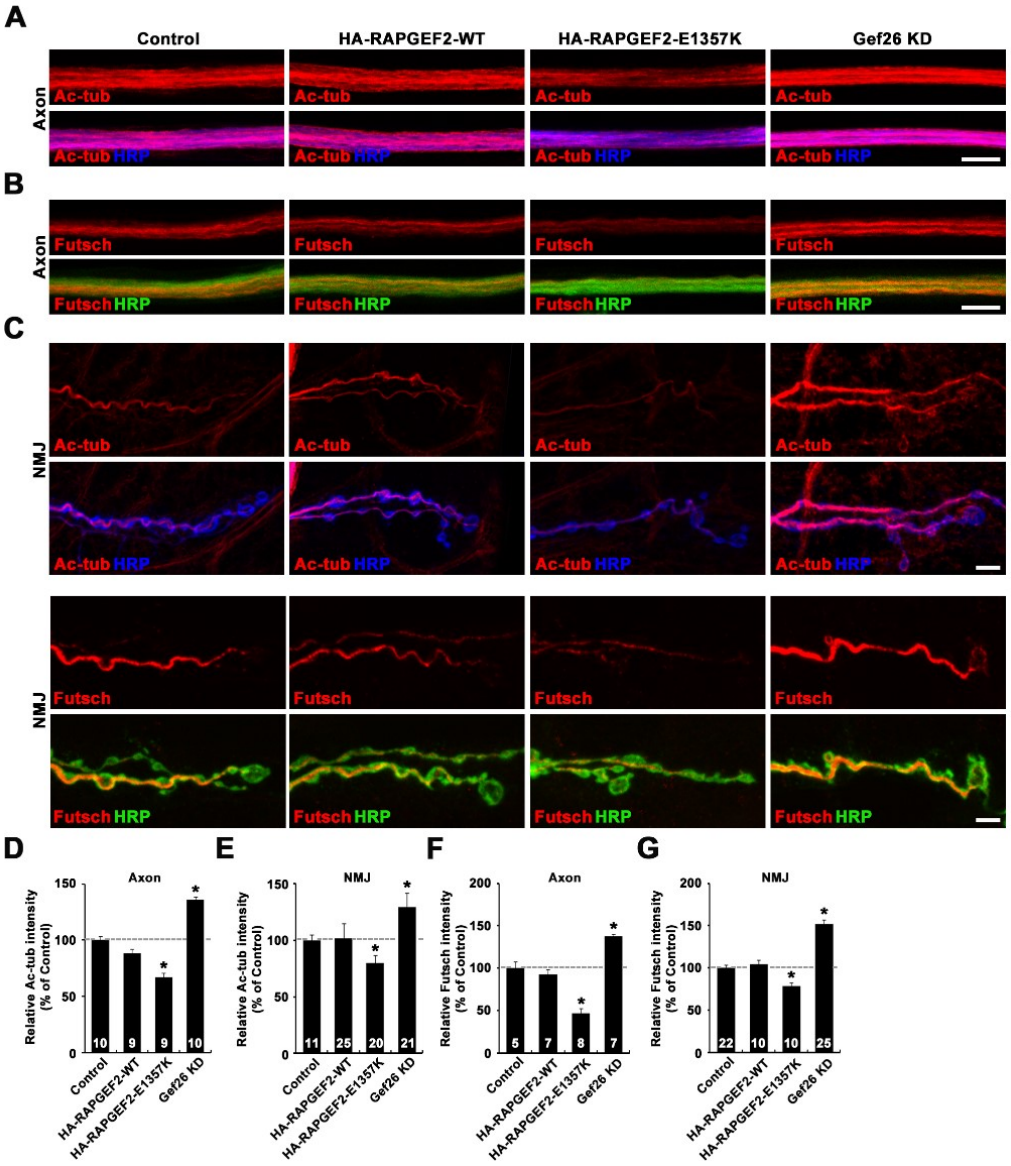

Figure 9. Motor neurons of transgenic flies over-expressing human RAPGEF2-E1357K display reduction of microtubule stability within axons and synaptic terminals

(A-C) Confocal images of distal (A5) axon segments (A and B) and synaptic terminals (NMJ 6/7) (C) double labeled with anti-Ac-tub (A and C) or anti-Futsch (B and C) and anti-HRP in motor neurons of *D42-GAL4*/+ (Control), *D42-GAL4*/*UAS-HA-RAPGEF2-WT* (HA-RAPGEF2-WT), *UAS-HA-RAPGEF2-E1357K*/+; *D42-GAL4*/+ (HA-RAPGEF2-E1357K), and *D42-GAL4*/*UAS-gef26*^{RNAi} (Gef26 KD) third-instar larvae. Scale bar: 5 μm. (D and E) Quantitative analysis of the Ac-tub to HRP level ratios in the axons (D) and the NMJs (E), and Futsch to HRP level ratios in the axons (F) and the NMJs (G) in each genotype. Data are presented as mean ± SEM. All data are compared with controls (*P <0.001).

Next, we examined mitochondrial distribution in two distinct regions: axonal segments, and synaptic terminals (NMJs) from each genotype. In flies expressing RAPGEF2 wild-type, similar distributions of GFP-tagged mitochondria were observed in all regions as the controls (Fig 10A and 10B). However, the distributions of Mito-GFP in distal axons and NMJs were different between flies expressing the RAPGEF2 wild-type and E1357K mutant (Fig 10A and 10B). The Mito-GFP puncta number and area in 100-μm lengths of distal axons (A5) were reduced, while the parameters were constant at proximal axons (A2) in motor neurons expressing RAPGEF2 E1357K mutant compare to RAPGEF2 wild-type (Fig 10C and 10D). Consequentially, the areas of Mito-GFP puncta at NMJs were also reduced in the RAPGEF2-E1357K mutant (Fig 10E). Unlike the RAPGEF2-E1357K mutant, the distributions of GFP-tagged mitochondria in flies expressing *gef26* dsRNA were constant in all regions as the controls (Fig 10A-E). From the results, we concluded that the disrupted mitochondrial distribution from proximal axons to distal axons in motor neurons of mutant flies expressing human RAPGEF2-E1357K is not caused by loss of RAPGEF2 expression.

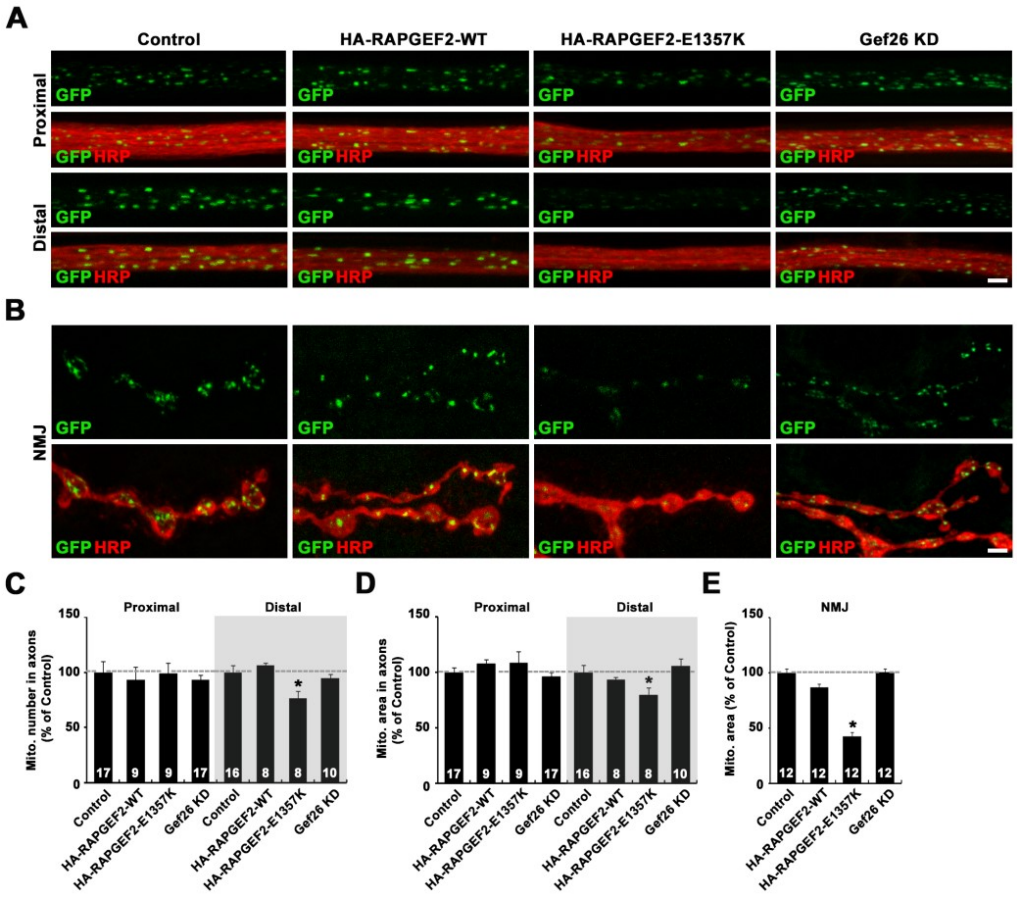

Figure 10. Motor neurons of transgenic flies expressing the human RAPGEF2-E1357K show decrease mitochondrial distribution in distal motor axons and NMJ
(A and B) Confocal images of Mito-GFP in proximal (A2) and distal (A5) axon segments (A), and synaptic terminals (NMJ 6/7) (B) in motor neurons of *D42-GAL4*,*UAS-mito-GFP*/+ (Control), *D42-GAL4*,*UAS-mito-GFP*/*UAS-HA-RAPGEF2-WT* (HA-RAPGEF2-WT), *UAS-HA-RAPGEF2-E1357K*/+; *D42-GAL4*,*UAS-mito-GFP*/+ (HA-RAPGEF2-E1357K), and *D42-GAL4*,*UAS-mito-GFP*/*UAS-gef26*^{RNAi} (Gef26 KD) third-instar larvae. Scale bars: 5 μm. (C-E) Quantification of number (C) and area (D) of Mito-GFP positive puncta in the proximal and distal axons, and area of Mito-GFP puncta at the NMJs (E) in each genotype. Data are presented as mean ± SEM. All data are compared with controls (*P <0.001).

7. Microtubule dysregulation induces BAX translocation to mitochondria in patient fibroblasts

Mitochondrial cristae remodeling and fragmentation occur at early stage of apoptosis, and induce massive cytochrome c release and decreases in membrane potential (Frank et al., 2001; Scorrano et al., 2002; Poncet et al., 2004). BAX is a proapoptotic regulator of BCL-2 proteins, which forms pores to release cytochrome c towards mitochondrial outer membrane (Frank et al., 2001; Wei et al., 2001; Sheridan et al., 2008). To determine the relevance of apoptotic pathway, we examined BAX distribution in the fibroblasts from the healthy controls and the patient carrying RAPGEF2-E1357K variant. We expressed GFP-tagged BAX in healthy and patient fibroblasts and then stained mitochondria with an anti-mitochondria antibody. BAX was predominantly localized in the cytosol in healthy cells (Fig 11A). Notably, BAX was co-localized with mitochondria in the fibroblasts (Fig 11A). We additionally fractionated the cells and tested the expression level of BAX in the mitochondrial fraction. We confirmed that the mitochondria fraction was successfully segregated from the cytosol fraction by examining α-tubulin level (Fig 11B). As expected, level of BAX was increased in the mitochondrial fraction in fibroblasts carrying the RAPGEF2-E1357K variant, unlike the controls (Fig 11B and 11C). We also proved that localization of BAX at mitochondria was re-localized to the cytosol after the tubastatin A treatment (Fig 11B and 11C). The total level of BAX was consistent in all samples (Fig 11D and 11E). Altogether, these results imply that impairment in mitochondrial function and

movement along the defective microtubule organization in cells carrying the RAPGEF2-E1357K variant promotes apoptotic cell death.

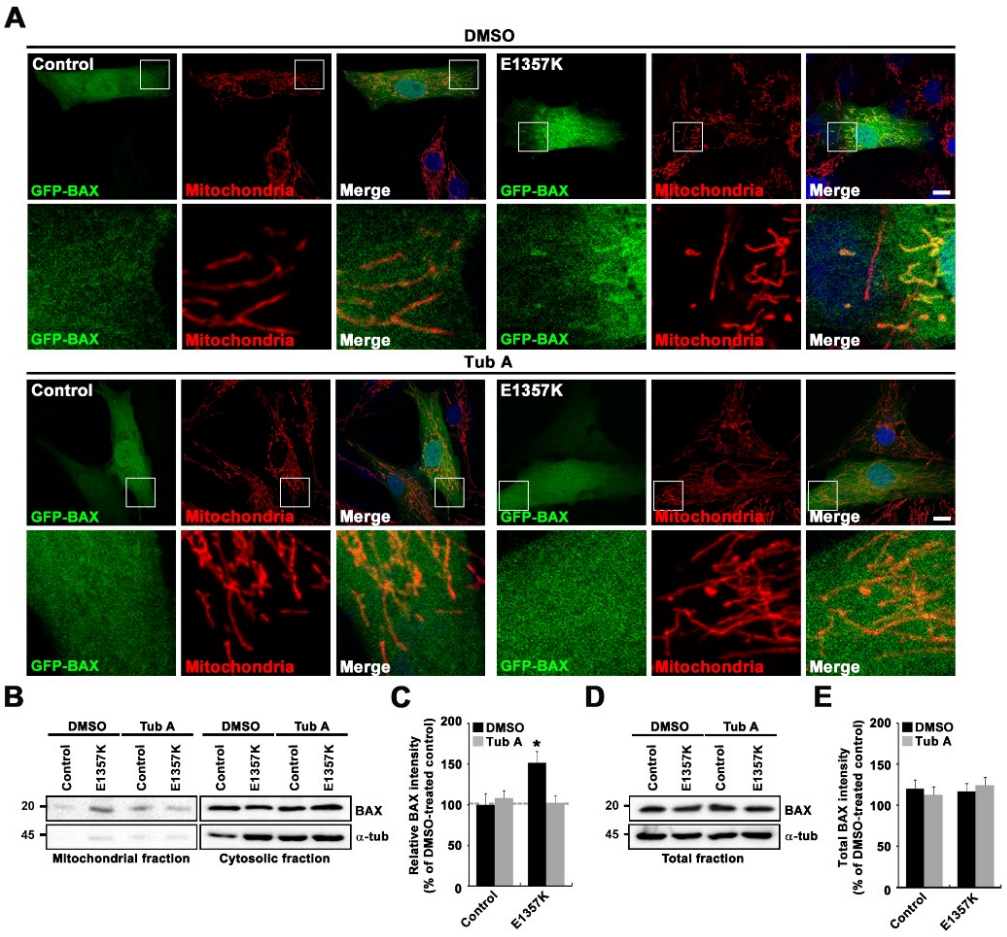

Figure 11. Translocation of the proapoptotic protein BAX towards mitochondria mediates in the patient fibroblasts

(A-E) BAX translocation to mitochondria from cytosol in patient fibroblasts carrying the RAPGEF2-E1357K variant is restored by tubastatin A (Tub A) treatment. (A) Confocal images of fibroblasts expressing GFP-BAX with or without Tub A treatment labeled with mitochondria (red), and DAPI (blue). Scale bar: 5 μm. (B) Western blot of fibroblasts from the ALS patients and healthy controls to examine BAX levels in mitochondria after the mitochondrial fractionation assay. The blots were incubated with anti-BAX, and anti-α-tub. (C) Quantitative analysis of BAX intensity from three independent blots using ImageJ. BAX levels at mitochondrial fraction were normalized

to the total BAX levels. All comparisons are made with healthy controls (*P<0.001). (D) Western blot of fibroblasts from the ALS patients and healthy controls to analyze total BAX level. The blots were incubated with anti-BAX, and anti-α-tub. (E) Quantitative analysis of total BAX levels from three independent blots using ImageJ. All comparisons are made with healthy controls (*P<0.001).

8. Defected motor function is observed in transgenic flies expressing human RAPGEF2-E1357K

Previously, fly models of TDP-43 and FUS mutation, known as ALS causing genes, mimics ALS-like symptom, such as locomotion deficits (Li et al., 2010; Hanson et al., 2010; Lanson et al., 2011). Therefore, we tested whether the transgenic flies expressing RAPGEF2-E1357K variants recapitulate motor inability presented in human ALS patients. To examine fly locomotion, we performed climbing assay through geotactic behavior analysis. In control group, most of the flies were crawled to the top of the glass cylinder, when they were at 20-days aged (Fig 12A and 12B). Unlike the controls, climbing ability in RAPGEF2-E1357K mutants was reduced, which is the resemblance of human ALS motor ability, when they are at 20-days aged (Fig 12A and 12B). These results imply the correlation between motor inability and impairments in mitochondria distribution in RAPGEF2-E1357K mutants. As results, we suspect that defects in mitochondrial trafficking in RAPGEF2-E1357K mutants would cause motor neuron death and weaken motor ability.

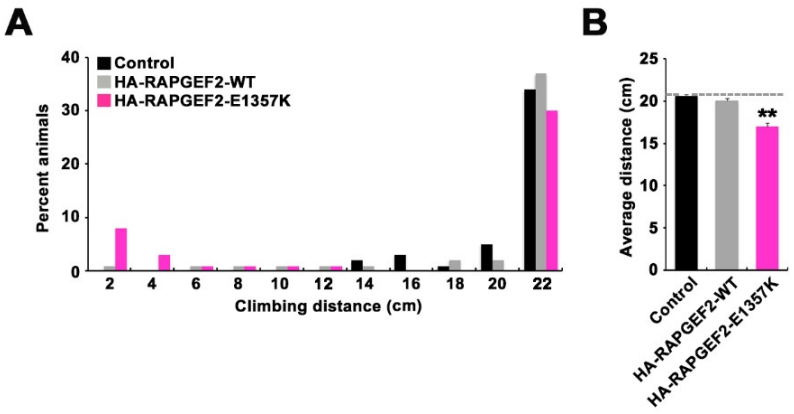

Figure 12. Transgenic flies expressing human RAPGEF2-E1357K display human ALS-like motor dysfunction
(A and B) Climbing ability is measured in 20 day old flies of the indicated genotype: *D42-GAL4*/+ (Control), *D42-GAL4*/*UAS-HA-RAPGEF2-WT* (HA-RAPGEF2-WT), and *UAS-HA-RAPGEF2-E1357K/+; D42-GAL4/+* (HA-RAPGEF2-E1357K). (A) Distribution of climbing distance of 20-day-aged flies during a 30-s period. (B) Quantification of the average climbing distance. All data are compared with GAL4 controls (**P <0.01).

9. The distribution of motor protein KIF5A is impaired in RAPGEF2-E1357K overexpressing cells

Previously, KIF5A is well-known neuron-specific kinesin-1, which participates in modulation of axonal mitochondria transport (Pilling et al., 2006; Hirokawa et al., 2010; Sheng et al., 2012; Franker et al., 2013; De Vos et al., 2017). Therefore, we explored the KIF5A expression in the cells overexpressing the RAPGEF2 E1357K to find whether RAPGEF2 E1357K variant has role in regulation of the motor protein. The localization of KIF5A was evenly distributed throughout the cells in RAPGEF2 wild-type (Fig 13A). Unlike the RAPGEF2 wild-type cells, the cells overexpressing RAPGEF2 E1357K variant showed abnormal aggregation of KIF5A (Fig 13A). We

additionally proved the phenomena by triple labeling with RAPGEF2, KIF5A, and Acetylated α-tubulin. As results, we observed that the expression of KIF5A is aggregated in the absence of the area, where the acetylated α-tubulin is absence from the RAPGEF2 E1357K cells (Fig 13B). These results proved that the function of motor protein is somehow impaired by RAPGEF2 E1357K variant. However, further studies are required to emphasize whether RAPGEF2-E1357K controls the KIF5A distribution.

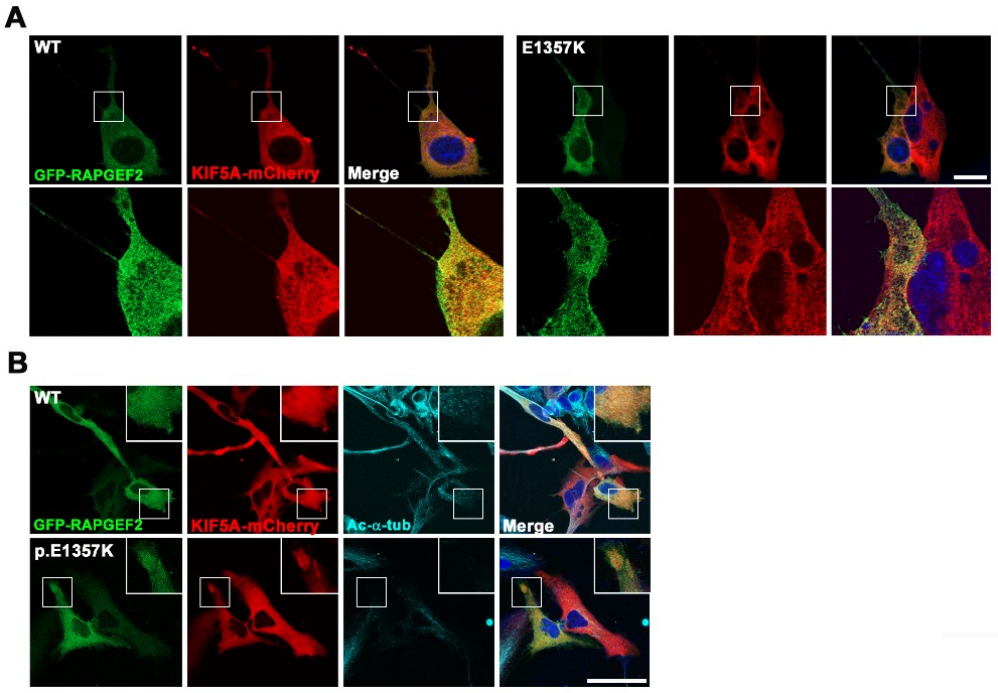

Figure 13. The distribution of KIF5A is altered in the Hela cells overexpressing the RAPGEF2-E1357K variant
(A) Images of cells using superresolution microscopy using stimulated emission depletion (STED) labeled with RAPGEF2 (green), KIF5A (red), and DAPI (blue). Scale bar: 5 μm. (B) Images of cells labeled with RAPGEF2 (green), KIF5A (red), Ac-α-tub (Cyan) and DAPI (blue). Scale bar: 5 μm.

V. Discussion

The microtubule-based transport throughout the cells is important for neuronal function and development (De Vos et al., 2007; Hirokawa et al., 2010). Defective microtubule-based transport has been suggested as a causative factor for neurodegenerative disease (Sasaki et al., 2004; Franker et al., 2013; Clark et al., 2016). In particular, the impairment in mitochondrial transport has been known to play a neuropathological mechanism related to ALS (Saxton et al., 2012; Schwarz et al., 2013; Sheng et al., 2014; Alami et al., 2014). Despite the fact, it is still unclear how alteration in mitochondria and microtubule stability significantly play in ALS progression (Franket et al., 2013; Clark et al., 2016). To prove the relevance of mitochondrial transport and microtubule dynamics in ALS, additional studies were required whether the malfunction in mitochondria and microtubule network are seen in sporadic cases of the disease (Clark et al., 2016). The discoveries of mutations in genes linked to the microtubule-based mitochondrial transport were suggested as a key to identify the relationship between the transport defects and ALS (Bilsland et al., 2010; Fallini et al., 2012; Franker et al., 2013; Wang et al., 2013).

In this study, we discovered a *de novo* missense substitution in *RAPGEF2* gene using trio-based WES approach, and elucidated that the RAPGEF2 dysfunction caused by E1357K variant impairs cytoskeleton organization. Cytoskeletal defects lead to impairment in mitochondrial movement, which is an established pathophysiological mechanism in ALS (Fallini et al., 2012). The patient skin fibroblasts with RAPGEF2 E1357K variant showed decreased level of acetylated α-tubulin and morphological and

functional defects of mitochondria. Importantly, mitochondrial defect shown in patient fibroblasts are rescued by HDAC6 inhibitor, tubastatin A, suggesting that the mitochondrial function is impaired followed by microtubule de-stabilization (Fig 14). We also proved that the defective mitochondrial movement and fragmentation induces apoptotic pathway by examining enhanced BAX level at mitochondrial fraction in the patient fibroblasts carrying RAPGEF2 E1357K variant.

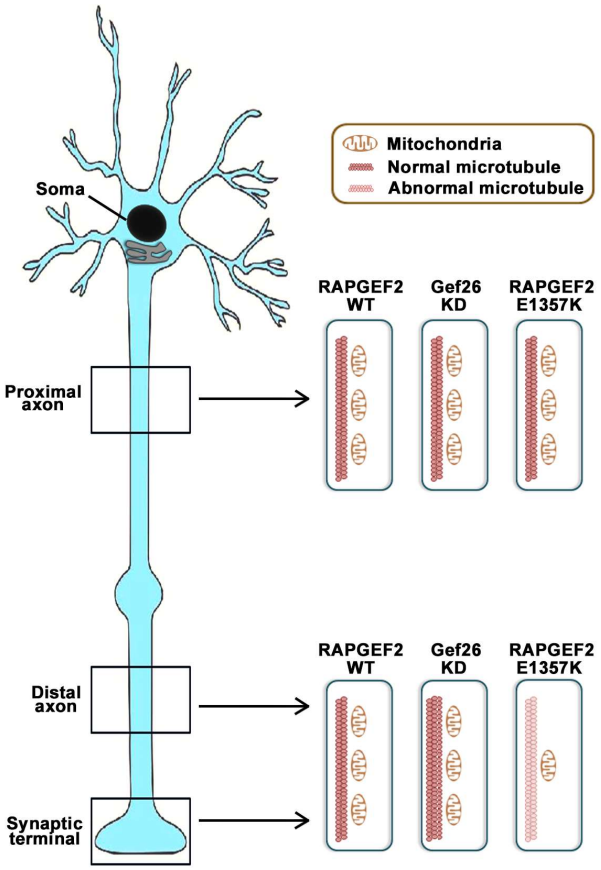

Figure 14. Summary of pathogenic effect of RAPGEF2 E1357K variant
When RAPGEF2 function is disrupted by E1357K variant, microtubule stability and mitochondrial distribution is disrupted in the distal axons and NMJ of transgenic flies expressing human RAPGEF2-E1357K. This phenomenon is caused by gain of toxicity. Unlike the E1357K variant, RAPGEF2 loss-of-function over-stabilizes the microtubules, but doesn't affect mitochondrial distribution.

Previously, we have reported that loss of *Drosophila RAPGEF2* (Gef26) induces synaptic overgrowth and neuronal cell death by modulating microtubule stability. We therefore examined the phenotypes of acetylated α-tubulin level and mitochondrial distribution at axonal segments and NMJs in MNs-specific knockdown of *Gef26* flies. Surprisingly, the acetylated α-tubulin level and mitochondrial distribution at the axons and the NMJs of the flies were normal, while reduced level of acetylated α-tubulin and mitochondria abnormality were observed in transgenic flies expressing human RAPGEF2-E1357K variant. These contrary results propose that RAPGEF2-E1357K may occur by gain of toxic effects (not by loss-of-function) to control microtubule stability and mitochondrial trafficking. Altogether, these evidences support another role of RAPGEF2 in regulation of microtubule stability either by 'loss-of-function' mechanism or 'gain-of-toxic function' mechanism. However, further study is required to identify molecular mechanism of RAPGEF2. Despite the fact, we verified that the maintenance of microtubule stability can be central pathological mechanism of motor neuron diseases.

Recent ALS studies using cell and mouse models of FUS or SOD1 have reported that kinesin function deficits are significant in ALS pathogenesis (Reed et al., 2006; Cho et al., 2007; Sirajuddin et al., 2014; Zhang et al., 2016). Notably, KIF5A is a neuron-specific motor protein from the kinesin-1 family, which facilitates neuronal mitochondria transport depends on the microtubule network, and its variants were recently found in genes associated with ALS (Glater et al., 2006; Russo et al., 2009; Baldwin et al., 2016). Such previous studies led us to suspect that RAPGEF2 might act

on neuronal mitochondrial function along the microtubules by functionally interacting with KIF5A protein. In fact, we found that expression of KIF5A is somehow altered in fibroblasts carrying RAPGEF2 E1357K variant compared to the controls. Therefore, KIF5A might be a key to understand ALS pathogenesis related to the axonal transport system. However, further studies are required to examine the correlation between RAPGEF2 and KIF5A function in detail.

Overall, the identification of *de novo* mutations using WES is recent method for detecting disease-related genes. Previous genetic studies were insufficient to emphasizing the significance of the mutations in identified ALS-associated genes. Our study revealed a *de novo* RAPGEF2 variant found by a trio-based WES method, which is a new technique to discover the genes that were not found by genome-wide association studies (GWAS). We also verified that this missense variant in the *RAPGEF2* gene is critical for mitochondrial movement, shape and function by regulation of microtubule organization. Previous studies have been reported that the morphological defects of mitochondria e.g., absence of cristae and swollen are the early event of the diseases in ALS patients carrying pathogenic variants either in TDP-43, FUS, C9orf72 or CHCHD10 (Deng et al., 2015; Genin et al., 2016; Smith et al., 2017; Wang et al., 2013). However, further study is required to support the relevance of RAPGEF2 role to ALS pathology. It would be more informative if the variants in *RAPGEF2* gene are found in additional ALS patient cohorts and perform extensive functional experiments using reliable cell (e.g., induced neurons or iPSC derived motor

neurons) and animal models, which recapitulate pathological finding observed in human for future studies.

VI. Literature Cited

1. Taylor JP, Brown RH, Cleveland DW. Decoding ALS: from genes to mechanism. (2016). Nature. 539(7628):197-206.
2. Brown RH, Al-Chalabi A. (2017). Amyotrophic Lateral Sclerosis. New Engl J Med. 377(2):162-72.
3. Mattson MP, Gleichmann M, Cheng A. (2008). Mitochondria in neuroplasticity and neurological disorders. Neuron. 60(5):748-66.
4. Clark, J.A., et al., (2016). A Case for Microtubule Vulnerability in Amyotrophic Lateral Sclerosis: Altered Dynamics During Disease. Frontiers in Cellular Neuroscience. 10.
5. De Vos KJ, Hafezparast M. (2017). Neurobiology of axonal transport defects in motor neuron diseases: Opportunities for translational research? Neurobiol Dis. 105:283-99.
6. Carri MT, D'Ambrosi N, Cozzolino M. (2017). Pathways to mitochondrial dysfunction in ALS pathogenesis. Biochem Biophys Res Commun. 483(4):1187-93.
7. Frank, S., et al., (2001). The role of dynamin-related protein 1, a mediator of mitochondrial fission, in apoptosis. Developmental Cell. 1(4): p. 515-525.
8. Safiulina, D. and A. Kaasik. (2013). Energetic and Dynamic: How Mitochondria Meet Neuronal Energy Demands. Plos Biology. 11(12).
9. Sheng, Z.H. (2017). The Interplay of Axonal Energy Homeostasis and Mitochondrial Trafficking and Anchoring. Trends in Cell Biology. 27(6): p. 403-416.
10. Sheng, Z.H. and Q. Cai. (2012). Mitochondrial transport in neurons: impact on synaptic homeostasis and neurodegeneration. Nature Reviews Neuroscience. 13(2): p. 77-93.
11. Fang D, Yan S, Yu Q, Chen D, Yan SS. (2016). Mfn2 is Required for Mitochondrial Development and Synapse Formation in Human Induced Pluripotent Stem Cells/hiPSC Derived Cortical Neurons. Sci Rep. 6:31462.
12. Hariharan IK, Carthew RW, Rubin GM. (1991). The Drosophila Roughened Mutation - Activation of a Rap Homolog Disrupts Eye Development and Interferes with Cell Determination. Cell. 67(4):717-22.
13. De Rooij J, Boenink NM, van Triest M, Cool RH, Wittinghofer A, Bos JL. (1999). PDZ-GEF1, a guanine nucleotide exchange factor specific for Rap1 and Rap2. J Biol Chem. 274(53):38125-30.
14. Asha H, de Ruiter ND, Wang MG, Hariharan IK. (1999). The Rap1 GTPase functions as a regulator of morphogenesis in vivo. Embo J. 18(3):605-15.
15. Boettner B, Van Aelst L. (2007). The rap GTPase activator drosophila PDZ-GEF regulates cell shape in epithelial migration and morphogenesis. Mol Cell Biol. 27(22):7966-80.

16. Asuri S, Yan JL, Paranavitana NC, Quilliam LA. (2008). E-Cadherin Dis-Engagement Activates the Rap1 GTPase. J Cell Biochem. 105(4):1027-37.
17. Gloerich M, Bos JL. (2011). Regulating Rap small G-proteins in time and space. Trends Cell Biol. 21(10):615-23.
18. Ye T, Ip JPK, Fu AKY, Ip NY. (2014). Cdk5-mediated phosphorylation of RapGEF2 controls neuronal migration in the developing cerebral cortex. Nat Commun. 2014;5.
19. Lim SM, Choi WJ, Oh KW, Xue YC, Choi JY, Kim SH, et al. (2016). Directly converted patient-specific induced neurons mirror the neuropathology of FUS with disrupted nuclear localization in amyotrophic lateral sclerosis. Mol Neurodegener. 2016;11.
20. Shin J, Salameh JS and Richter JD. (2016). Impaired neurodevelopment by the low complexity domain of CPEB4 reveals a convergent pathway with neurodegeration. Sci Rep. 6:29395.
21. Heo K, Nahm M, Lee MJ, Kim YE, Ki CS, Kim SH, et al. (2017). The Rap activator Gef26 regulates synaptic growth and neuronal survival via inhibition of BMP signaling. Mol Brain. 2017;10.
22. Lee, J.H., et al. (2002). Drosophila PDZ-GEF, a guanine nucleotide exchange factor for Rap1 GTPase, reveals a novel upstream regulatory mechanism in the mitogen-activated protein kinase signaling pathway. Molecular and Cellular Biology. **22**(21): p. 7658-7666.
23. Westermann, S. and K. Weber. (2003). Post-translational modifications regulate microtubule function. Nature Reviews Molecular Cell Biology. 4(12): p. 938-947.
24. Conde C, Caceres A. (2009). Microtubule assembly, organization and dynamics in axons and dendrites. Nat Rev Neurosci. 10(5):319-32.
25. Wloga, D. and J. Gaertig. (2010). Post-translational modifications of microtubules. Journal of Cell Science. 123(20): p. 3447-3455.
26. Brooks BR, Miller RG, Swash M, Munsat TL, Gr WFNR. (2000). El Escorial revisited: Revised criteria for the diagnosis of amyotrophic lateral sclerosis. Amyotroph Lateral Sc. 1(5):293-9.
27. Portran D, Schaedel L, Xu ZJ, Thery M, Nachury MV. (2017). Tubulin acetylation protects long-lived microtubules against mechanical ageing. Nat Cell Biol. 19(4):391-+.
28. Vossler MR, Yao H, York RD, Pan MG, Rim CS and Stork PJ. (1997). cAMP activates MAP kinase and Elk-1 through a B-Raf- and Rap1-dependent pathway. Cell. 89(1):73-82.
29. Park JY, Jang SY, Shin YK, Koh H, Suh DJ, Shinji T, et al. (2013). Mitochondrial Swelling and Microtubule Depolymerization Are Associated with Energy Depletion in Axon Degeneration. Neuroscience. 238:258-69.

30. Kaasik A, Safiulina D, Choubey V, Kuum M, Zharkovsky A, Veksler V. (2007). Mitochondrial swelling impairs the transport of organelles in cerebellar granule neurons. J Biol Chem. 282(45):32821-6.
31. Zala D, Hinckelmann MV, Yu H, da Cunha MML, Liot G, Cordelieres FP, et al. (2013). Vesicular Glycolysis Provides On-Board Energy for Fast Axonal Transport. Cell. 152(3):479-91.
32. Lim SM, Choi BO, Oh SI, Choi WJ, Oh KW, Nahm M, et al. (2016). Patient fibroblasts-derived induced neurons demonstrate autonomous neuronal defects in adult-onset Krabbe disease. Oncotarget. 7(46):74496-509.
33. Hubbert C, Guardiola A, Shao R, Kawaguchi Y, Ito A, Nixon A, et al. (2002). HDAC6 is a microtubule-associated deacetylase. Nature. 417(6887):455-8.
34. d'Ydewalle C, Krishnan J, Chiheb DM, Van Damme P, Irobi J, Kozikowski AP, et al. (2011). HDAC6 inhibitors reverse axonal loss in a mouse model of mutant HSPB1-induced Charcot-Marie-Tooth disease. Nat Med. 17(8):968-U86.
35. Guo WT, Naujock M, Fumagalli L, Vandoorne T, Baatsen P, Boon R, et al. (2017). HDAC6 inhibition reverses axonal transport defects in motor neurons derived from FUS-ALS patients. Nat Commun. 2017;8.
36. Chen HC, Chan DC. (2009). Mitochondrial dynamics-fusion, fission, movement, and mitophagy-in neurodegenerative diseases. Hum Mol Genet. 18:R169-R76.
37. Smiley ST, Reers M, Mottolahartshorn C, Lin M, Chen A, Smith TW, et al. (1991). Intracellular Heterogeneity in Mitochondrial-Membrane Potentials Revealed by a J-Aggregate-Forming Lipophilic Cation Jc-1. P Natl Acad Sci USA. 88(9):3671-5.
38. Genin EC, Plutino M, Bannwarth S, Villa E, Cisneros-Barroso E, Roy M, et al. (2016). CHCHD10 mutations promote loss of mitochondrial cristae junctions with impaired mitochondrial genome maintenance and inhibition of apoptosis. EMBO. 8(1):58-72.
39. Pilling AD, Horiuchi D, Lively CM, Saxton WM. (2006). Kinesin-1 and dynein are the primary motors for fast transport of mitochondria in Drosophila motor axons. Molecular Biology of the Cell. 17(4):2057-68.
40. Wang XN, Schwarz TL. (2009). Imaging Axonal Transport of Mitochondria. Methods in Enzymology, Vol 457: Mitochondrial Function, Partb Mitochondrial Protein Kinases, Protein Phosphatases and Mitochondrial Diseases. 457:319-33.
41. Schwarz, TL. (2013). Mitochondrial Trafficking in Neurons. Csh Perspect Biol. **5**(6).

42. Sandoval H, Yao CK, Chen KC, Jaiswal M, Donti T, Lin YQ, et al. (2014). Mitochondrial fusion but not fission regulates larval growth and synaptic development through steroid hormone production. Elife. 2014;3.
43. Babic M, Russo GJ, Wellington AJ, Sangston RM, Gonzalez M, Zinsmaier KE. (2015). Miro's N-Terminal GTPase Domain Is Required for Transport of Mitochondria into Axons and Dendrites. Journal of Neuroscience. 35(14):5754-71.
44. Frank S, Gaume B, Bergmann-Leitner ES, Leitner WW, Robert EG, Catez F, et al. (2001). The role of dynamin-related protein 1, a mediator of mitochondrial fission, in apoptosis. Dev Cell. 1(4):515-25.
45. Scorrano L, Ashiya M, Buttle K, Weiler S, Oakes SA, Mannella CA, et al. (2002). A distinct pathway remodels mitochondrial cristae and mobilizes cytochrome c during apoptosis. Dev Cell. 2(1):55-67.
46. Poncet D, Larochette N, Pauleau AL, Boya P, Jalil AA, Cartron PF, et al. (2004). An anti-apoptotic viral protein that recruits bax to mitochondria. J Biol Chem. 279(21):22605-14.
47. Wei MC, Zong WX, Cheng EHY, Lindsten T, Panoutsakopoulou V, Ross AJ, et al. (2001). Proapoptotic BAX and BAK: A requisite gateway to mitochondrial dysfunction and death. Science. 292(5517):727-30.
48. Sheridan C, Delivani P, Cullen SP, Martin SJ. (2008). Bax- or Bak-induced mitochondrial fission can be uncoupled from cytochrome c release. Mol Cell. 31(4):570-85.
49. Li Y, Pay, P, Rao EJ, Shi C, Guo W, Chen X, et al. (2010). A Drosophila model for TDP-43 proteinopathy. PNAS. 107(7);3169-3174.
50. Hanson KA, Kim SH, Wassarman DA, Tibbetts RS. (2010). Ubiquilin modifies TDP-43 toxicity in a Drosophila model of Amyotrophic Lateral Sclerosis (ALS). J of Biol Chem. 285: 11068-11072.
51. Lanson NA, Maltare A, King H, Smith R, Kim JH, Taylor JP, et al. (2011). A Drosophila model of FUS-related neurodegeneration reveals genetic interaction between FUS and TDP-43. Hum Mol Genet. 20(13):2510-23.
52. Hirokawa N, Niwa S, Tanaka Y. (2010). Molecular Motors in Neurons: Transport Mechanisms and Roles in Brain Function, Development, and Disease. Neuron. 68(4):610-38.
53. De Vos KJ, Chapman AL, Tennant ME, Manser C, Tudor EL, Lau KF, et al. (2007). Familial amyotrophic lateral sclerosis-linked SOD1 mutants perturb fast axonal transport to reduce axonal mitochondria content. Hum Mol Genet. 16(22):2720-8.

54. Sasaki S, Warita H, Abe K, Iwata M. (2004). Slow component of axonal transport is impaired in the proximal axon of transgenic mice with a G93A mutant SOD1 gene. Acta Neuropathol. 107(5):452-60.
55. Franker MAM, Hoogenraad CC. (2013). Microtubule-based transport - basic mechanisms, traffic rules and role in neurological pathogenesis. J Cell Sci. 126(11):2319-29.
56. Clark JA, Yeaman EJ, Blizzard CA, Chuckowree JA, Dickson TC. (2016). A Case for Microtubule Vulnerability in Amyotrophic Lateral Sclerosis: Altered Dynamics During Disease. Front Cell Neurosci. 2016;10.
57. Saxton WM, Hollenbeck PJ. (2012). The axonal transport of mitochondria. J Cell Sci. 125(9):2095-104.
58. Sheng ZH. (2014). Mitochondrial trafficking and anchoring in neurons: New insight and implications. J Cell Biol. 204(7):1087-98.
59. Alami NH, Smith RB, Carrasco MA, Williams LA, Winborn CS, Han SSW, et al. (2014). Axonal Transport of TDP-43 mRNA Granules Is Impaired by ALS-Causing Mutations. Neuron. 81(3):536-43.
60. Bilsland, L.G., et al. (2010). Deficits in axonal transport precede ALS symptoms in vivo. Proceedings of the National Academy of Sciences of the United States of America. 107(47): p. 20523-20528.
61. Fallini, C., G.J. Bassell, and W. Rossoll, (2012). The ALS disease protein TDP-43 is actively transported in motor neuron axons and regulates axon outgrowth. Human Molecular Genetics. 21(16): p. 3703-3718.
62. Reed, N.A., et al. (2006). Microtubule acetylation promotes kinesin-1 binding and transport. Current Biology. 16(21): p. 2166-2172.
63. Cho, K.I., et al. (2007). Association of the kinesin-binding domain of RanBP2 to KIF5B and KIF5C determines mitochondria localization and function. Traffic. 8(12): p. 1722-1735.
64. Sirajuddin, M., L.M. Rice, and R.D. Vale. (2014). Regulation of microtubule motors by tubulin isotypes and post-translational modifications. Nature Cell Biology. 16(4): p. 335-+.
65. Zhang, Y., et al. (2016). Induction of Posttranslational Modifications of Mitochondrial Proteins by ATP Contributes to Negative Regulation of Mitochondrial Function. Plos One. **11**(3).
66. Glater, E.E., et al.. (2006). Axonal transport of mitochondria requires milton to recruit kinesin heavy chain and is light chain independent. Journal of Cell Biology, 2006. **173**(4): p. 545-557.
67. Russo, G.J., et al. (2009). Drosophila Miro Is Required for Both Anterograde and Retrograde Axonal Mitochondrial Transport. Journal of Neuroscience. **29**(17): p. 5443-5455.
68. Baldwin, K.R., et al. (2016). Axonal transport defects are a common phenotype in Drosophila models of ALS. Human Molecular Genetics. **25**(12):

p. 2378-2392.
69. Deng J, Yang M, Chen Y, Chen X, Liu J, Sun S, Cheng H, Li Y, Bigio EH, Mesulam M, Xu Q, Du S, Fushimi K, Zhu L, and Wu JY. (2015). FUS interacts with HSP60 to promote mitochondrial damage. PloS Genet. 11(9): e1005357.
70. Wang W, Li L, Lin WL, Dickson DW, Petrucelli L, Zhang T, and Wang X. (2013). The ALS disease-associated mutant TDP-43 impairs mitochondrial dynamics and function in motor neurons. Human Mol Gen. 22(23):4706-4719.
71. Smith EF, Shaw PJ and De Vos KJ. (2017). The role of mitochondria in amyotrophic lateral sclerosis. Neurosci Letter. pii: S0304-3940(17)30544-X.

Chapter VI
Conclusion and perspective

During my Ph.D courses, I was interest in research to explore the pathological mechanisms of ALS, which is one of neurodegenerative diseases resulting from loss of motor neurons selectively. Because neuron has long axon, and requires high energy consumption compared to other cellular types, I believe studying the molecular mechanisms of microtubule dynamics is important to understand the developmental processes of synapse or growth cone and neuronal survival. From the previous studies, the function of microtubule dynamics is known to be regulated by post-translational modifications of α-tubulin, motor proteins, or intracellular pathways related to the neuronal development, for example BMP signaling. This conclusion is organized into two parts. The first part is about my past works, which is to identify roles of a novel gene in controlling of microtubule stability to modulate NMJ development and neuronal survival via BMP signaling pathway, and to define the pathogenic effects of the novel genetic variants found from the sporadic ALS patients in the area of neurodegeneration. The second part is about my future plan in the respective areas.

Summary of my work

My research was focus on the identification of novel genes affecting NMJ growth and neuronal survival by modulating stability of microtubules. Among the several genes I studied, my dissertation was focused on functional role of RAPGEF2 at synaptic terminals and the pathogenic effect of RAPGEF2 variant (p.E1357K), which was newly identified from the whole exome sequencing (WES) analysis of sporadic amyotrophic lateral sclerosis (ALS) patients. Previously, RAPGEF2 is known as a

GEF for Rap1, which convert GDP to GTP-bound Rap1 to activate developmental processes, e.g., eye, productive organs, and neuronal development (Asha et al., 1999; Singh et al., 2006; Bos et al., 2001; Pannekoek et al., 2009). However, role of RAPGEF2 in synaptic development and neuronal survival was unclear. My first publication is about the synaptic role of GEF26 (human ortholog of RAPGEF2), which governs microtubule stability via BMP signaling to inhibit neuromuscular junction (NMJ) growth and neuronal survival. I proved that GEF26 retrains BMP signaling by attenuating the endocytic internalization of surface BMP receptor. In addition, I clearly showed that GEF26 acts as an upstream molecule of Rap1 to control NMJ growth, motor function, and neuronal cell survival. For experimental approach, I genetically recombined the fly strains carrying distinct genes and interpreted the genetic epitasis through the test of trans-heterozygous interaction to define the genetic interactions between the molecules, or the suppression test to explore regulatory hierarchy between the molecules. Using the strategies, I scrutinized genetic relations between GEF26, BMP-related components, and microtubule-associated proteins (MAPs) by examining the phenotypic similarity of NMJ growth and morphology among the molecules. From this study, I clarified the GEF26 loss-of-function in regulation of synaptic development by controlling microtubule stability. Furthermore, I investigated lifespan, locomotor ability, and brain neurodegeneration to study the pathological role of GEF26. As results, I found that the loss of GEF26 induces age-dependent shorten lifespan, progressive locomotor dysfunction and neurodegeneration in fly brain, which further leads to neuronal cell death. In conclusion, I discovered that GEF26 inhibits BMP

signaling to regulate synaptic outgrowth and neuronal survival through regulation of microtubule stability.

My second publication is focused on defining the pathogenic effect of a *de novo* RAPGEF2 variant (p.E1357K), which is discovered from a sporadic ALS patient. For this study, I used skin fibroblasts obtained from the ALS patient carrying the RAPGEF2 variant and various types of cells, such as HeLa, Nsc34 and HEK293 cells. When the RAPGEF2 function is disrupted by E1357K variant, decrease in microtubule stability and enhancement of fragmented or short mitochondria were examined. In particular, defective mitochondrial distributions and microtubule stability were observed in distal axons of transgenic flies, which are generated to carry a transgene of RAPGEF2-E1357K motor neuron specifically. For this research, I concluded that the RAPGEF2-E1357K variant disrupts microtubule-dependent moving of mitochondria, which induces apoptotic cell death based on the three evidences. First, enlarged mitochondria with absence of cristae were detected in patient-derived fibroblasts by electron microscopy (EM) analysis. Mitochondria cristae are known as the site for ATP generation, thus absence of cristae implies the weaken mitochondria activity (Cogliati et al., 2016). Second, the mitochondrial membrane potential was severely depolarized in ALS patient-derived fibroblasts, which implies mitochondrial activity is disrupted. Third, I examined the trans-localization of pro-apoptotic regulator BAX, which phenomena is restored by pharmacological treatment of HDAC6 inhibitor, tubastatin A, in cells overexpressing the RAPGEF2 variant. BAX dimerization is well-known to induce mitochondrial outer membrane permeabilization (MOMP) and Cytochrome C

release resulting of apoptosis (Patra et al., 2016). Altogether, I proved that the disruption in microtubule dynamics and mitochondrial distribution is detrimental effect caused by gain-of-toxicity from E1357K variant, which is located in the low-complexity domain (LCD) of human RAPGEF2. My past works demonstrate that maintenance of microtubule stability is significant for neuronal survivability.

My future plan and my perspective

My research goal of my thesis was to find the specific molecules controlling the regulatory mechanism of microtubule dynamics causing selective neuronal cell death. My previous findings support that the maintenance of proper microtubule stability is the key to prevent neurodegenerative processes. The first part of my studies highlights that the proper microtubule stability controlled by BMP signaling is significant for synaptic outgrowth and neuronal survival. Despite the fact, these finding was limited to pinpoint that this is the only causes of selective death of neurons related to motor behavior. My second part of the studies highlights that the proper microtubule stability is important for mitochondrial trafficking. From the studies, I expect that the identification of a novel gene, which has roles in regulation of post-translational modification of α-tubulin or trafficking of microtubule-associated motor proteins, is necessary for therapeutic development in motor neuron diseases. Mitochondrial transport provide energy supplies to demanded areas, thus finding molecular causes affecting microtubule stability and deliveries of axonal mitochondria could be a major clue to understand selective neuronal death underlying the behaviors. Therefore, I think

that the possessing the technical strategy to examine the specific type of cortical neurons' activities, which affects to the motor function in animal models carrying particular mutation of disease-related gene, might be necessary to further define the mechanisms of neurodegenerative diseases.

Literature Cited

1. Asha H, deRuiter ND, Wang MG, and Hariharan IK. (1999). The Rap1 GTPase functions as a regulator of morphogenesis in vivo. EMBO J. *18*, 605–615.
2. Singh SR, Oh SW, Liu W, Chen X, Zheng Z, and Hou SX. (2006). Rap-GEF/Rap signaling restricts the formation of supernumerary spermathecae in *Drosophila melanogaster*. Devlop Growth Differ. *48*, 169-175.
3. Bos JL, Rooij J, and Reedquist KA. (2001). Rap1 signalling: Adhering to new models. Nat Rev Mol Cell Bio. 2(5):369-377.
4. Pannekoek WJ, Kooistra MR, Zwartkruis FJ and Bos JL. (2009). Biochim Biophys Acta. 1788(4):790-6.
5. Cogliati S, Enriquez JA, and Scorrano L. (2016). Mitochondria Cristae: Where beauty meets functionality. Trends in Biochem Sci. 41(3):261-73.
6. Patra M, Malata SK, Padhan DK and Sen M. (2016). CCN6 regulates mitochondrial function. J Cell Sci. 129(14):2841-51.

국 문 초 록

RAPGEF2/GEF26 의 생리적-병태생리적 기능

서울대학교 대학원
뇌인지과학과
허근정

신경세포는 여러 세포기관을 미소세관에 기반하여 양방향으로 전달 할 수 있는 분극화 된 세포다. 이러한 신경세포의 구조 때문에 미소세관 안정화를 조절하는 기전을 이해하는 것은 운동 신경계질환을 치료하는데 있어 중요하다. 이 학위 논문은 미소세관 안정화를 조절하여 신경근 접합부의 성장과 세포사멸을 조절하는 *RAPGEF2/GEF26* 유전자 발견에 대한 연구내용으로 구성되어 있다. 본 연구는 BMP 신호전달을 통해 FMRP-Futsch 를 조절하는 RAPGEF2/GEF26 의 기능적 역할과 산발적인 ALS 환자들을 대상으로 whole exome sequencing 을 수행하여 발견한 de novo RAPGEF2 변이인 E1357K 의 병원의 영향을 규명했다.

첫 번째 연구는 BMP 신호전달의 활성화를 억제하여 미소세관 안정화를 조절하여 시냅스의 성장과 신경세포 사멸을 조절하는 GEF26 (초파리 ortholog: RAPGEF2)의 시냅스에서의 역할에 관한 내용이다. 특히 GEF26 가 BMP receptors 의 endocytic internalization 를 조절하여 BMP receptor endocytosis 과정에서 역할을 한다는 것을 밝혔다. 또한 Gef26 가 Rap1 의 상위단계에 존재하며 시냅스 성장, 운동기능, 그리고 세포사멸을 조절한다는 것을 증명했다. 이 연구를 통해 저는 미소세관 안정화를 조절하는 GEF26 의 기능을 Gef26, Rap1, BMP 구성원들, 그리고 미소세관 관련 단백질 (MAP)의 유전학적 관계를 통해 새롭게 밝히는데 기여했다.

두 번째 연구는 산발적인 ALS 환자들을 대상으로 whole exome sequencing 을 수행하여 발견한 *de novo RAPGEF2* (c.4069G>A; p.E1357K) 변이의 기능연구에 관한 내용이다. 이 연구에서, RAPGEF2 의 기능이 E1357K 변이에 의해 방해되면, 비정상적인 미토콘드리아의 형태, 활동 그리고 분배와 약해진 미세소관 안정화가 조사되었다. 특히 RAPGEF2-E1357K 를 인위적으로 발현시킨 형진 전환 초파리의 distal axon 에서 약해진 미세소관 안정화를 따라 미토콘드리아의 수송에 결함이 있는 것을 확인했다. 또한 RAPGEF2-E1357K 을 발현시킨 세포에서 비정상적인 미토콘드리아의 기능과 형태는 세포사멸을 증가시킨다는 것을 확인했다. 이 연구를 통해 저는 RAPGEF2-E1357K 에 의한 gain-of-toxicity 가 미세소관 안정화를 약화시켜 미세소관에 의존해 있는 미토콘드리아의 수송을 방해하여 세포사멸과 운동기능을 저해하는 것이 아닌가 의심할 수 있었다. 따라서 제

학위논문은 미소세관 안정화를 유지하는 것이 신경세포의 생존능력에 얼마나 중요한 역할을 하는 것과 미소세관 안정화 조절이 신경계 질환의 치료표적으로 중요하다는 것을 증명한다.

주요어: RAPGEF2/GEF26, BMP 신호경로, 미소세관 안정화, 미토콘드리아의 운송, FMRP-Futsch 경로, 시냅스 성장, 세포사멸

학 번: 2014-21333